Development and Application of Thermodynamic Models of Chemical Equilibrium in Multi-phase Organic/Electrolyte/Water Mixtures for Prediction of Atmospheric Organic Particulate Matter Levels

Elsa I-Hsin Chang
B.S., Environmental Engineering, National Chung-Hsing University, 1999
M.S., Environmental and Biological Engineering, Cornell University, 2001

A dissertation presented to the faculty of the
OGI School of Science & Engineering
at Oregon Health & Science University
in partial fulfillment of the
requirements for the degree
Doctor of Philosophy
in
Environmental Science and Engineering

March 2008

The dissertation "Development and Application of Thermodynamic Models of Chemical Equilibrium in Multi-phase Organic/Electrolyte/Water Mixtures for Prediction of Atmospheric Organic Particulate Matter Levels" by Elsa I-Hsin Chang has been examined and approved by the following Examination Committee:

Dr. James Pankow, Thesis Advisor
Professor

Dr. James Huntzicker
Department Head
Department of Management in Science & Technology

Dr. Paul Tratnyek
Professor

Dr. Eladio Knipping
Senior Technical Manager – Air Quality
Electrical Power Research Institute

ACKNOWLEDGEMENTS

I would like to thank all the people who have helped and inspired me during my doctoral study. I especially want to thank my advisor Jim Pankow for bringing me to OGI, an excellent research environment and a warm, friendly community. I have gained tremendous professional and personal development throughout the years at OGI and this would be impossible without Jim. I want to thank him for providing me with scientific and personal advice as well as a lot of support and encouragement. His sense of humor always brightens my day and makes the toughest research problems fun to tackle with. I am truly grateful for his guidance. I see him as my academic father.

I would like to acknowledge my thesis committee, Jim Huntzicker, Paul Tratnyek, and Eladio Knipping for their insightful suggestions and comments on my research. In particular, I would like to thank Jim Huntzicker for guiding me through my independent study of Aerosol Physics. During this study, Jim Huntzicker has spent so much personal time helping me to have a better understanding of Aerosol and giving me a lot of encouragement.

I would like to thank OGI staffs, who made my research and personal life so much easier. Wentai Luo and Lorne Isabelle have helped me with GC/MS and have given me many useful suggestions on experimental QA/QC. Nancy Christie has assisted me with almost everything everyday. She and Jim Pankow also let me join their weekly Bluegrass Jam. As a classical piano player, that was a brand new experience to me and I had a lot fun jamming with them. I thank Bill Asher for helping me with programming problems.

Special thanks to fellow students Kelley Barsanti, Cai Chen, Vaishnavi Sarathy, Zhenhong Li, and Ryan Holland for enriching me in research and life through our interactions. Specifically, I would like to thank Vaishnavi Sarathy for her friendship, help, and delicious Indian food in the past five years.

My deepest gratitude goes to my family for their everlasting love and support throughout my life; this dissertation is simply impossible without them. I am indebted to my parents, Len-Fu Chang and Kee-Kung Kao, who spare no effort to provide the best possible environment for me to grow up and to receive education. I owe my loving thanks to my husband, Danny Chen. His constant love, understanding, and support have helped me to overcome all the obstacles along the years. My special gratitude is due to my sister, Echa Chang, for her loving support and companionship.

TABLE OF CONTENTS

LIST OF TABLES

LIST OF FIGURES

ABSTRACT

Development and Application of Thermodynamic Models of Chemical Equilibrium in Multi-phase Organic/Electrolyte/Water Mixtures for Prediction of Atmospheric Organic Particulate Matter Levelsiii

Elsa I-Hsin Chang, B.S., M.S.

Ph.D., OGI School of Science & Engineering
at Oregon Health & Science University
March 2008

Research Advisor: Dr. James F. Pankow

In the first part of the dissertation, a thermodynamic model is presented for predicting the formation of particulate matter (PM) within an aerosol that contains organic compounds, inorganic salts, and water. Neutral components are allowed to partition from the gas phase to the PM, with the latter potentially composed of both a primarily aqueous (α) liquid phase and a primarily organic (β) liquid phase. Partitioning is allowed to occur without any artificial restraints: when both α and β PM phases are present, ionic constituents are allowed to partition to both. X-UNIFAC.2, an extended UNIFAC method based on Yan et al. (1999), was developed for activity coefficient estimation. X-UNIFAC.2 utilizes the standard UNIFAC terms, a Debye-Hückel term, and a virial equation term that represents the middle-range (MR) contribution to activity coefficient effects. A large number (234) of MR parameters are already available from Yan et al. (1999). Six additional MR parameters were optimized here to enable X-

UNIFAC.2 to account for interactions between the carboxylic acid group and Na^+, Cl^-, and Ca^{2+}. Predictions of PM formation were made for a hypothetical sabinene/O_3 system with varying amounts of NaCl in the PM. Predictions were also made for the chamber experiments with α-pinene/O_3 (and $CaCl_2$ seed) carried out by Cocker et al. (Atmospheric Environment, 2001, 35, 6049-6072); good agreement between the predicted and chamber-measured PM mass concentrations was achieved.

In the second part of the dissertation, the commonly used existing two-product model (Odum et al., 1996) is advanced to account for the relative humidity effects on levels of organic particulate matter (OPM) mass. The two-product model predicts secondary organic aerosol (SOA) formation in the atmosphere using a multiple lumped "two-product" ($N{\bullet}2\mathrm{p}$) approach. The $N{\bullet}2\mathrm{p}$ approach neglects: 1) variation of activity coefficient (ζ_i) values and mean molecular weight $\overline{\mathrm{MW}}$ in the particulate matter (PM) phase; 2) water uptake into the PM; and 3) the possibility of phase separation in the PM. This study considers these effects by adopting an $(N{\bullet}2\mathrm{p})^{\zeta,\overline{\mathrm{MW}},\theta}$ approach (θ is a phase index). Specific chemical structures are assigned to 25 lumped SOA 2p compounds and to 15 representative primary organic aerosol (POA) compounds to allow calculation of ζ_i and $\overline{\mathrm{MW}}$ values. The SOA structure assignments are based on chamber-derived 2p gas/particle partition coefficient values coupled with known effects of structure on vapor pressure $p^{\mathrm{o}}_{\mathrm{L},i}$ (atm). To facilitate adoption of the $(N{\bullet}2\mathrm{p})^{\zeta,\overline{\mathrm{MW}},\theta}$ approach in large-scale models, this study also develops CP-Wilson.1, a group-contribution ζ_i–prediction method that is more computationally economical than the UNIFAC model of Fredenslund et. al (1975). Group parameter values required by CP-Wilson.1 are obtained by fitting ζ_i values to predictions from UNIFAC. The $(N{\bullet}2\mathrm{p})^{\zeta,\overline{\mathrm{MW}},\theta}$ approach is applied (using CP-Wilson.1) to several real α–pinene/O_3 chamber cases for high reacted hydrocarbon levels (ΔHC $\approx$ 400 to 1000 μg m^{-3}) when relative humidity (RH) $\approx$ 50%. Good agreement between the chamber and predicted results is obtained using both the $(N{\bullet}2\mathrm{p})^{\zeta,\overline{\mathrm{MW}},\theta}$ and $N{\bullet}2\mathrm{p}$ approaches, indicating relatively small water effects under these conditions. However, for a hypothetical α–pinene/O_3 case at ΔHC = 30 μg m^{-3} and RH = 50%, the

$(N{\bullet}2\mathrm{p})^{\zeta,\overline{\mathrm{MW}},\theta}$ approach predicts that water uptake will lead to an organic PM level that is more than double that predicted by the $N{\bullet}2\mathrm{p}$ approach. Adoption of the $(N{\bullet}2\mathrm{p})^{\zeta,\overline{\mathrm{MW}},\theta}$ approach using reasonable lumped structures for SOA and POA compounds is recommended for ambient PM modeling.

The third part of the dissertation focuses on the practical applicability of the activity coefficient model to computationally demanding, large-scale air quality models. The study used two very simple basis sets of compound characteristic parameters, vapor pressure ($p^{\mathrm{o}}_{\mathrm{L},i}$) and octanol-water partition coefficient ($K_{\mathrm{ow},i}$), to predict compound distribution in gas and particle phases. The foundation of this approach is the development of the new activity coefficient (ζ_i) model, Simple Activity Coefficient Model.1 (SimAct.1) to express ζ_i as a function of $p^{\mathrm{o}}_{\mathrm{L},i}$ and $K_{\mathrm{ow},i}$. Four parameters were fitted for SimAct.1 and the model performance was evaluated by the comparison against the UNIFAC model. An example calculation using the 2-dimentional basis set ($p^{\mathrm{o}}_{\mathrm{L},i}$ vs. $K_{\mathrm{ow},i}$) method for a hypothetical atmospheric system is demonstrated in the study. This 2-dimentional basis set ($p^{\mathrm{o}}_{\mathrm{L},i}$ vs. $K_{\mathrm{ow},i}$) method is very simple, yet it accounts for effects of volatility, polarity, and compound size on G/P partitioning of compounds in atmosphere. This method bypasses the requirement of the knowledge of the individual molecular structures for estimating the effects of compound polarity. This is advantageous to current atmospheric modeling because currently very limited information regarding specific compound identities is available. Moreover, this simple approach can advance the accuracy of current large scale air quality models with very economical computation cost.

References

Cocker, D. R., Clegg, S. L., Flagan, R. C., Seinfeld, J. H., 2001. The effect of water on gas-particle partitioning of secondary organic aerosol. Part I: α-pinene/ozone system. Atmospheric Environment 35, 6049-6072.

Odum, J. R., Hoffmann, T., Bowman, F., Collins, D., Flagan, R. C., Seinfeld, J. H., 1996. Gas/particle partitioning and secondary organic aerosol yields. Environmental Science & Technology 30, 2580-2585.

Yan, W., Topphoff, M., Rose, G., Gmehling, J., 1999. Prediction of vapor-liquid equilibria in mixed-solvent electrolyte systems using the group contribution concept. Fluid Phase Equilibria 162, 97-113.

CHAPTER 1

Overview

Gas and particle (G/P) partitioning process controls the formation and evaporation of particulate matter (PM) in both regional and global atmosphere. The formation of PM in the atmosphere is a topic of critical importance in almost every area of atmospheric science. Indeed, atmospheric PM can affect human health (EPA, 1996), ecosystem health, visibility, the earth's radiation balance, properties and lifetimes of clouds (IPCC, 2001), and thus global climate. Concerns related to human health and visibilities have led U.S. EPA to establish National Ambient Air Quality Standards for PM. Achievement of compliance with such standards can likely only be achieved by the aids of new air quality models that fully consider the complex composition and associated thermodynamic properties of atmospheric PM. Specifically, these models will provide the tools that will enable scientists and air quality regulators to understand the relationships between emissions and ambient PM levels.

Predictions of atmospheric PM levels have been widely implemented using the absorptive G/P partitioning model proposed by Pankow (1994a,b). Two of these predictions are models of Odum et al. (1996,1997) and Strader et al. (1999), which assume atmospheric PM as a single, primarily organic phase that excludes the presence of water and inorganic salts. Other predictions like models of Pun et al. (2002) and Griffin et al. (2003) consider two phases (one primarily organic and one primarily aqueous) existing in PM, but do not allow for the inter-PM-phase equilibrium or for the ionic effects due to the presence of salts on the activity coefficients of PM components. All current models have serious deficiencies because the atmospheric PM often contains water (in correspond to levels of relative humidity) and significant amounts of inorganic salts and it can split into multiple liquid phases. The current model, therefore, are unable to accurately predict PM formation under the important atmospheric conditions. The first objective of this research is to improve the current models by the development of a more completed thermodynamic modeling framework accounting for three major missing compartments of the current existing models: (1) The complex PM composition, which includes organics, water (relative humidity effects), and salts. (2) Ionic effects, due to the presence of salts, on the activity coefficients of PM components, on the G/P portioning, and ultimately on the levels of atmospheric PM formation; and (3) the multiphasic properties of PM.

There is no doubt that it is important to understand the detailed atmospheric physics and chemistry, so the complex atmospheric PM system can be better described and, therefore, more accurately predicted. However, the incorporation of increasing detail in the atmospheric science employed large-scale, multi-day, 3-D air quality modeling is accompanied by tremendous increases in computational demand. This is especially true when modeling secondary organic aerosol (SOA) formed from the gas/particle (G/P) condensation of numerous oxidation products generated from multiple parent hydrocarbons. In modeling the G/P partitioning involved in SOA formation, the dynamic phase equilibrium of each partitioning organic species is established by iteratively solving for values of the composition- and species-dependent G/P partitioning constant. Computationally, these iterative calculations become especially demanding when considering the activity coefficient dependency of the G/P partitioning constants. The second objective of this research is to develop simple models that can greatly reduce computational demand without significant loss of real predictive power. The resulting models will afford greatly expanded PM modeling capability without consuming tremendous computational power.

This dissertation contains reproductions of two manuscripts (permission to reproduce manuscripts granted by Elsevier and Copernicus Publications) that have been accepted for publications and one manuscript suitable for publication:

Chapter 2: Chang and Pankow (2006)

Chapter 3: Chang and Pankow (2008)

Chapter 4: Chang and Pankow (2008) (in preparation)

1.1 References

Chang, E.I., Pankow, J.F., 2006. Prediction of activity coefficients in liquid aerosol particles containing organic compounds, dissolved inorganic salts, and water-Part 2: Consideration of phase separation effects by an X-UNFIAC model. Atmospheric Environment 40, 6422-6436.

Chang, E.I., Pankow, J. F., 2008. Organic particulate matter formation at varying relative humidity using surrogate secondary and primary organic compounds with activity corrections in the condensed phase obtained using a method based on the Wilson equation. Atmospheric Chemistry and Physics Discussion 8, 995-1039.

Chang, E.I., Pankow, J. F., 2008. Using two simple pure compound properties to model complex gas/particle partitioning for atmospheric organic particulate matter (OPM) (in preparation).

EPA, 1996. Air Quality Criteria for Particulate Matter, EPA/600/P-95/001. Washington, D.C.

Griffin, R.J., Nguyen, K., Dabdub, D., Seinfeld, J.H., 2003. A combined hydrophobic-hydrophilic module for predicting secondary organic aerosol formation. Journal of Atmospheric Chemistry 44, 171-190.

Intergov. Panel Climate Change (IPCC). 2001. Climate Change 2001, Cambridge University Press: Cambridge, U.K.

Odum, J.R., Hoffmann, T., Bowman, F., Collins, D., Flagan, R.C.; Seinfeld, J.H. 1996. Gas/particle partitioning and secondary organic aerosol yields. Environmental Sciience & Technology 30, 2580-2585.

Odum, J.R., Jungkamp, T.P.W., Griffin, R.J., Flagan, R.C., Seinfeld, J.H. 1997. The atmospheric aerosol-forming potential of whole gasoline vapor. Science 276, 96-99.

Pankow, J.F. 1994a. An absorption model of gas/particle partitioning of organic compounds in the atmosphere. Atmospheric Environment 28, 185-188.

Pankow, J.F. 1994b. An absorption model of the gas/aerosol partitioning involved in the formation of 9isecondary organic aerosol. Atmospheric Environment 28, 189-193.

Pun, B. K., Griffin, R. J., Seigneur, C., Seinfeld, J. H., 2002. Secondary organic aerosol 2. Thermodynamic model for gas/particle partitioning of molecular constituents. Journal of Geophysical Research 107, 10.1029/2001JD000542.

Strader, R., Lurmann, F., Pandis, S.N. 1999. Evaluation of secondary organic aerosol formation in winter. Atmospheric Environment 33, 4849-4863.

CHAPTER 2

Prediction of Activity Coefficients in Liquid Aerosol Particles Containing Organic Compounds, Dissolved Inorganic Salts, and Water: Consideration of Phase Separation Effects by an X-UNIFAC Model

2.1 Introduction

2.1.1. General

Samples of atmospheric particle matter (PM) typically contain a myriad of different organic compounds, significant amounts of different inorganic salts, and water (e.g., Saxena and Hildemann, 1996; Middlebrook et al., 1998). Under such circumstances, multiple liquid phases may be present in the PM, with the presence of more than one liquid phase affecting the properties of the PM. Proper modeling of atmospheric PM (including amount formed) requires an understanding of multiphasic PM. This requires prediction of chemical activity coefficients as a function of PM composition: a liquid phase will undergo phase separation when the chemical activities underlying enough material in the phase can be reduced by creation of a separate phase.

Most thermodynamic models for organic-electrolyte-water PM focus on predicting aerosol hygroscopic growth (e.g., Clegg et al., 2001; Ming and Russell, 2002; Marcolli et al., 2004; Chan and Chan, 2003; Chan et al., 2005). This type of model predicts only the gas-particle partitioning of water; the organic and inorganic components are locked in the PM. A few models seek to simulate the formation of organic particulate matter (OPM) containing organic compounds, electrolytes, and water (Pun et al., 2002; Griffin et al., 2003). Pun et al. (2002) assumed that OPM may be located in two phases, an organic phase that contains 100% of the "hydrophobic" organic compounds and no water, and an aqueous phase that contains 100% of the "hydrophilic" organic compounds and 100% of the inorganic salts. Griffin et al. (2003) modified the Pun et al. (2002) model to allow equilibration of all organic compounds between both phases, but did not allow similar equilibration of either the water or the salts. In a given circumstance, though the difference may be small, higher OPM levels will be predicted by the Griffin et al. (2003) model as compared to the Pun et al. (2002) model: the freedom to occupy both PM phases corresponds to a state with an overall lower free energy.

The models of Pun et al. (2002) and Griffin et al. (2003) provide useful approximations when modeling OPM formation. They also, however, place some artificial constraints on the overall gas/particle (G/P) partitioning equilibrium. In this work we develop and describe a model that: 1) allows the formation of PM composed of either one or two liquid phases (α, primarily aqueous; and β, primarily organic); 2) considers the complete partitioning of all organic compounds and water among all phases; and 3) when the PM is predicted to be composed of both an α and β phase, allows the salt ions to distribute between both those phases.

2.1.2. Activity coefficient models for organic compound+salt+water mixtures

A thermodynamic model of a solution phase requires a means to predict activity coefficient (ζ) values for each species of interest in the phase. In the atmosphere, the relative humidity (RH, %) varies widely, as do the levels and identities of the salts and organic compounds found in atmospheric PM. Liquid PM can range from being mainly aqueous to mainly organic. When not mainly aqueous, it may not even be characterizable as having a primary solvent. ζ models for atmospheric PM must therefore be applicable over wide ranges in composition. And, since the compounds making up the majority of the organic portion of atmospheric PM are unknown and thus uncharacterized regarding their physical properties, a ζ model for atmospheric PM cannot presume knowledge of the physical properties of the organic constituents.

As a group contribution method (GCM), UNIFAC as developed by Fredenslund et al. (1975) carries considerable potential for modeling complex atmospheric PM because it assumes that ζ_i for each species i can be expressed as a summation of interaction terms between the groups that constitute i and all other groups in the solution. The interaction terms can be deduced by pooling the data from multiple simple experimental studies of phase equilibrium. Important types of phase-equilibrium experiments include vapor-liquid equilibrium (VLE) and liquid-liquid equilibrium (LLE) experiments. The advantage of the GCM approach is that it allows complex interactions between solution species to be broken down into interactions among group building blocks: knowledge of the interaction effects among a relatively small number of building blocks (which may include individual ions) allows prediction of interactions between the great variety of species that can be built from those groups.

Existing predictive ζ models for organic-salt-water mixtures are in many cases extensions of UNIFAC (e.g., Kikic et al., 1991; Yan et al., 1999; Erdakos et al., 2006). The interaction parameters used in these UNIFAC extensions are obtained by fitting primarily to experimental phase equilibrium data obtained for solutions containing short-chain monofunctional compounds, and not the longer-chain and/or multifunctional species that can be found in atmospheric PM. Kikic et al. (1991) combine the basic UNIFAC term for short-range (SR) interactions with a Debye-Hückel term for long-range (LR) interactions. Erdakos et al. (2006) describe X-UNIFAC.1, a derivative of the Kikic et al. (1991) model, for consideration of ions and functional groups of particular interest for atmospheric PM. The models of Kikic et al. (1991) and Erdakos et al. (2006) were developed to predict activity coefficients for neutral compounds in organic-salt-water mixtures, and do not provide ζ expressions for any ions. The LIFAC model of Yan et al. (1999) utilizes a middle range (MR) interaction term in addition to SR and LR terms to express ζ values for organic compounds, water, and certain ions. Yan et al. (1999) report that LIFAC predicts ζ values for solutions with a wider salt concentration range than does the Kikic et al. (1991) model.

Some efforts have been made to fit ζ models using data for compound types that have been identified in atmospheric PM. Among them, Ming and Russell (2002) used data for long chain alkanes, monosaccharides, and carboxylic acids. Raatikainen and

Laaksonen (2005) used data for dicarboxylic acids and for hydroxycarboxylic acids to refit parameters for the LIFAC model and for the Ming and Russell (2002) model. They concluded that the Ming and Russell (2002) model performs better for complex aqueous multi-salt solutions than for organic-salt-water solutions, the problem for the latter relating to the use of a low number of fitted organic-ion interactions. Raatikainen and Laaksonen (2005) also concluded that the MR term in LIFAC enhances the accuracy of that model, but that LIFAC performs best when only a single salt is present.

Although interest is growing rapidly in fitting ζ models using experimental phase equilibrium data, both the amount of such data and the ranges of compound structures and mixture types considered in the data are extremely limited. These limitations in turn limit model predictability (Raatikainen and Laaksonen, 2005). The lack of atmospheric-relevant organic-salt-water mixture data is thus the largest impediment for the development of atmospheric-relevant ζ prediction models: more phase equilibrium data covering a wider range of compound structures, salts, and mixture types is needed.

2.1.3. Goals and approaches of this work

This work: 1) describes the development of a ζ prediction model for neutral compounds and ions in organic-salt-water mixtures; and 2) applies that model in several example cases that involve simultaneous: a) G/P equilibration of organic compounds and water between the gas and liquid-PM phases; b) equilibration of all organic compounds and water between multiple liquid PM phases, when phase separation in the PM occurs; and c) equilibration of ions between multiple liquid PM phases, when phase separation occurs. For the ζ prediction model, we describe X-UNIFAC.2, a LIFAC-based method that considers SR, MR, and LR interactions. Needed group-group interaction parameters were obtained as follows: SR UNIFAC-based neutral-neutral group parameters were obtained from Hansen et al. (1991); SR ion-solvent group and SR ion-ion interaction parameters were set to zero following Yan et al. (1999) who argue that these interactions have negligible influence; selected MR ion-solvent group parameters were obtained from Yan et al. (1991); and MR parameters for Ca^{2+}-COOH, Na^{+}-COOH, and Cl^{-}-COOH interactions were obtained from optimizations carried out here based on existing phase equilibrium data. LIFAC parameters as refitted by Raatikainen and Laaksonen (2005) were not used because parameters for the aldehyde and ketone groups were not included in that study. The overall coverage for interaction parameters provided by X-UNIFAC.2 is summarized in Fig. S2.1. The case examples considered here include: a) hypothetical sabanine-O_3 systems with varying particle-phase NaCl; and b) several α-pinene-O_3 chamber experiments carried out by Cocker et al. (2001) in the presence of $CaCl_2$ seed aerosol.

2.2 Governing equations for X-UNIFAC.2

2.2.1. Short–range (SR) term

In this work a given species *i* may either be a neutral solvent molecule of type *o*, or an inorganic ion of type *j*. The possibility of organic ions is not considered here. To maintain consistency with prior studies, the term "solvent" is reserved here for neutral molecules, though we explicitly note that all ions *j* will certainly play roles in determining the solvent power of any given liquid phase. The governing expression for ζ_i is the same as used by Yan et al. (1991) in the development of LIFAC. It assumes contributions SR, MR, and LR interactions. For a given species *i*, we have $\ln \zeta_i = \ln \zeta_i^{\mathrm{SR}} + \ln \zeta_i^{\mathrm{MR}} + \ln \zeta_i^{\mathrm{LR}}$. For solvent molecule *o* and ion *j*,

$$\ln \zeta_o^{\mathrm{SR}} = \ln \zeta_o^{\mathrm{UNIFAC}} \tag{2.1}$$

and

$$\ln \zeta_j^{\mathrm{SR}} = \ln \zeta_j^{\mathrm{UNIFAC}} - \ln \zeta_{j(s)}^{\mathrm{UNIFAC}} \tag{2.2}$$

where $\ln \zeta_{j(s)}^{\mathrm{UNIFAC}}$ is the activity coefficient of *j* at infinite dilution in solvent *s*; it normalizes $\ln \zeta_j^{\mathrm{UNIFAC}}$ from the pure compound reference state to an infinite dilution reference state. The group-dependent values for the UNIFAC volume parameter R_k and the surface area parameter Q_k used here are given in Table 2.S1.

2.2.2. Middle-range (MR) term

MR interactions are assumed to result from charge↔dipole interactions between ions and molecules, and charge↔induced dipole interactions between ions. The MR contribution to the ζ value for a specific group *k* within a solvent molecule is expressed as:

$$\ln\zeta_k^{\mathrm{MR}} = \sum_{\mathrm{ion}} B_{k,\mathrm{ion}} m_{\mathrm{ion}} - \frac{M_k}{M_{\mathrm{m}}} \sum_{l} \sum_{\mathrm{ion}} [B_{l,\mathrm{ion}} + IB'_{l,\mathrm{ion}}] x'_l m_{\mathrm{ion}} - M_k \sum_{c} \sum_{a} [B_{c,a} + IB'_{c,a}] m_c m_a \tag{2.3}$$

and for ion *j*:

$$\ln\zeta_j^{\mathrm{MR}} = \frac{1}{M} \sum_{l} B_{l,j} x'_l + \frac{z_j^2}{2M} \sum_{l} \sum_{\mathrm{ion}} B'_{l,\mathrm{ion}} x'_l m_{\mathrm{ion}} + \sum_{c} B_{c,a} m_c + \frac{z_j^2}{2} \sum_{c} \sum_{a} B'_{c,a} m_c m_a - \frac{1}{M_s} \sum_{l(s)} B_{l(s),j} \tag{2.4}$$

The summations in Eqs.(2.3-2.4) occur variously over: all ions (anions+cations) at molalities m_{ion}; all solvent groups with index *l*; all anions at their individual molality values m_{a}; all cations at their molalities m_{c}; and all solvent groups in solvent *s* with index *l*(*s*). M_{m} = mole-fraction average weight (g mol^{-1}) as averaged over all solvent groups; M_k = group weight (g mol^{-1}) of the specific solvent group *k* for which ζ_k^{MR} is being estimated; *I* = ionic strength; x'_l = "solvent group mole fraction" of group *l* (computed by including only solvent groups and no ions); *M* = mean molecular weight (g mol^{-1}) of the mixed solvents; z_j = the charge of *j* (e.g. ±1, ±2, etc.); $B_{l,\mathrm{ion}}$, $B_{\mathrm{c,a}}$, and $B_{l(s),j}$ = second virial coefficients; $B'_{l,\mathrm{ion}} = \partial B_{l,\mathrm{ion}}/\partial I$; $B'_{\mathrm{c,a}} = \partial B_{\mathrm{c,a}}/\partial I$; and M_s = molecular weight of the pure solvent *s* selected for the reference state (g mol^{-1}).

By GCM principles, the value of ζ_o^{MR} for solvent *o* can be assembled from the individual ζ_k^{MR} values:

$$\ln\zeta_o^{\mathrm{MR}} = \sum_{k} \nu_k^{(o)} \ln\zeta_k^{\mathrm{MR}} \tag{2.5}$$

where $\nu_k^{(o)}$ is the number of solvent groups of type *k* present in solvent *o* (e.g., 2 for CH_3 in acetone).

The expressions used by Yan et al. (1999) for the solvent group-ion second virial coefficient $B_{l,\mathrm{ion}}$ and the cation-anion second virial coefficient $B_{c,a}$ are

$$B_{l,\mathrm{ion}} = b_{l,\mathrm{ion}} + c_{l,\mathrm{ion}} \exp(-1.2I^{1/2} + 0.13I) \tag{2.6}$$

$$B_{c,a} = b_{c,a} + c_{c,a} \exp(-I^{1/2} + 0.13I) \tag{2.7}$$

where $b_{l,\mathrm{ion}}$ and $c_{l,\mathrm{ion}}$ are MR interaction parameters between the solvent group *l* and the ion; $b_{c,a}$ and $c_{c,a}$ are the MR interaction parameters between *c* and *a*. All MR interaction parameters are assumed symmetrical. For example, for the pair (l = 1, ion = 1), then $b_{l=1,\text{ion}=1} = b_{\text{ion}=1,\ l=1}$. MR interaction parameters are set to zero for interactions between groups or ions of the same kind (e.g. $b_{l=1,l=1} = 0$ and $b_{\text{ion}=1,\ \text{ion}=1} = 0$). Where possible, optimized values of MR parameters for Eqs. (2.6) and (2.7) were obtained from Yan et al. (1999). Because they were not addressed by Yan et al. (1999), MR parameters were optimized as discussed below for Ca^{2+}-COOH, Na^{+}-COOH, and Cl^{-}-COOH interactions based on available experimental data for relevant organic+salt+water solutions.

2.2.3. Long-range (LR) term

The LR ζ expressions for solvent *o* and ion *j* are

$$\ln \zeta_o^{\mathrm{LR}} = \frac{2A\mathrm{MW}_o\rho}{b^3\rho_o}\left[1+b\sqrt{I}-\frac{1}{1+b\sqrt{I}}-2\ln(1+b\sqrt{I})\right] \tag{2.8}$$

$$\ln \zeta_j^{LR} = z_j^2 A\frac{\sqrt{I}}{1+b\sqrt{I}} \tag{2.9}$$

where: MW_o (kg mol^{-1}) = molecular weight of *o*; ρ_o (kmol m^{-3}) = molar density of pure *o* as a liquid; ρ (kmol m^{-3}) = molar density of the solvent mixture at the composition of interest; $A = 1.327757 \times 10^5\ \rho^{1/2}/(\varepsilon T)^{3/2}$; $b = 6.359696\ \rho^{1/2}/(\varepsilon T)^{1/2}$; ε (dimensionless) = dielectric constant of the solvent mixture; T (K) = temperature. The density and the dielectric constant of a solvent mixture are estimated using the volume-fraction based mixing rules

$$\rho = \sum_o v_o\rho_o \tag{2.10}$$

$$\varepsilon = \sum_o v_o\varepsilon_o \tag{2.11}$$

where ε_o is the dielectric constant of pure solvent *o*; v_o is the salt-free volume fraction of solvent *o* in the solution according to

$$v_o = \frac{x'_o V_o}{\sum_q x'_q V_q} \tag{2.12}$$

x'_q is the mole fraction of solvent q (excluding ions) and V_q is the molar volume of solvent q. ρ_o and ε_o for pure compounds were obtained from Yaws (1999) and Wohlfarth (1995).

2.2.4. ζ Expressions for solvents and ions

The full ζ expression for solvent o is:

$$\ln \zeta_o = \ln \zeta_o^{\mathrm{SR}} + \ln \zeta_o^{\mathrm{LR}} + \ln \zeta_o^{\mathrm{MR}} \tag{2.13}$$

The assumed concentration scale for o is the mole fraction scale. The reference state for o is represented as: $x_o \rightarrow 1,\ \zeta_o \rightarrow 1$. The standard state is pure o at the system temperature and pressure. The component terms $\ln\zeta_o^{\mathrm{SR}}$, $\ln \zeta_o^{\mathrm{MR}}$, $\ln \zeta_o^{\mathrm{LR}}$ are computed based on Eqs. (2.1), (2.5), and (2.8) respectively.

The full ζ expression for ion j is:

$$\ln \zeta_j = \ln \zeta_j^{\mathrm{SR}} + \ln \zeta_j^{\mathrm{LR}} + \ln \zeta_j^{\mathrm{MR}} - \ln\left(\frac{M_s}{M_m} + M_s \sum_{ion} m_{ion}\right) \tag{2.14}$$

The assumed concentration scale for j is the molality scale. The reference state for j is represented as: $x_s \rightarrow 1,\ I \rightarrow 0,\ \zeta_j \rightarrow 1$. The standard state is j at unit molality in s behaving as an ideal dilute solution at the system temperature and pressure. Water is selected here as the reference state solvent s. The component terms $\ln\zeta_j^{\mathrm{SR}}$, $\ln \zeta_j^{\mathrm{MR}}$, $\ln \zeta_j^{\mathrm{LR}}$ are computed based on Eqs. (2.2), (2.4), and (2.9) respectively.

2.2.5. Mean ionic properties and solution electroneutrality

Although Eq. (2.14) gives ζ of each ion, ζ for cation or anion (ζ_+ or ζ_-) can not be measured individually. Hence, mean ionic activity coefficient, $\zeta_\pm$ is defined according to:

$$\zeta_\pm = \left(\zeta_+^{\nu_+} \zeta_-^{\nu_-}\right)^{\frac{1}{\nu_+ + \nu_-}} \tag{2.15}$$

where ν_+ and ν_- are stoichiometric coefficients for the salt dissociation reaction: $\mathrm{M}_{\nu_+}\mathrm{X}_{\nu_-} \rightarrow \nu_+\mathrm{M}^{z+} + \nu_-\mathrm{X}^{z-}$; ζ_+ and ζ_- are calculated based on Eq. (2.14). Similarly, mean ionic mole fraction, $x_\pm$, is defined as:

$$x_\pm = (x_+^{\nu_+} x_-^{\nu_-})^{\frac{1}{\nu_+ + \nu_-}} \tag{2.16}$$

The assumption of solution electroneutrality is used in the model and it is achieved by using mean ionic activity ($a_\pm$) defined by $a_\pm = \zeta_\pm x_\pm$. When using $a_\pm$, M^{z+} and X^{z-} are implicitly assumed "chemically linked" and therefore the solution net charge always remains zero.

2.2.6. Phase equilibrium and selection of standard state

Debye-Hückel theory can be used to estimate the LR contribution to ζ values. For a salt dissolved in a solvent mixture composed of organic compounds with water, the solvent mixture is considered to be equivalent to a single dielectric medium. The standard state for ion j is unit concentration in the mixed solvent, with the mixed solvent behaving as an ideal dilute solution. However, as mentioned above regarding Eq. 2.14, the standard state for j is unit concentration in water, with the water behaving as an ideal dilute solution. This seems to create a standard state discrepancy for an ion. Fortunately, as explained by Zerres and Prausnitz (1994), the problem can be resolved by assuming that only LR forces contribute to ζ_j^{LR}. In this manner, the two standard states can be assumed identical: the chemical potential of an ion in an ideal dilution solution of water is the same as that in an ideal dilute solution of a mixed-solvent solution, given that the concentrations of the ion are the same in both solutions. This concept enables us to select a unified standard state for an ionic species regardless the composition of the solvent medium the ions are in. The unified standard state is especially important when modeling phase equilibrium between multiple liquid phases. At phase equilibrium, equality of mean ionic activities ($a_\pm$) of an ion species in all liquid phases can establish, only when provided that standard states for that ion species in all liquid phases being identical.

2.3 Optimization of selected group interaction parameters for X-UNIFAC.2

A total of 234 MR interaction parameters were taken from Yan et al. (1999), the parameters having been obtained by fitting using a large data set with salt concentrations up to 22 molal. Six additional interaction parameters for Na^+-COOH, Cl^--COOH, and Ca^{2+}-COOH were obtained here by fitting 97 VLE data points from systems of the following types: acetic acid/$CaCl_2$/water; propionic acid/$CaCl_2$/water; and propionic acid/NaCl/water (Pereyra et al., 2001, Banat et al., 2002, and Banat et al., 2003). Both isobaric x-y-T data (29 points) involving measured solution-phase ζ values and isothermal x-y data (68 points) involving measured gas-phase mole fraction (y) values were used.

Parameter optimization (fitting) occurred by minimization of the objective function F_{obj}

$$F_{\text{obj}} = \sum_{n=1}^{97} \frac{\left| Q_n^{\text{exp}} - Q_n^{\text{pred}} \right|}{Q_n^{\text{exp}}} \tag{2.17}$$

which gives the sum of all relative error values. Q_n^{exp} is the measured value for a specific thermodynamic parameter (either a solvent solution-phase activity coefficient ζ or a solvent vapor mole fraction y) for data point n, and Q_n^{pred} is the corresponding predicted value based on the fitted values of all relevant b and c as indicated in Eqs.(2.6-2.7). For the isothermal x-y data, predicted y values were calculated using

$$y_o = \frac{\zeta_o \, x_o \, p_{\text{L},o}^{\text{o}}}{P} \tag{2.18}$$

$$P = \sum_o \frac{\zeta_o \, p_{\text{L},o}^{\text{o}}}{y_o} \tag{2.19}$$

where: P (Torr) is the total system pressure; x_o is the mole fraction of solvent o (including all solvents and all ions); ζ_o is calculated using Eq. (2.13); $p_{\text{L},o}^{\text{o}}$ (Torr) is the vapor pressure of pure liquid solvent o. The values of p_o^{o} for acetic acid and propionic acid were calculated using tabulated parameters for the Antoine Equation (McDonald et al., 1959; Dreisbach and Shader, 1949).

Optimization of F_{obj} involved 1000 sets of initial values for the six fitting parameters (b_{Na^+-COOH}, b_{Cl^--COOH}, $b_{Ca^{2+}-COOH}$, c_{Na^+-COOH}, c_{Cl^--COOH}, $c_{Ca^{2+}-COOH}$). For each of the first 500 sets, a single random number in the range -5.0 and 3.0 was assigned to all six parameters. For each of the second 500 sets, each of the six parameters was assigned a different random number from the same range. This range was selected because all *b* and *c* values reported by Yan et al. (1999) parameters fall in this range. Also, values outside this range tended to cause computational overflow. Each optimization run was carried out using Small Scale Solver DLL (Frontline Systems, Incline Village, NV), which utilizes the generalized reduced gradient method to seek the minimum on a multidimensional F_{obj} surface. The first partial derivative of F_{obj} was approximated by central differencing. The initial values for the parameters at the beginning of each one-dimensional line search were estimated by linear extrapolation. The Quasi-Newton method was used to approximate the Hessian of F_{obj} to determine the direction vector for the parameters being changed during a given iteration.

2.4 Applications of X-UNIFAC.2 to complex particulate matter systems

2.4.1. Model approaches

2.4.1.1. Equilibrium-phase (EP) modeling

In the EP model, aerosol PM may have either one or two liquid phases; two liquid phases occur when thermodynamic equilibrium for the PM indicates phase separation. Each organic compound and water distributes among the gas phase and liquid phase(s). If two liquid PM phases are present, each ion distributes between the two phases. Each salt ion is considered to be 100% non-volatile as well as 100% dissociated (including no involvement in ion pairing). X-UNIFAC.2 was used to predict all solution-phase activity coefficients.

In an adaptation of the approach of Pankow (1994b), the total mass concentration T_i (ng m^{-3}) of every component (volatilizable compound or ion) in the aerosol is expressed here as

$$T_i = A_i + D_i \qquad \text{with} \qquad D_i = \sum_{\theta} F_i^{\theta} \tag{2.20}$$

where: A_i (ng m^{-3}) is the gas-phase concentration of i; D_i (ng m^{-3}) is the total mass concentration of i associated with the PM; and F_i^{θ} (ng m^{-3}) is the mass concentration of i in phase θ. When there is a single PM phase, the phase index θ refers to that single phase; when phase separation occurs, then θ refers to either the α or β phase.

Based on the gas/particle partitioning constant K_p (m^3 μg^{-1}) for volatilizable compounds (Pankow, 1994a), A_i can be expressed as:

$$A_i = x_i^{\theta}\zeta_i^{\theta} p_{i,\mathrm{L}}^{\mathrm{o}} \mathrm{MW}_i (1.33\times10^{11})/(RT) \tag{2.21}$$

where: for i in phase θ, x_i^{θ} and ζ_i^{θ} are mole fraction and activity coefficient, respectively; R is the gas constant; T is temperature (K); and MW$_i$ (g mol^{-1}) is molecular weight of i. $p_{\mathrm{L},i}^{\mathrm{o}}$ (Torr) values were obtained using SPARC online calculator (Hilal et al., 1994). 1.33 x 10^{11} is a unit conversion factor.

For each ion, $D_i = T_i$ and thus is fixed. For all volatilizable components except water, T_i is specified, and thus governed by mass balance requirements. Based on Eqs. (2.20) and (2.21):

$$T_i - x_i^{\theta}\zeta_i^{\theta} p_{i,\mathrm{L}}^{\mathrm{o}} \mathrm{MW}_i (1.33\times10^{11})/(RT) - D_i \;=\; 0 \tag{2.22}$$

For water, instead of fixing T_i, RH is fixed so that in place of Eq.(2.22) we have:

$$\mathrm{RH}/100 - x_i^{\theta}\zeta_i^{\theta} = 0 \tag{2.23}$$

The solution process used here involved an iterative variation of the set of D_i for the volatilizable compounds in search of the set pertaining to the equilibrium corresponding to the set of T_i and the RH. For each iteration, an LLE flash calculation (Koak, 1997; von Bochove, 2003) was used with the guess set of D_i to obtain the corresponding values of F_i^{θ}, x_i^{θ}, and ζ_i^{θ} for all i and θ. The obtained values of x_i^{θ} and ζ_i^{θ} for the organic compounds and water were then utilized in Eqs. (2.22) and (2.23) in the given iteration.

A stability test based on the Gibbs tangent plane stability criterion (Michelsen, 1982) was included within the LLE flash calculation to check if a different number of phases would produce a more stable mixture. Within the LLE flash calculation, the equilibrium condition can be expressed as (Koak, 1997; von Bochove, 2003):

$$\sum_{\theta}(a_i^{\theta} - a_i^{\text{avg}} + \Theta^{\theta}) = 0 \qquad \text{with} \qquad a_i^{\text{avg}} = \sum_{\theta}\eta^{\theta} a_i^{\theta} \tag{2.24}$$

where a_i^{θ} is activity of i in θ (for ions, $a_{\pm}^{\theta}$ is used); a_i^{avg} is averaged activity coefficient of i over all liquid phases; $\Theta^{\theta} = RT\ln\sum_i X_i^{\theta}$ and is related to stability test wherein i denotes each PM component and X_i^{θ} is a composition variable (see Phoenix et al., 1998); η^{θ} is moles in θ over total moles in PM. The governing mass balance equations are (Koak, 1997; von Bochove, 2003):

$$\sum_{\theta}\eta^{\theta} x_i^{\theta} = w_i \qquad \text{and} \qquad 1 - \sum_i x_i^{\theta} = 0 \tag{2.25}$$

where w_i is the overall mole fraction of i associated with PM.

At equilibrium, TPM (μg m^{-3}) (the total suspended PM concentration) is given by:

$$\text{TPM} = \sum_{\theta}\text{TPM}^{\theta} \tag{2.26}$$

with

$$\text{TPM}^{\theta} = 10^{-3}\sum_i F_i^{\theta} \tag{2.27}$$

where TPM$^{\theta}$ (μg m^{-3}) is the contribution from the θ phase. Also,

$$\text{TPM} = M_{\text{o}} + M_{\text{w}} + M_{\text{salt}} \tag{2.28}$$

with

$$M_{\text{o}} = \sum_{\theta} M_{\text{o}}^{\theta}, \quad M_{\text{w}} = \sum_{\theta} M_{\text{w}}^{\theta}, \quad M_{\text{salt}} = \sum_{\theta} M_{\text{salt}}^{\theta} \tag{2.29}$$

M_{o} (μg m^{-3}) is the total organic mass concentration associated with the PM; M_{w} (μg m^{-3}) is the total PM water content; M_{salt} (μg m^{-3}) is the total salt content. M_{o}^{θ}, M_{w}^{θ}, and M_{salt}^{θ} (μg m^{-3}) are the mass concentrations in PM phase θ. Lastly,

$$M_{\text{o+w}} = \sum_{\theta} M_{\text{o+w}}^{\theta} = \sum_{\theta}(M_{\text{o}}^{\theta} + M_{\text{w}}^{\theta}) \tag{2.30}$$

Net change of PM mass, $\Delta M_{\text{o+w}}$ (μg m^{-3}), may be considered to be the result of net change in liquid water content and the formation of individual condensable oxidation products with stoichiometric yield factors α_i according to $T_i = 10^3\ \alpha_i\ \Delta\text{HC}$ (Odum1996). $\Delta M_{\text{o+w}}$ is defined as (Cocker et al., 2001):

$$\Delta M_{\text{o+w}} = M_{\text{o}} + \Delta M_{\text{w}} \tag{2.31}$$

where ΔM_{w} (μg m^{-3}) is the net change of liquid water mass concentration. When the initial seed aerosol is wet, ΔM_{w} is determined as the difference between the final total PM water content (M_{w}) and the water content of the initial seed ($M_{\text{w,seed}}$). Values for M_{w} were estimated by the model described above; values for $M_{\text{w,seed}}$ were estimated by means of the ZSR equation (Stokes and Robinson 1966):

$$M_{\text{w,seed}} = 10^9 \times \sum_e \frac{M_e}{m_{\text{o},e}(a_{\text{w}})} \tag{2.32}$$

where M_e (mol m^{-3}) is the volume concentration of salt e in air; and $m_{\text{o},\,e}(a_{\text{w}})$ is the molality (mol (kg water)$^{-1}$) of a solution containing only salt e and water that exhibits the water activity a_{w} for the RH of interest. Our applications of Eq. (2.32) only involved one salt at a time, either $CaCl_2$ or NaCl. The polynomial expressions of a_{w} vs. $m_{\text{o},\,e}$ in Table 2.1 near the temperatures of interest were obtained by fitting osmotic coefficient data for aqueous $CaCl_2$ solutions (Ananthaswamy and Atkison, 1985) and for NaCl solutions (Hubert at al., 1995).

2.4.1.2. One-phase (1P) modeling

In 1P modeling, the G/P partitioning is assumed to occur to PM that is one homogeneous liquid phase that includes all salt ions, all PM organic compounds, and all PM water. For a selected RH and a given set of T_i, when EP modeling also predicts one PM phase (i.e., no phase separation), the predictions of the two models will be identical. However, when EP modeling predicts two stables phases, then the results will be different from those predicted (incorrectly) by 1P modeling.

Assumption of a single PM phase is, and can be expected to continue to be, an attractive/simplified way to model atmospheric PM. 1P modeling was thus carried out here for comparison with the EP modeling results. As with the EP modeling, G/P partitioning was assumed to follow Eqs.(2.20-2.23) and (2.26-2.32). With only one phase, however, the LLE flash calculation was not necessary. X-UNIFAC.2 was used to predict all ζ values.

2.4.2. Systems studied

The EP and 1P approaches were each applied to two aerosol systems: 1) a hypothetical sabinene/O_3 system with NaCl seed aerosol; and 2) the experimental α-pinene/O_3 system studied by Cocker et al. (2001) using wet $CaCl_2$ seed aerosol. For each system, the PM formed, the phase composition(s) of the PM, the PM-phase activity coefficients, and the G/P distributions were predicted by both modeling approaches. The predicted $\Delta M_{\text{o+w}}$ values for the α-pinene/O_3 system were compared with the experimental values reported by Cocker et al. (2001).For the hypothetical sabinene/O_3 system, the assumed conditions are: ΔHC = 800 μg m^{-3}, M_{NaCl} ranging from 3 to 18 μg m^{-3}, T = 306 K, and RH = 80%. ($NaCl_{(s)}$ deliquesces at RH = 72% when T = 306 K.) For the α-pinene/O_3 system studied by Cocker et al. (2001), the conditions were: ΔHC = 406 to 1204 μg m^{-3}, M_{CaCl_2} = 17 to 32 μg m^{-3}, T = 302-303 K, and RH = 48 to 51%. ($CaCl_{2(s)}$ deliquesces at RH < 35% when $T \approx$ 302 K.) The values of the mass stoichiometric yield factors α_i for product formation from sabinene/O_3 and α-pinene/O_3 oxidation were assumed equal to those reported by Yu et al. (1999). For products not fully identified measured by Yu et al. (1999), the lumping method of Pankow et al. (2001) was used to obtain a single surrogate compound X with an appropriate structure and p_{L}^{o}. Table 2.2 summarizes the sabinene and α-pinene oxidation products. Measured ε_o values are not available for these compounds. An estimated ε_o value was therefore assigned to each product based on reported ε_o values for similar compounds. In particular, ε_o values for organic compounds with one or two carboxylic acid groups are typically ~2.5; ε_o values for compounds with one hydroxyl, aldehyde, or ketone group are typically less than 20 (Wohlfarth, 1995). In all simulations it was assumed that compound volatility was not altered due to the Kelvin Effect (surface tension). For particles with smaller diameters, Kelvin Effect can be an important factor in determining final PM concentrations. Unfortunately, neither experimental data nor predictive models for surface tension of pure atmospheric organics are currently available. Moreover, the lack the theory to describe the mixing effects on surface tension of a multi-component PM makes the consideration of Kelvin effect in the current modeling not feasible.

2.5 Results

2.5.1. Parameter optimization

The optimized values of the MR interaction parameters *b* and *c* are given in Table 2.3. For each data set used in the optimization, the average unsigned fractional error ($\overline{\mathrm{err}}$) was calculated according to

$$\overline{\mathrm{err}} = \frac{\sum_{k}^{n} \{ \left| Q_k^{\exp} - Q_k^{calc} \right| / Q_k^{\exp} \}}{n} \tag{2.33}$$

where *n* is the number of data points in a specific data set. Values of $\overline{\mathrm{err}}$ for the isothermal *x-y* data sets are generally lower than that for the isobaric *x-y-T* data set (see Table 2.4). For all 97 data points, $\overline{\mathrm{err}}$ = 0.06, indicating a good overall fit, especially given the fact that only six MR interaction parameters were varied during the optimization, 20 having been set equal to the previously optimized values of Yan et al. (1999) (Table 2.3).

2.5.2. Sabinene/O$_3$ with $\Delta HC = 800\ \mu g\ m^{-3}$, $M_{NaCl} = 2.9$ to $17.5\ \mu g\ m^{-3}$, RH = 80%.

2.5.2.1. EP model results

Phase compositions. EP modeling predicted that two liquid PM phases would be present over the entire M_{NaCl} range. PM composition results are provided in Fig. 2.1.a for $M_{\mathrm{NaCl}} = 17.5\ \mu\mathrm{g\ m}^{-3}$. For that case, the mostly aqueous (α) phase contains nearly all of the NaCl and only a small fraction of the OPM, and the mostly organic (β) phase contains nearly all of the OPM, and only small fractions of the PM water and M_{NaCl}. The organic compounds are largely excluded from the α phase. The converse is also true.

Mass concentrations. Predicted values for $M_{\mathrm{o}}^{\alpha+\beta}$, $M_{\mathrm{w}}^{\alpha+\beta}$, $M_{\mathrm{o+w}}^{\alpha+\beta}$ by EP modeling as functions of M_{NaCl} are given in Fig. 2.2. M_{w}^{α}, M_{w}^{β}, M_{o}^{α}, and M_{o}^{β} as functions of M_{NaCl} are given in Fig. 2.3. $M_{\mathrm{o+w}}^{\alpha+\beta}$ increases with increasing M_{NaCl} due to increasing values of $M_{\mathrm{w}}^{\alpha+\beta}$ (the $M_{\mathrm{o}}^{\alpha+\beta}$ values remain nearly constant). Because the large ζ_{Na^+} and ζ_{Cl^-} in the β phase essentially limit Na^+ and Cl^- to the α phase, increasing M_{NaCl} has little effect on either M_o^β or M_w^β. With M_o^α very small for all M_{NaCl} considered, one net result is constancy in $M_o^{\alpha+\beta}$. On the other hand, increasing M_{NaCl} increases M_w^α because RH is assumed held constant, and with M_w^β relatively small, the net result is increasing $M_w^{\alpha+\beta}$. Though small in absolute terms, M_o^α does increase with increasing M_{NaCl} because of the increasing size of that phase per m^3.

*Effects of the PM concentration (*Λ, mols m^{-3}*) and of the activity coefficients (ζ).* Based on a consideration of absorptive gas/particle partitioning theory (Pankow, 1994a), the mol-based concentration of PM phase θ in the aerosol is defined here as

$$\Lambda^\theta\ (\text{mols m}^{-3}) \quad = \quad \text{TPM}^\theta \Big/ (10^6\,\overline{\text{MW}}^\theta) \tag{2.34}$$

so that the particle to gas mass-concentration ratio for compound *i* condensing into phase θ is given by

$$\frac{F_i^\theta}{A_i} \quad = \quad 760RT\Lambda^\theta \frac{1}{\zeta_i^\theta p_{L,i}^o} \tag{2.35}$$

The effects of increasing M_{NaCl} on Λ^α and Λ^β obtained by the EP model are illustrated in Fig. 2.4; the effects on ζ_i^α and ζ_i^β for norsabonic acid (as an example organic compound) and for water are illustrated in Fig. 2.5. The exclusion of Na^+ and Cl^- from the β phase cause ζ_i^β of each organic compound as well as Λ^β to remain largely unchanged as M_{NaCl} increases. With Λ^β remaining nearly constant, M_o^β remains nearly constant. For the α phase, Λ^α increases with increasing M_{NaCl} because the constant RH requires near constancy in the concentrations of Na^+ and Cl^-. The increases in M_o^α are thus due almost entirely to the increases in Λ^α (all ζ_i^α values are largely unaffected given near constancy in the Na^+ and Cl^- concentrations).

2.5.2.2. 1P model results

As noted above, when the EP model predicts two stables phases, then the results will be different from those predicted (incorrectly) by the 1P model (Fig. 2.2). With the entire M_{NaCl} range considered here characterized by two PM phases, we can consider the error magnitudes associated with assuming one phase. With the 1P model underpredicting both M_{o} and M_{w}, the errors are negative (Fig. 2.6). The errors initially become more severe with increasing M_{NaCl} because the assumption of a single phase worsens the amount of salt increases: the ζ values of the organic compounds increase (Fig. 2.5). Then, as M_{NaCl} increases above 10 μg m^{-3} the errors begin to decrease because the system is moving back towards stability as a single phase: the increasing size of the α phase would eventually allow that phase to accommodate enough of the organic mass that a separate primarily-organics phase cannot form.

2.5.3. Comparison of EP and 1P model predictions for chamber data obtained in the α-pinene/O$_3$ system studied by Cocker et al. (2001)

Phase stability. Four cases involving wet $CaCl_2$ seed were derived from Cocker et al. (2001) and modeled using both the EP and 1P approaches (Table 2.5). EP modeling predicted two stable PM phases in Cases 1 and 2 (and therefore more PM formation than from 1P modeling). For Cases 3 and 4, EP modeling predicted one stable PM phase (with compositions and PM amounts therefore identical to those from 1P modeling). Fig. 2.7 utilizes Case 2 to provide an example of the differences in the PM composition between the EP and 1P model results when two PM phases are stable.

Overall mass concentrations. Predicted M values for water and total organics for Cases 1-4 are given in Table 2.5. Predicted and measured $\Delta M_{\mathrm{o+w}}$ values vs. ΔHC are given in Fig. 2.8. (Note: $\Delta M_{\mathrm{o+w}} = \Delta M^{\alpha+\beta}_{\mathrm{o+w}}$ when two phases are stable.) By EP modeling, the prediction error for $\Delta M_{\mathrm{o+w}}$ is 24 to 37% for Cases 1-2 (two stable phases), and only 1 to 4% for Cases 3 and 4 (one stable phase). That the errors for Cases 1-2 are larger than for the other two cases may partially be a consequence of the fact that two liquid PM phases necessarily means that the required activity corrections are more extreme and thus more subject to error. In addition, there will be greater reliance on accurate α_i factors for HC oxidation product formation. Nevertheless, given the extent of the assumptions that were required, the EP modeling results obtained here agree quite well with the measured results of Cocker et al. (2001). And, while verification of the actual existence of two PM phases in systems such as Cases 1-2 will require further experimental work, the results obtained here indicate that neglecting phase separation when it occurs can result in significant prediction errors.

Individual compound mass concentration. Fig. 2.9 uses Case 2 to provide an example of the differences between EP and 1P modeling for predicted F_i values. When two PM phases are stable, we define the compound-dependent error:

$$\Delta F_{\mathrm{P},i} = F_{i,\mathrm{EP}} - F_{i,\mathrm{1P}} \tag{2.36}$$

For the most volatile compounds (norpinonaldehyde and pinonaldehyde), $\Delta F_{\mathrm{P},i}$ values are not significant because only very small amounts are present in the PM regardless of whether EP or 1P modeling is conducted. And, $\Delta F_{\mathrm{P},i}$ values for the least volatile compounds (pinic acid, hydroxy pinonic acid, and X) are small because nearly 100% of their T_i values are assigned to the PM regardless of whether EP or 1P modeling is conducted. In contrast, $\Delta F_{\mathrm{P},i}$ is significant (11,000 to 27,000 ng m^{-3}) for the compounds of intermediate volatility (hydroxy pinonaldehyde, norpinonic acid, and pinonic acid); most of the underprediction of PM observed for 1P modeling is due to the underprediction for those compounds.

2.6 Conclusions

X-UNIFAC.2 has been developed as a useful tool for predicting activity coefficient (ζ) values of organic compounds, a number of salt ions, and water when modeling the formation of complex atmospheric PM. (As usual, any such modeling effort requires good input information regarding the identities and stoichiometric yield factor (α_i) values for the organic products from the oxidation of parent hydrocarbons.) Because the ζ values of some organic compounds can become large in the presence of salt ions and water (and vice versa), it is necessary to consider the possibility of phase separation in these types of PM systems, and the X-UNIFAC.2 model was found to have adequate prediction range to allow consideration of PM that simultaneously contains large mass fractions of organic compounds, certain salt ions, and water. Good prediction was obtained for the amount of PM formed in selected α-pinene/O_3 chamber experiments conducted by Cocker et al. (2001); in several of the cases, the presence of two liquid PM phases was predicted.

Modeling PM formation by forcing a single PM phase when two PM phases is the preferred state necessarily leads to an underprediction in PM formation. The extent of the expected error was examined for several α-pinene/O_3 cases considered by Cocker et al. (2001), and for several hypothetical sabinene/O_3 cases. Errors in total PM formed as large as 50% can be expected.

2.7 References

Ananthaswamy, J., Atkinson, G., 1985. Thermodynamics of concentrated electrolyte mixtures. 5. A review of the thermodynamic properties of aqueous calcium chloride in the temperature range 273.15–373.15 K. Journal of Chemical Engineering Data 30, 120-128.

Banat, F., Al-Asheh, S., Simandl, J., 2002. Effect of dissolved inorganic salts on the isothermal vapor-liquid equilibrium of the propionic acid-water mixture. Chemical Engineering and Processing 41, 793-798.

Banat, F., Al-Asheh, S., Simandl, J., 2003. Vapor-liquid equilibria of propionic acid-water system in the presence of different types of inorganic salts: effect of temperature and salt concentration. Chemical Engineering and Processing 42, 917-923.

Chan, M. N., Chan, C. K., 2003. Hygroscopic properties of two model humic-like substances and their mixtures with inorganics of atmospheric importance. Environmental Science & Technology 37, 5109-5115.

Chan, M. N., Choi, M.Y., Ng, N. L., Chan, C. K., 2005. Hygroscopicity of water-soluble organic compounds in atmospheric aerosols: Amino acids and biomass burning derived organic species, Environmental Science & Technology 39, 1555-1562.

Clegg, S. L., Seinfeld, J. H., Brimblecombe, P., 2001. Thermodynamic modeling of aqueous aerosols containing electrolytes and dissolved organic compounds. Journal of Aerosol Science 32, 713-738.

Cocker, D. R., Clegg, S. L., Flagan, R. C., Seinfeld, J. H., 2001. The effect of water on gas-particle partitioning of secondary organic aerosol. Part I: α-pinene/ozone system. Atmospheric Environment 35, 6049-6072.

Dreisbach, R. R., Shrader, S. A., 1949. Vapor pressure-temperature data on some organic compounds. Industrial Engineering Chemistry. 41, 2879-2880.

Erdakos, G. B., Asher, W. E., Seinfeld, J. H. Pankow, J. F., 2006. X-UNIFAC.1: A method for predicting activity coefficients of neutral compounds in liquid aerosol particles containing organic compounds, dissolved inorganic salts, and water. Atmospheric Environment (in press).

Fredenslund, A., Jones, R. L., Prausnitz, J. M., 1975. Group-contribution estimation of activity coefficients in non ideal liquid mixtures. American Institute of Chemical Engineers Journal 21, 1086-1099.

Griffin, R. J., Nguyen, K., Dabdub, D., Seinfeld, J. H., 2003. A combined hydrophobic-hydrophilic module for predicting secondary organic aerosol formation. Journal of Atmospheric Chemistry 44, 171-190.

Hilal, S. H., Carreira, L. A., Karickhoff, S. W., 1994. Estimation of chemical reactivity parameters and physical properties of organic molecules using SPARC. In: Murray, P.P.a.J.S.(Ed.), Quantitative Treatments of Solute/Solvent Interactions. Elsevier, Amsterdam.

Hansen, H. K., Rasmussen, P., Fredenslund, A., Schiller, M., Gmehling, J., 1991. Vapor-liquid equilibria by UNIFAC group contribution. 5. Revision and extension. Industrial & Engineering Chemistry Research 30, 2352-2355.

Hubert, N., Gabes, Y., Bourdet, J., Schuffenecker, L., 1995. Vapor pressure measurements with a nonisothermal static method between 293.15 and 363.15 K for electrolyte solutions. Application to the H_2O + NaCl system. Journal of Chemical Engineering Data 40, 891-894.

Kikic, I., Fermeglia, M., 1991. UNIFAC prediction of vapor-liquid equilibria in mixed solvent-salt systems. Chemical Engineering Science 46, 2775-2780.

Koak, N., 1997. Polymer Solution Phase Behavior, Ph.D. Dissertation. University of Calgary, Calgary, Canada.

Marcolli, C., Luo, B., Peter, T., 2004. Mixing of the organic aerosol fractions: liquids as the thermodynamically stable phases. Journal of Physical Chemistry A 108, 2216-2224.

McDonald, R. A., Shrader, S. A., Stull, D.R., 1959. Vapor pressures and freezing points of 30 organics, Journal of Chemical Engineering Data 4, 311-313.

Michelsen, M. L., 1982. The isothermal flash problem. Part I. Stability. Fluid Phase Equilibria 9, 1-19.

Middlebrook, A. M., Murphy, D. M., Thomson, D. S., 1998. Observations of organic material in individual marine particles at Cape Grim during the first aerosol characterization experiment (ACE 1). Journal of Geophysical Research 103, 16475-16483.

Ming, Y., Russell, L. M., 2002. Thermodynamic equilibrium of organic-electrolyte mixtures in aerosol particles. American Institute of Chemical Engineers Journal 48, 1331-1348.

Odum, J. R., Hoffmann, T., Bowman, F., Collins, D., Flagan, R. C., Seinfeld, J. H., 1996. Gas/particle partitioning and secondary organic aerosol yields. Environmental Science & Technology 30, 2580-2585.

Pankow, J. F., 1994a. An absorption model of gas/particle partitioning of organic compounds in the atmosphere. Atmospheric Environment 28, 185-188.

Pankow, J. F., 1994b. An absorption model of the gas/aerosol partitioning involved in the formation of secondary organic aerosol. Atmospheric Environment 28, 189-193.

Pankow, J. F., Seinfeld, J. H., Asher, W. E., Erdakos, G. B., 2001. Modeling the formation of secondary organic aerosols. 1. Theory and measurements for the α-pinene-, β-pinene-, sabinene-, Δ3-carene, and cyclohexene-ozone systems. Environmental Science & Technology 35, 1164-1172. See also Errata 2001, Environmental Science & Technology 35, 3272.

Pereyra, C., de la Ossa, E. M., 2001. A semiempirical equation for vapor-liquid equilibrium in water-acetic acid-calcium chloride systems. Journal of Chemical Engineering Data 46, 188-192.

Phoenix, A. V., Heidemann, R. A., 1998. A non-ideal multiphase chemical equilibrium algorithm. Fluid Phase Equilibria 150-151, 255-265.

Pun, B. K., Griffin, R. J., Seigneur, C., Seinfeld, J. H., 2002. Secondary organic aerosol 2. Thermodynamic model for gas/particle partitioning of molecular constituents. Journal of Geophysical Research 107, 10.1029/2001JD000542.

Raatikainen, T., Laaksonen, A., 2005. Application of several activity coefficient models to water-organic-electrolyte aerosols of atmospheric interest. Atmospheric Chemistry and Physics Discussions 5, 3641-3699.

Saxena, P., Hildemann, L. M., 1996. Water-soluble organics in atmospheric particles: A critical review of the literature and application of thermodynamics to identify candidate compounds. Journal of Atmospheric Chemistry 24, 57-109.

Saxena, P., Hildemann, L. M., 1997. Water adsorption by organics: survey of laboratory evidence and evaluation of UNIFAC for estimating water activity. Environmental Science & Technology 31, 3318-3324.

Seinfeld, J. H., Erdakos, G. B., Asher, W. E., Pankow, J. F., 2001. Modeling the formation of secondary organic aerosols. 2. The predicted effects of relative humidity on aerosol formation in the α-pinene-, β-pinene-, sabinene-, Δ3-carene, and cyclohexene-ozone systems. Environmental Science & Technology 35, 1806-1817.

Stokes, R. H., Robinson, R. A., 1966. Interactions in aqueous nonelectrolyte solutions. I. Solute-solvent equilibria. Journal of Physical Chemistry 70, 2126-2131.

van Bochove, G. H., 2003. Two- and three-liquid phase equilibria in industrial mixed-solvent electrolyte solutions: experiments and modeling of systems of importance for the extraction of caprolactam, Ph.D. Dissertation. Delft University Press, Delft, Netherlands.

Wohlfarth, C., 1995. Temperature dependence of the permittivity (dielectric constant) of liquids. In: Lide, D.R. (Editor-in-Chief), CRC Handbook of Chemistry and Physics. CRC Press, Boca Raton.

Yaws, C. L., 1999. Chemical Properties Handbook: Physical, Thermodynamic, Environmental, Transport, Safety, and Health Related Properties for Organic and Inorganic Chemicals, McGraw-Hill, New York.

Yan, W., Topphoff, M., Rose, G., Gmehling, J., 1999. Prediction of vapor-liquid equilibria in mixed-solvent electrolyte systems using the group contribution concept. Fluid Phase Equilibria 162, 97-113.

Yu, J., Cocker, D. R., Griffin, R. J., Flagan, R. C., Seinfeld, J. H., 1999. Gas-phase ozone oxidation of monoterpenes: gaseous and particulate products. Journal of Atmospheric Chemistry 34, 207-258.

Zerres, H., Prausnitz., J. M., 1994. Thermodynamics of phase equilibria in aqueous-organic systems with salt. American Institute of Chemical Engineers Journal 40, 676-691.

2.8 Acknowledgements

This work was supported by the Electric Power Research Institute, and by National Science Foundation grant ATM-0513492.

Table 2.1. Fitted cubic equation parameters ($b, c, d,$ and e) for $m_{\mathrm{o},e}$ vs. a_{w} according to:

$m_{\mathrm{o},e}(a_{\mathrm{w}}) = b\, a_{\mathrm{w}}^3 + c\, a_{\mathrm{w}}^2 + d\, a_{\mathrm{w}} + e$

Solution	T (K)	b	c	d	e	R^2
NaCl + H_2O §	304	-43.042	89.569	-81.631	35.108	0.9999
$CaCl_2$ + H_2O †	303	-28.391	54.592	-42.035	15.88	0.9996

§Data obtained from Hubert et al. (1995). † Data obtained from Ananthaswamy and Atkison (1985)

Table 2.2. Stoichiometric yield factors (α_i), liquid vapor pressures (p_L^o), densities (ρ_o), and dielectric constant (ε_o) of the oxidation products in the two studied systems.

Product	α_i [a]	p_L^o [b] (Torr)	ρ_o [b] (g ml^{-1})	ε_o [c]
Sabinene/O_3 system				
NaCl (3-18 μg m^{-3}), RH: 80%, ΔHC: 800 μg m^{-3}, T: 306 K				
S_5(2-2(isopropyl)-2-formyl-cyclopropyl-methanoic acid)	0.003	3.17×10^{-5}	1.050	15
hydroxysabina ketone	0.4729	1.01×10^{-3}	1.045	15
sabina ketone	0.0793	2.01×10^{-1}	0.929	15
norsabinonic acid	0.0588	1.52×10^{-5}	1.026	2.5
norsabinic acid	0.0032	2.02×10^{-7}	1.114	2.5
sabinic acid	0.0164	1.68×10^{-8}	1.087	2.5
pinic acid	0.0191	3.55×10^{-8}	1.104	2.5
S_{10}(1-(2-isopropyl)-3-(1-oxo-2-hydroxy-ethyl)-cyclopropyl-ethanoic acid)	0.0021	2.14×10^{-9}	1.111	15
X [d]	0.0001	1.00×10^{-12}	1.025	15
α-pinene/O_3 system				
$CaCl_2$ (17-32 μg m^{-3}), RH: 48-51%, ΔHC: 406-1204 μg m^{-3}, $T \approx$ 302 K				
norpinonaldehyde	0.0208	1.74×10^{-1}	0.966	15
pinonaldehyde	0.1458	4.63×10^{-2}	0.946	15
hydroxy pinonaldehyde	0.0762	2.29×10^{-4}	1.043	15
norpinonic acid	0.1129	8.17×10^{-6}	1.039	2.5
norpinic acid	0.0012	7.50×10^{-6}	1.125	2.5
pinonic acid	0.0568	2.22×10^{-6}	1.020	2.5
pinic acid	0.0661	2.10×10^{-6}	1.107	2.5
hydroxy pinonic acid	0.0397	2.03×10^{-6}	1.127	2.5

Table 2.3. Fitted middle range interaction parameters $b_{k,\mathrm{ion}}$, $c_{k,\mathrm{ion}}$, $b_{c,a}$, and $c_{c,a}$

	$b_{k,\mathrm{ion}}$			$c_{k,\mathrm{ion}}$		
Main group	Na^+	Cl^-	Ca^{2+}	Na^+	Cl^-	Ca^{2+}
CH_2	-0.2698	0.2971	-0.8179	-0.3446	0.343	-1.1583
OH	0.1252	-0.1575	0.0160	0.5979	-0.3737	2.5117
CH_3OH	-0.5567	0.527	-1.6630	0.5044	-0.3825	0.573
H_2O	-0.2571	0.1284	-0.7894	-0.0239	0.0196	-0.0491
CHO	0[a]	0[a]	0[a]	0[a]	0[a]	0[a]
CH_2CO	-0.3507	0.5569	0[a]	0.5511	-1.1024	0[a]
COOH	-0.9048[b]	0.1230[b]	-1.3469[b]	1.3085[b]	0.9020[b]	-1.9639[b]
Salt	$b_{c,a}$	$c_{c,a}$				
NaCl	0.2111	-0.0910				
$CaCl_2$	0.6406	-0.5258				

Source: Yan et al. (1999) unless otherwise indicated:

[a] Not available and set to zero in this work.

[b] Optimized by this work.

Table 2.4. Averaged unsigned fractional errors ($\overline{\mathrm{err}}$) from parameter optimization using vapor-liquid equilibrium (VLE) experimental data sets.

Solution	Number of data points	Temperature (K)	Salt molality	Data type	$\overline{\mathrm{err}}$
acetic acid-water-$CaCl_2$ [a]	29	377-398	0.9-2.3	Isobaric x- y-T	0.10
propionic acid-water-$CaCl_2$ [b]	25	313-333	0.2-1.0	Isothermal x, y	0.06
propionic acid-water-NaCl [b]	43	313-333	0.2-2.0	Isothermal x, y	0.03
				overall $\overline{\mathrm{err}}$	: 0.06

[a] Pereyraet al. (2001). [b] Banat et al. (2002) and Banat et al. (2003).

Table 2.5. Comparison of EP model and 1P model predictions and the measured results for α-pinene/O_3 chamber experiment.

					Initial	Final						Net change				
Case	ΔHC (μg/m^3)	T (K)	RH (%)	$CaCl_2$ (μg/m^3)	$M_{w,seed}$ (μg/m^3)	M_o (μg/m^3)		M_w (μg/m^3)		M_{o+w} (μg/m^3)		ΔM_{o+w} (μg/m^3)			Error in ΔM_{o+w} (%)	
					ZSR*	EP	1P	EP	1P	EP	1P	Measured§	EP	1P	EP	1P
1	406.0	301.5	49.2	30	46	81	50	48	29	129	79	60	82	32	+36.6	-46.3
2	628.2	301.5	50.0	32	56	145	81	72	43	217	124	130	162	68	+24.2	-47.9
3	933.9	302.0	47.5	17	31	234	234	14	14	248	248	215	217	217	+1.2	+1.2
4	1204.3	302.0	51.2	18	29	321	321	14	14	335	335	295	306	306	+3.7	+3.7

Numbers of liquid phases predicted by EP model are: two for Case1 and 2, and one for Case 3 and 4. *Estimated based on aqueous $CaCl_2$ data (Ananthaswamy and Atkison, 1985). §Measured by Cocker et al. (2001).

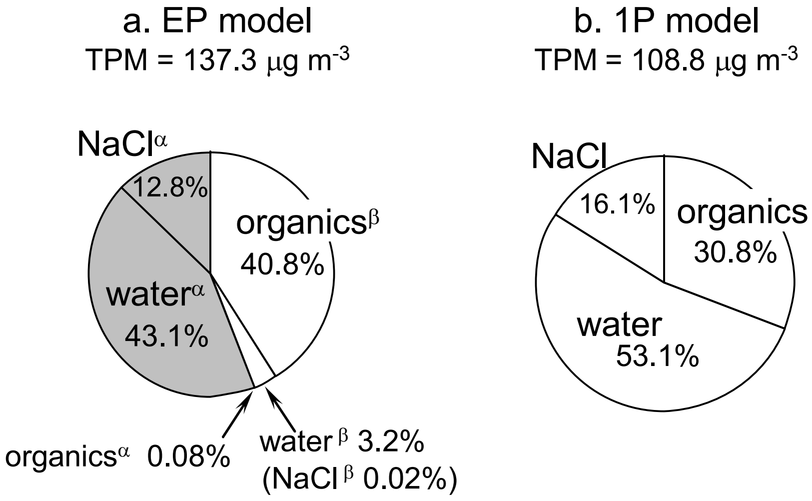

Figure 2.1. Comparison of PM mass distributions predicted by equilibrium-phase (EP) modeling and one-phase (1P) modeling in a sabinene/O_3 system (ΔHC = 800 μg m^{-3}, T = 306 K, RH = 80%, and M_{NaCl}= 17.5 μg m^{-3}). α = mostly aqueous PM phase; β = mostly organic PM phase.

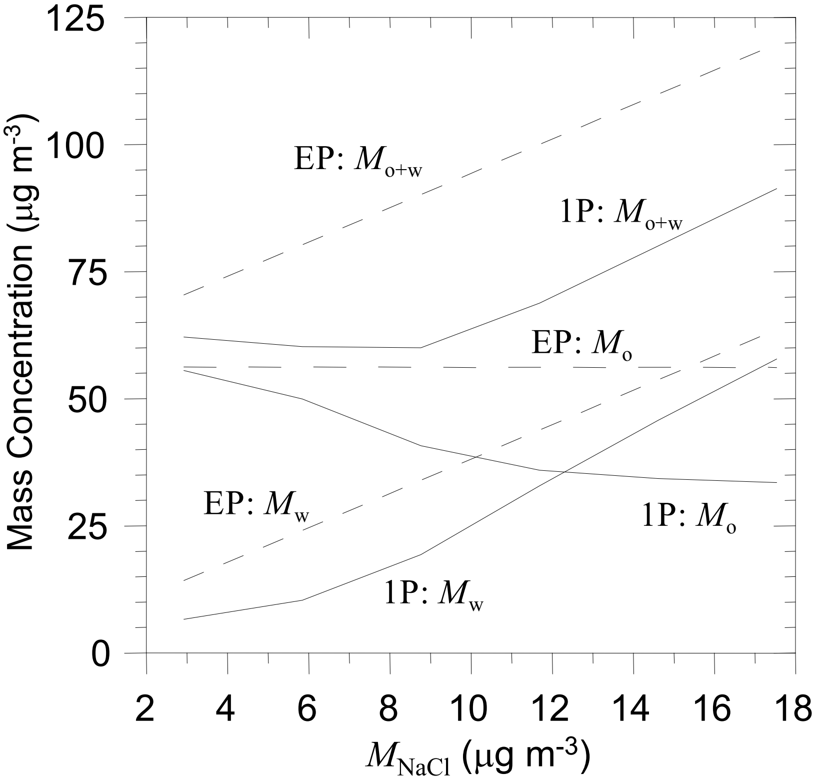

Figure 2.2. Organic mass concentrations (M_o), final PM water content (M_w), and total mass concentrations (M_{o+w}) in a sabinene/O_3 system, all as functions of M_{NaCl} as predicted by both equilibrium-phase (EP) and one-phase (1P) modeling (ΔHC = 800 µg m^{-3}, T = 306 K, RH = 80%). Note: for the EP results, $M_o = M_o^{\alpha+\beta}$, $M_w = M_w^{\alpha+\beta}$, and $M_{o+w} = M_{o+w}^{\alpha+\beta}$. α = mostly aqueous PM phase; β = mostly organic PM phase.

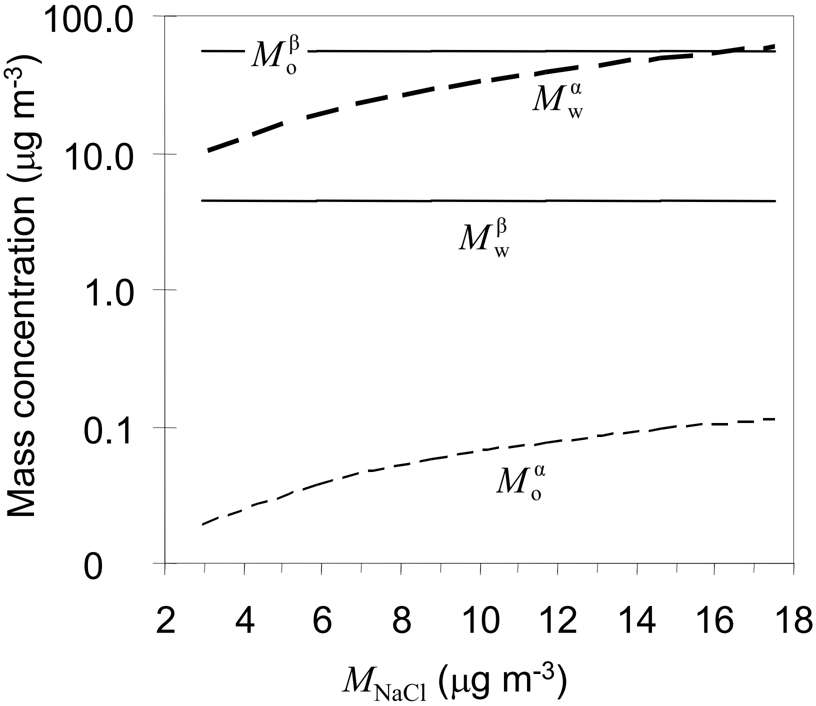

Figure 2.3. Phase-specific mass concentrations predicted by equilibrium-phase (EP) modeling for PM water concentration (M_w^α, M_w^β) and organic mass concentration (M_o^α, M_o^β) all as functions of M_{NaCl} in a sabinene/O_3 system (ΔHC = 800 µg m^{-3}, T = 306 K and RH = 80%). α = mostly aqueous PM phase; β = mostly organic PM phase.

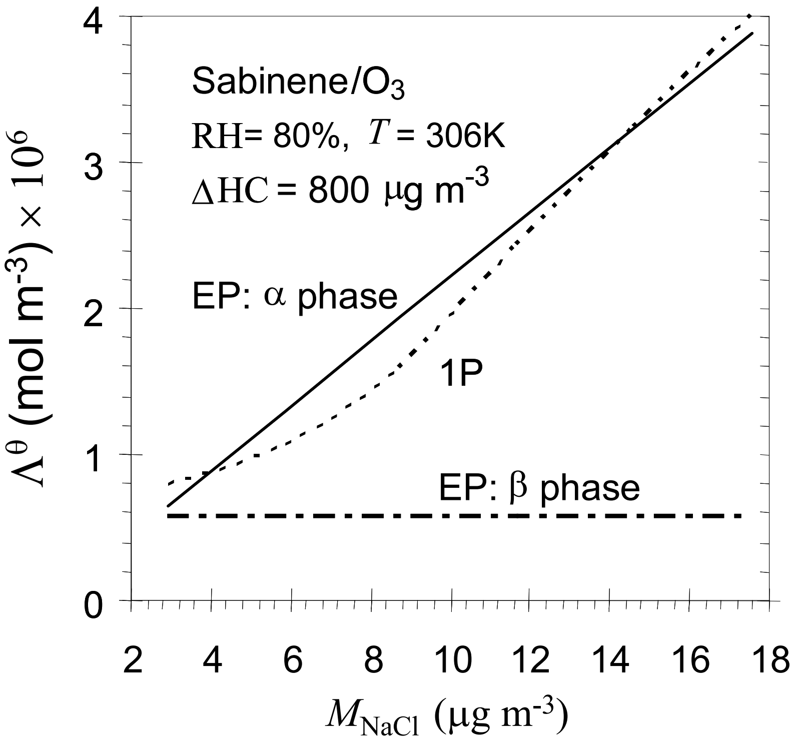

Figure 2.4. Mol-based concentrations of PM phases (Λ^{θ}) vs. M_{NaCl} in a sabinene/O_3 system ($\Delta\mathrm{HC}$ = 800 μg m^{-3}, T = 306 K and RH = 80%) as predicted by equilibrium-phase (EP) and one-phase (1P) modeling. For EP modeling, two liquid PM phases are predicted over the entire M_{NaCl} range. α = mostly aqueous PM phase; β = mostly organic PM phase.

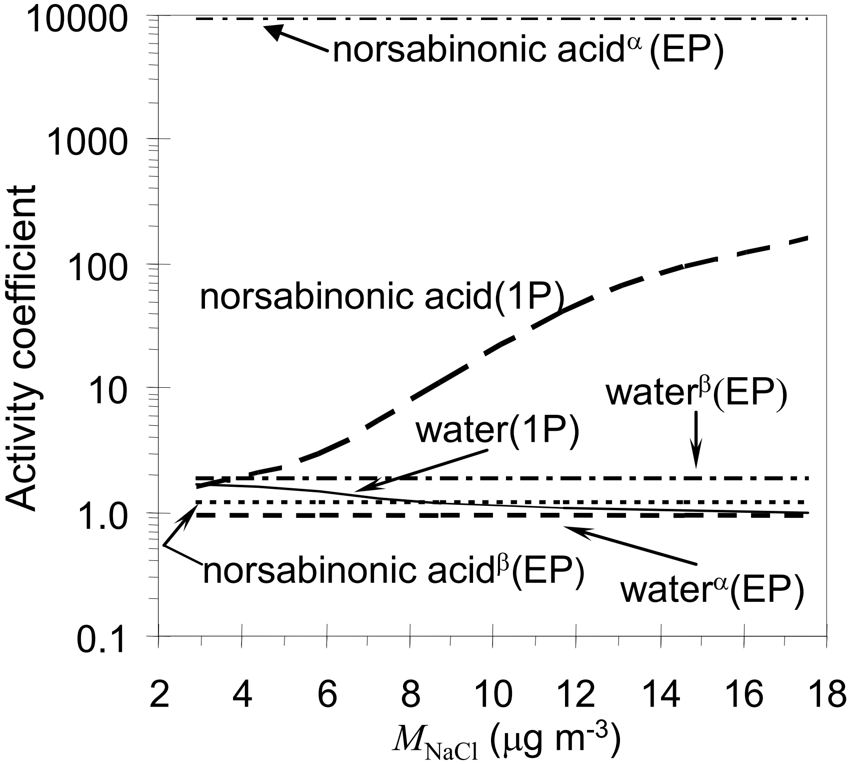

Figure 2.5. Activity coefficients of water and norsabinonic acid as predicted by equilibrium-phase (EP) modeling and one-phase (1P) modeling, all as functions of M_{NaCl} in a sabinene/O$_3$ system (ΔHC = 800 μg m^{-3}, 306 K, and RH = 80%). For EP modeling, two liquid PM phases are predicted over the entire M_{NaCl} range. α = mostly aqueous PM phase; β = mostly organic PM phase.

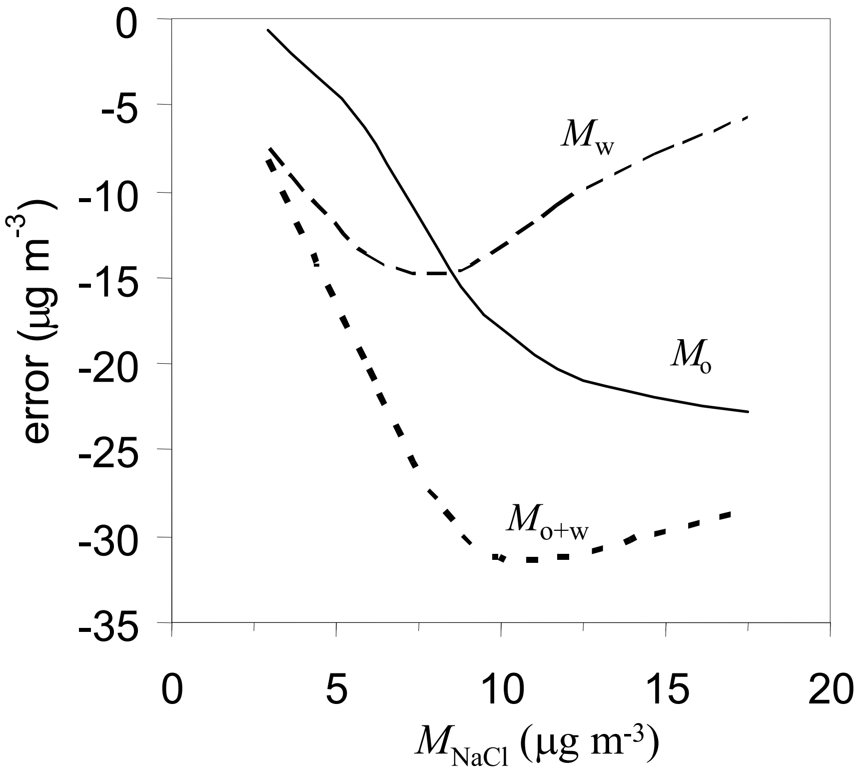

Figure 2.6. Predicted errors for M_o, M_w, M_{o+w} vs. M_{NaCl} due to assumption of one PM phase in a sabinene/O$_3$ system (ΔHC = 800 μg m^{-3}, T = 306 K, and RH = 80%).

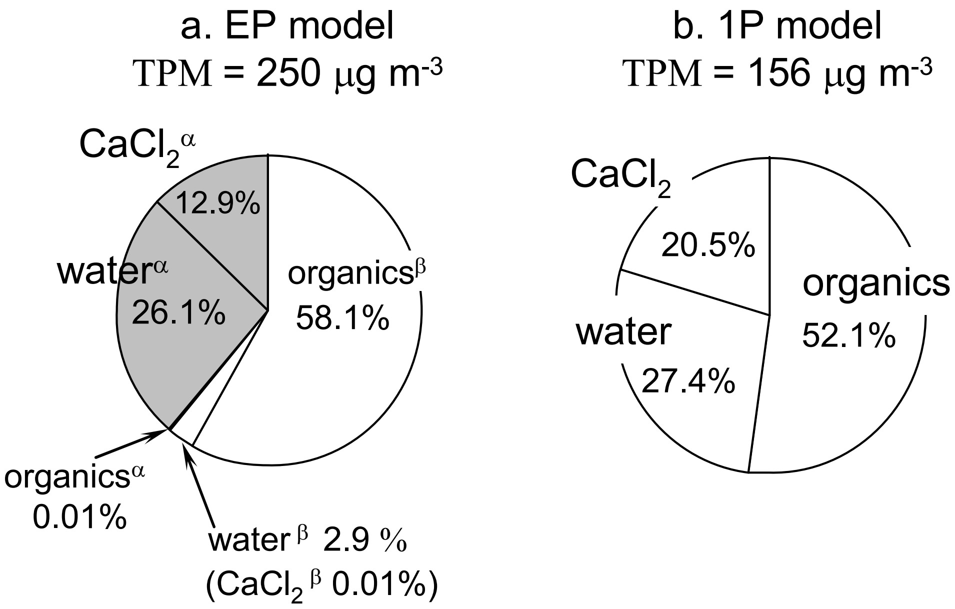

Figure 2.7. Comparison of PM mass distributions predicted by equilibrium-phase (EP) modeling and one-phase (1P) modeling in an α-pinene/O$_3$ system (ΔHC = 628 μg m^{-3}, T = 301.5 K, RH = 47.5%, $M_{\mathrm{CaCl_2}}$ = 32.2 μg m^{-3}). α = mostly aqueous PM phase; β = mostly organic PM phase.

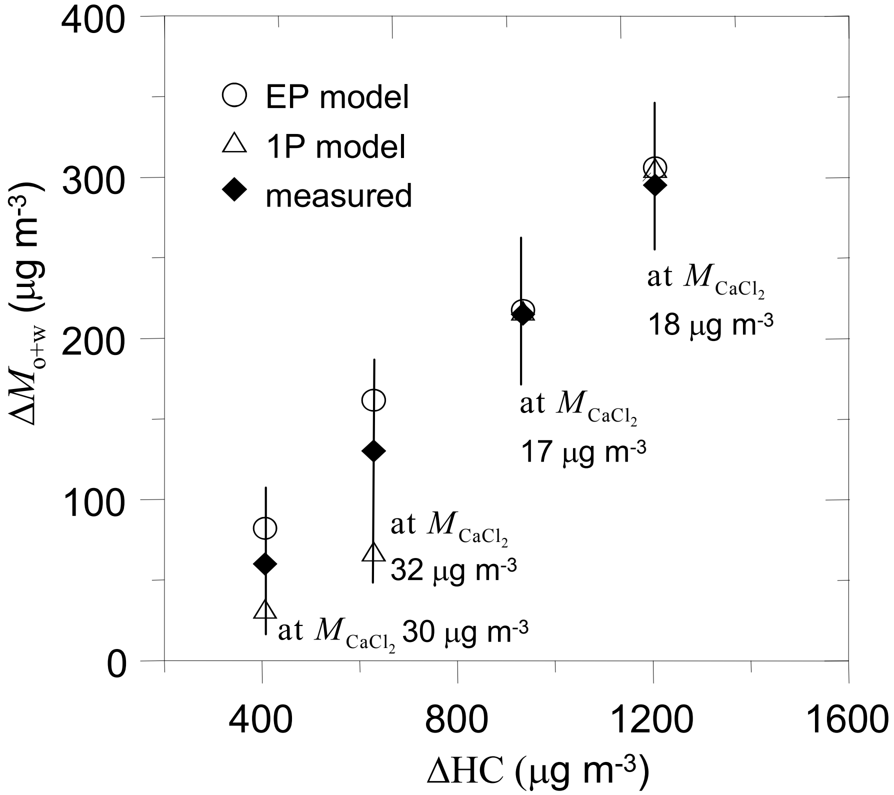

Figure 2.8. Change in total PM mass concentration (ΔM_{o+w}) as predicted by EP modeling and by 1P modeling, together with corresponding measured values of Cocker et al. (2001) for four cases involving α-pinene/O$_3$. Note: for the EP modeling results, $M_{o+w} = M_{o+w}^{\alpha+\beta}$.

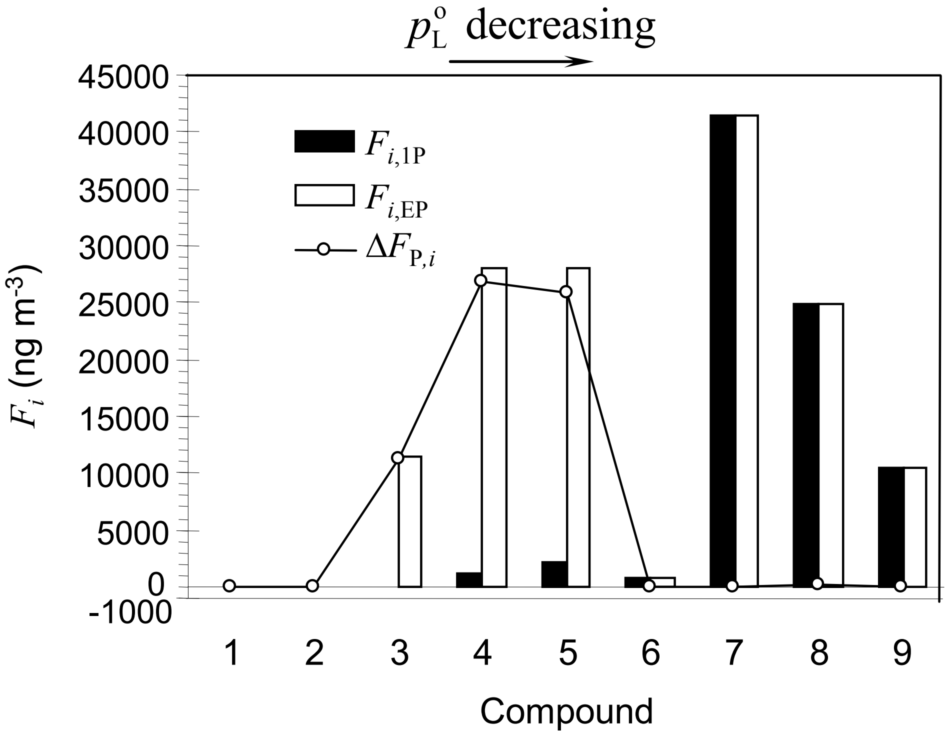

Figure 2.9. Compound F_i values by EP and 1P modeling together with the EP minus 1P model difference ($\Delta F_{i,P}$) values for Case 2 in the α-pinene/O$_3$ system (ΔHC = 628 μg m^{-3}, T = 301.5K, RH = 47.5%, M_{CaCl_2} = 32.2 μg m^{-3}). Compound key: 1 = norpinonaldehyde, 2 = pinonaldehyde, 3 = hydroxy pinonaldehyde, 4 = norpinonic acid, 5 = pinonic acid, 6 = norpinic acid, 7 = pinic acid, 8 = hydroxy pinonic acid, 9 = compound "X".

Table S2.1. Relative van der Waals group volume (R_k) and surface area(Q_k) parameters

Solvent group[a]	R_k	Q_k
CH_3	0.9011	0.848
CH_2	0.6744	0.54
CH	0.4469	0.228
OH	1.0000	1.200
CH_3OH	1.4311	1.432
H_2O	0.9200	1.400
CH_3CO	1.6724	1.488
CH_3COO	1.9031	1.728
COOH	1.3013	1.224
Ion[b]	**R_k**	**Q_k**
Na^+	3.0000	3.000
Ca^{2+}	1.0000	1.000
Cl^-	0.9861	0.992

[a]Hansen et al. (1991). [b]Yan et al. (1999)

Figure S2.1. Present status of interaction parameter availability for X-UNIFAC.2

X 21 UNIFAC parameters published by Hansen et al.

O 234 middle range parameters published by Yan et al.

\# Six middle range parameters fitted in this study

▨ Not available

	group																												
1	CH_2																												
2	OH	X																											
3	CH_3OH	X	X																										
4	H_2O	X	X	X																									
5	CH_2CO	X	X	X	X																								
6	CH_3COOH	X	X	X	X	X																							
7	CCOO	X	X	X	X	X	X																						
8	CH_2O	X	X	X	X	X	X	X																					
9	Li^+	O	O	O	O	O	▨	▨	▨																				
10	Na^+	O	O	O	O	▨	O	▨	#	▨																			
11	K^+	O	O	O	O	O	O	O	▨	▨	▨																		
12	NH_4^+	O	O	O	▨	▨	▨	▨	▨	▨	▨	▨																	
13	Ca^{2+}	O	O	O	O	▨	▨	▨	#	▨	▨	▨	▨																
14	Mg^{2+}	O	▨	▨	▨	▨	▨	▨	▨	▨	▨	▨	▨	▨															
15	Ba^{2+}	O	O	O	O	▨	▨	▨	▨	▨	▨	▨	▨	▨	▨														
16	Sr^{2+}	O	O	O	O	▨	▨	▨	▨	▨	▨	▨	▨	▨	▨	▨													
17	Cu^{2+}	O	O	▨	O	▨	▨	▨	▨	▨	▨	▨	▨	▨	▨	▨	▨												
18	Zn^{2+}	O	O	O	O	O	O	▨	▨	▨	▨	▨	▨	▨	▨	▨	▨	▨											
19	Co^{2+}	O	O	▨	O	▨	▨	▨	▨	▨	▨	▨	▨	▨	▨	▨	▨	▨	▨										
20	Ni^{2+}	O	O	▨	O	▨	▨	▨	▨	▨	▨	▨	▨	▨	▨	▨	▨	▨	▨	▨									
21	Hg^{2+}	O	O	O	O	▨	▨	▨	▨	▨	▨	▨	▨	▨	▨	▨	▨	▨	▨	▨	▨								
22	F^-	O	O	O	▨	▨	▨	▨	▨	▨	O	O	▨	▨	▨	▨	▨	▨	▨	▨	▨	▨							
23	Cl^-	O	O	O	O	O	O	▨	#	O	O	O	O	O	O	O	O	O	O	O	O	O	▨						
24	Br^-	O	O	O	O	O	▨	▨	▨	O	O	O	▨	▨	O	▨	▨	▨	▨	▨	▨	▨	▨	▨					
25	I^-	O	O	O	O	O	▨	▨	▨	▨	O	O	O	▨	▨	▨	▨	▨	▨	▨	▨	▨	▨	▨	▨				
26	NO_3^-	O	O	O	O	▨	▨	▨	▨	▨	O	O	▨	O	▨	O	O	▨	▨	▨	▨	▨	▨	▨	▨	▨			
27	$CH3COO^-$	O	O	O	O	▨	▨	▨	▨	▨	O	O	▨	▨	▨	▨	▨	▨	▨	▨	▨	▨	▨	▨	▨	▨	▨		
28	SCN^-	O	▨	O	▨	O	O	▨	▨	▨	O	▨	▨	▨	▨	▨	▨	▨	▨	▨	▨	▨	▨	▨	▨	▨	▨	▨	
		1	2	3	4	5	6	7	8	9	10	11	12	13	14	15	16	17	18	19	20	21	22	23	24	25	26	27	28

CHAPTER 3

Organic Particulate Matter at Varying Relative Humidity Using Surrogate Primary and Secondary Organic Compounds with a Method Based on the Wilson Equation for Activity Corrections in the Condensed Phase

3.1 Introduction

A significant fraction of the fine particulate matter (PM) in the atmosphere can be organic in nature, and so that fraction is of interest for visibility, health effect, and climate effect reasons (Mazurek et al., 1997; Pope, 2000; Bates et al., 2006). Organic PM (OPM) is always a complex mixture, and usually contains compounds loosely categorized as primary organic aerosol (POA) compounds and secondary organic aerosol (SOA) compounds. OPM can also contain compounds that have been formed by a variety of accretion reactions in which reactive SOA and POA compounds combine to yield products of appreciable molecular weight and low vapor pressure (Kalberer et al., 2004; Barsanti and Pankow; 2004, 2005, 2006).

Absorptive gas/particle (G/P) partitioning may be parameterized according to the model of Pankow (1994a). In the case of one absorbing phase within the PM, for compound i the equilibrium partitioning constant $K_{\mathrm{p},i}$ (m^3 μg^{-1}) is given by

$$K_{\mathrm{p},i} = \frac{c_{\mathrm{p},i}}{c_{\mathrm{g},i}} = \frac{RT\,f}{10^6\,\overline{\mathrm{MW}}\,\zeta_i\,p^{\mathrm{o}}_{\mathrm{L},i}} \qquad (3.1)$$

where: $c_{\mathrm{p},i}$ = P-phase concentration (ng μg^{-1}); $c_{\mathrm{g},i}$ = G-phase concentration (ng m^{-3}); R is the gas constant (8.2×10^{-5} m^3 atm mol^{-1} K^{-1}); T (K) = temperature; f is the weight fraction of the PM that is the absorbing phase (often taken to be unity for OPM calculations); $\overline{\mathrm{MW}}$ (g mol^{-1}) = mean molecular weight of the absorbing phase; $p^{\mathrm{o}}_{\mathrm{L},i}$ (atm) = vapor pressure of i; and ζ_i = mole-fraction-based activity coefficient of i. $K_{\mathrm{p},i}$ values generally depend strongly on T because $p^{\mathrm{o}}_{\mathrm{L},i}$ is usually a strong function of T. Significant temporal and spatial variations in $K_{\mathrm{p},i}$ values can also be caused by variations in ζ_i and $\overline{\mathrm{MW}}$ due to changes in the types and levels of the compounds (including water) in the P phase mixture.

Many of the applications of the Pankow (1994a,b) model for predicting secondary OPM formation in the atmosphere have been based on the "two-product" simplification of Odum et al. (1996). This implementation acknowledges that a parent hydrocarbon (HC, e.g. toluene, α-pinene, etc.) will be oxidized to a range of secondary products, but assumes that the mix of products can be represented using up to two hypothetical "lumped" surrogate compounds. For each parent HC, yield and compound characteristics for two lumped compounds are obtained by fitting chamber yield data to four-parameters: two stoichiometric formation α_i factors and two $K_{\mathrm{p},i}$ values (with one lumped product, one α_i and one $K_{\mathrm{p},i}$ value are invoked). With ΔHC (μg/m^3) giving the amount of reacted HC, for each of the lumped products, the total (G+P) amount formed is assumed to be given by $\mathcal{T}_i = \alpha_i \Delta\mathrm{HC}$ (μg/m^3).

Many two-product parameters obtained have been acquired in a chamber at a single temperature and under "dry" conditions (i.e., very low relative humidity (RH)). Extrapolations of $K_{\mathrm{p},i}$ values for a given OPM composition to another temperature under dry conditions have proceeded using the Clausius-Clapeyron equation with an estimate of the enthalpy of vaporization ($\Delta H_{\mathrm{vap},i}$) for each hypothetical lumped product. Utilizing chamber data in a theoretical consideration of the effects of RH is more difficult, and is a topic of this work.

In a chamber study of the oxidation of a mix of parent HCs, Odum et al. (1997) sought to predict the amount of OPM formed by using the collection of two-product α_i and $K_{\mathrm{p},i}$ values measured for oxidation of the individual parent HCs. This approach implicitly assumes similarity in both the MW and the polarity characteristics of all the various two-product compounds so that in the OPM formed from all mixes of parent

HCs, $\overline{\mathrm{MW}}$ remains approximately constant and all $\zeta_i \approx 1$. Pankow and Barsanti (2007) have designated this the "N•2p approach"; its range of applicability in the atmosphere remains uncertain, but nevertheless the N•2p approach has been widely utilized in the prediction of secondary OPM levels in the ambient atmosphere (e.g., Hoffman et al., 1997; Kanakidou et al., 2000; Pun et al., 2001;Tsigaridis and Kanakidou, 2003).

The computational advantage of the N•2p approach in 3-D air quality models (e.g., as in MADRID 1 as described by Pun et al., 2001) may be understood as follows. Any multi-component G/P model requires an iterative solution to determine the PM composition and level at each point in space and time. The N•2p approach assumes a limited number of secondary products, and provides a fixed $K_{\mathrm{p},i}$ value for each i for each iteration cycle at the T of interest. In contrast, if the $K_{\mathrm{p},i}$ values were allowed to vary because of dependence of the ζ_i and $\overline{\mathrm{MW}}$ on PM composition, then each solution within the series of solutions performed during each iteration cycle would require added computation time to estimate the ζ_i and $\overline{\mathrm{MW}}$ for the PM phase. Bowman and Melton (2004) compare the computational requirements of a number of ζ_i prediction methods, including the UNIFAC method of Fredenslund et al. (1975).

Parent HCs considered in the MADRID 1 model are known to produce oxidation products with a range of polarities. For example, α-pinene quickly leads to products like hydroxyacids and diacids that contain significant polarity, while humulene initially leads to products of considerably lower polarity. The current assumption within MADRID 1 that all $\zeta_i = 1$ for the OPM from all mixes of parent HCs is thus problematic. Moreover, the assumption that the organic portion of the PM formed is essentially free of water will certainly be in error whenever a significant portion of the PM is comprised of relatively high polarity compounds, and the RH is not low. In such circumstances, RH-driven water uptake into the PM phase can occur, further affecting ζ_i values (especially of the lower polarity products), and the value of $\overline{\mathrm{MW}}$. (A consideration of the potential magnitude of the effects of changing RH on PM levels at high ΔHC values (244 to 501 $\mu\mathrm{g\ m^{-3}}$) is provided by Seinfeld et al. (2001) for the ozone oxidation of several different biogenic HCs as well as cyclohexene.) Also, increasing RH levels will increase the likelihood of phase separation in the PM, especially whenever the OPM contains significant mass fractions of both SOA and POA compounds: the generally significant polarities of the former contrast with the generally low polarities of the latter (e.g., as with long chain alkanes and PAHs). When phase separation does occur, a phase index θ is needed, with $\theta = \alpha$ referring to a relatively more polar, hydrophilic phase (α mnemonically suggesting "aqueous"), and $\theta = \beta$ referring to the relatively less polar, less hydrophilic phase (Erdakos and Pankow, 2004). When the possibility of variation in the ζ_i and $\overline{\mathrm{MW}}$ and the possibility of phase separation are added to the $N{\bullet}2\mathrm{p}$ approach, the result is referred to as the "$(N{\bullet}2\mathrm{p})^{\zeta,\overline{\mathrm{MW}},\theta}$ approach" (Pankow and Barsanti, 2007).

With a superscript * used to denote a value determined under particular chamber conditions with a specific parent HC, Bowman and Karamalegos (2002) employ Eq.(3.1) to extrapolate a $K^*_{\mathrm{p},i}$ to different conditions. In the 2p view, the OPM formed from a given parent HC could be composed of significant amounts of both lumped compounds. Thus, given the level of approximation already allowed in that view, it may be reasonable to assume that $\zeta^*_i \approx 1$ for both products in that OPM. For partitioning to a significantly different type of OPM, however, it may be that $\zeta_i \neq 1$. Thus, with $\overline{\mathrm{MW}}$ and T also subject to variation, a $K^*_{\mathrm{p},i}$ value may be extrapolated using the ratios: a) $\zeta^*_i/\zeta_i \approx 1/\zeta_i$; b) $\overline{\mathrm{MW}}^*/\overline{\mathrm{MW}}$; c) T/T^*; and d) $p^{\mathrm{o}}_{\mathrm{L},i}(T^*)/p^{\mathrm{o}}_{\mathrm{L},i}(T)$. Assuming that $\Delta H_{\mathrm{vap},i}$ is constant over the temperature interval of interest (i.e., from T^* to T), correction for the effect of T on $p^{\mathrm{o}}_{\mathrm{L},i}$ occurs according to the integrated Clausius-Clapeyron equation which gives $p^{\mathrm{o}}_{\mathrm{L},i}(T^*)/p^{\mathrm{o}}_{\mathrm{L},i}(T) = \exp[\Delta H_{\mathrm{vap},i}(1/T - 1/T^*)]$. Assuming that $f = 1$, the overall result is (Bowman and Karamalegos, 2002)

$$K_{\mathrm{p},i}(T, x_i, x_2, x_3, \ldots x_n) = K^*_{\mathrm{p},i}\left(\frac{\overline{\mathrm{MW}}^*}{\overline{\mathrm{MW}}}\right)\left(\frac{1}{\zeta_i}\right)\left(\frac{T}{T^*}\right)\exp\left[\frac{\Delta H_{\mathrm{vap},i}}{R}\left(\frac{1}{T}-\frac{1}{T^*}\right)\right] \quad (3.2)$$

where $K_{\mathrm{p},i}(T, x_i, x_2, x_3, \ldots x_n)$ here denotes that $K_{\mathrm{p},i}$ depends on T and on the PM composition, the latter being characterized by the set of mole fraction values x_j. Eq.(3.2) has been applied in global modeling of SOA in the troposphere by Tsigaridis and

Kanakidou (2003), with the needed ζ_i values estimated using the Wilson (1964) equation. However, while Tsigaridis and Kanakidou (2003) demonstrate the computational practicality of using Eq.(3.2) in a large-scale 3-D model with the Wilson equation used for the ζ_i corrections, the Wilson equation parameters were assigned without regard to probable compound structure and functionality.

This work has four goals: 1) assign reasonable, specific surrogate structures to 25 lumped secondary compounds pertaining to a range of parent HCs of interest, and to 15 surrogate primary OPM compounds; 2) develop and implement a Wilson-equation-based group contribution method for prediction of ζ_i values for use with the 40 surrogate compounds that is computationally more economical than UNIFAC; 3) relax four key assumptions of the $N\bullet 2\mathrm{p}$ approach (all $\zeta_i = 1$; no RH effects; $\overline{\mathrm{MW}}$ = constant; and a single OPM phase) thereby permitting use of the $(N\bullet 2\mathrm{p})^{\zeta,\overline{\mathrm{MW}},\theta}$ approach; then 4) use the $(N\bullet 2\mathrm{p})^{\zeta,\overline{\mathrm{MW}},\theta}$ approach to calculate OPM formation in selected cases using: a) experimentally determined or estimated values of the $K^*_{\mathrm{p},i}$; b) Eq.(3.2); c) the assigned chemical structures; and d) the ζ_i prediction method developed here. For comparison, calculations were also made using the $N\bullet 2\mathrm{p}$ approach.

3.2 Method

3.2.1. Partitioning SOA Compounds

A total of 25 lumped secondary products were considered to arise from a total of 14 HC oxidation processes. Based on Odum et al. (1997), Griffin et al. (1999), Pun et al.(2003), Henze et al. (2006), and Griffin (2007), 11 of the processes assume two lumped products, and three of the processes (β-pinene reacting with NO_3 radical, humulene reacting with OH radical, and an *n*-alkane (C_{16}) reacting with OH radical) assume one lumped product each. Reaction 13 (2-ring PAH with OH) and Reaction 14 (C_{16} *n*-alkane with OH) were included as representative secondary reactions involving intermediate volatility parent HC compounds. Table 3.1 summarizes the information on the final set of the 40 surrogate compounds considered (25 lumped secondary products and 15 primary compounds).

As noted above, if ζ_i values are to be estimated in a mixture of interest, specific structural information is required for the compounds in the mixture. Griffin (2007) and our study here considered known gas phase reaction mechanisms and kinetics (Griffin et al., 1999, 2002a, 2002b, 2003; Surratt et al., 2006) to obtain the assignments for each lumped secondary product used in Table 3.1 for: 1) number of carbon atoms $\nu_{\mathrm{C},i}$; 2) whether cyclic or acyclic; (3) whether aromatic; and 4) retention (or not) of a double bond found in the parent HC. As summarized in Eq.(3.5) below, a corresponding initial estimate of MW_i was then assigned herein for each lumped product compound. Then, as summarized in Eq.(3.6) below, an initial estimate of $\overline{\mathrm{MW}}^*$ was computed as the mean of the MW_i estimates for the lumped products (two or one) from a given HC oxidation reaction (for two lumped products, this is equivalent to assuming that the OPM is a 1:1 molar mixture of the two products). An initial estimate of each $\log_{10} p^{\mathrm{o}}_{\mathrm{L},i}(T^*)^{\mathrm{chamber}}$ was then obtained as summarized in Eq.(3.7) below, i.e., as based on Eq.(3.1) and $K^*_{\mathrm{p},i}(T^*)$ at T^* using the $\overline{\mathrm{MW}}^*$ estimate and assuming $\zeta^*_i \approx 1$ for each lumped product (see discussion preceding Eq.(3.2)).

With the task denoted in Eq.(3.7) below completed, an approximation of the specific functionality was needed for each of the 25 surrogate secondary compounds (ultimately, for use as input to the ζ_i prediction method). The approach taken was to utilize known relationships between $p^{\mathrm{o}}_{\mathrm{L},i}$ values and structure. For organic compounds, $p^{\mathrm{o}}_{\mathrm{L},i}$ values decrease as $\nu_{\mathrm{C},i}$ increases, and as compound polarity increases. In the SIMPOL.1 group-contribution model for prediction of $p^{\mathrm{o}}_{\mathrm{L},i}$ (atm) values, Pankow and Asher (2007) write

$$\log_{10} p^{\mathrm{o}}_{\mathrm{L},i}(T) = \sum_k \nu_{k,i} b_k(T) \qquad k = 0,1,2,3,\text{ etc.} \tag{3.3}$$

where: $\nu_{k,i}$ is the number of groups of type k in compound i; $b_k(T)$ is the T-dependent contribution to $\log_{10} p^{\mathrm{o}}_{\mathrm{L},i}(T)$ from one group of type k. Eq.(3.3) provides a means to assemble the aggregate effects of structure on $p^{\mathrm{o}}_{\mathrm{L},i}(T)$. SIMPOL.1 utilizes a zeroeth group ($k = 0$), with $\nu_{0,i} = 1$ for all i and $b_0(293.15) = 1.99$. The $k = 1$ group pertains to molecular carbon; e.g., for hexane, $\nu_{1,i} \equiv \nu_{\mathrm{C},i} = 6$. Because $b_1(293.15) \equiv b_{\mathrm{C}}(293.15) = -0.47$, within any given compound class, $p^{\mathrm{o}}_{\mathrm{L},i}$ values decrease by ~½ order of magnitude for every unit increase in carbon number. And, $p^{\mathrm{o}}_{\mathrm{L},i}$ can also be decreased for a given carbon skeleton by adding polar functional groups. Eq.(3.3) may thus be re-written as

$$\log_{10} p^{\mathrm{o}}_{\mathrm{L},i}(T) = \nu_{0,i} b_k(T) + \nu_{\mathrm{C},i} b_{\mathrm{C}}(T) + \omega_i(T) \tag{3.4}$$

wherein all the structural aspects beyond carbon number are placed in the term $\omega_i(T)$. With $\nu_{0,i} = 1$ and using the assumed value of $\nu_{\mathrm{C},i}$, then $p^{\mathrm{o}}_{\mathrm{L},i}(T^*)^{\mathrm{chamber}}$ allows an estimate of $\omega_i(T^*)^{\mathrm{chamber}}$ (see also Eq.(3.8) below). Four groups are of special interest: hydroxyl ($b_7(293.15) \equiv b_{\mathrm{OH}}(293.15) = -2.29$); aldehyde ($b_8(293.15) \equiv b_{\mathrm{CHO}}(293.15) = -1.06$); ketone ($b_9(293.15) \equiv b_{\mathrm{CO}}(293.15) = -0.99$); and carboxylic acid ($b_{10}(293.15) \equiv b_{\mathrm{COOH}}(293.15) = -3.59$). Thus, for example, the conversion of cyclohexene to adipic acid is accompanied by about a seven order of magnitude drop in $\log_{10} p^{\mathrm{o}}_{\mathrm{L},i}(293.15)$.

Compound-to-compound differences in polarity are the primary drivers of differences among the ζ_i values in a mixture. Considering the groups that contribute significantly to $\omega_i(T)$ by adding polarity to a molecule (e.g., the four groups noted above, nitrate (ONO_2), nitrite (NO_2)), as well as other structural groups assumed to be retained from the parent HC (e.g., rings), the goal was to manually vary the $\nu_{k,i}$ to obtain an estimate of $\omega_i(T^*)^{\mathrm{fitted}}$ that would match $\omega_i(T^*)^{\mathrm{chamber}}$ (see Eq.(3.9)). The goal was to thereby derive a reasonable approximation of the functionality for each surrogate lumped secondary product for subsequent use in ζ_i prediction. Each resulting new $\nu_{k,i}$ set (including $\nu_{\mathrm{C},i}$) implied a new MW_i for the lumped product. When executed in concert with the other lumped product (if it exists) from each particular parent HC, as summarized in Eq.(3.10) below the process led to updated estimates of the MW_i and $\overline{\mathrm{MW}}^*$. Consequently, the approach used led naturally to an iterative process producing a possible best-fit $\nu_{k,i}$ set for each lumped product.

The overall scheme by which the values of each $\nu_{k,i}$ set were assigned is summarized below. (The character "→" should be read as "gives".)

$$\boxed{\nu_{\mathrm{C},i}} \rightarrow \mathrm{MW}_i \tag{3.5}$$

$$\mathrm{MW}_i \rightarrow \overline{\mathrm{MW}}^{*} \text{ estimated as the simple mean of the } \mathrm{MW}_i \text{ values from Eq.(3.5)} \tag{3.6}$$

$$\overline{\mathrm{MW}}^{*} \text{ with } \boxed{K^{*}_{\mathrm{p},i}(T^{*})} \rightarrow \text{estimate of } p^{\mathrm{o}}_{\mathrm{L},i}(T^{*})^{\mathrm{chamber}} \text{ by Eq.(3.1), with } \boxed{\zeta^{*}_{i} = 1} \tag{3.7}$$

$$p^{\mathrm{o}}_{\mathrm{L},i}(T^{*})^{\mathrm{chamber}} \text{ with } \boxed{\nu_{0,i} \text{ and } \nu_{\mathrm{C},i}} \rightarrow \omega_i(T^{*})^{\mathrm{chamber}} \text{ by Eq.(3.4)} \tag{3.8}$$

$$\omega_i(T^{*})^{\mathrm{chamber}} \rightarrow \text{fitted } \nu_{k,i} \text{ set} \rightarrow \omega_i(T^{*})^{\mathrm{fitted}} \text{ by inverse application of Eq.(3.4)} \tag{3.9}$$

$$\text{fitted } \nu_{k,i} \text{ set (including } \boxed{\nu_{\mathrm{C},i}}\text{)} \rightarrow \mathrm{MW}_i \tag{3.10}$$

iterate

Boxed values represent quantities that were held fixed during the iteration. A set of preliminary structures for the 25 SOA surrogate compounds obtained prior to full convergence of the process is given in the Supplementary Materials. At the end of the process, for every surrogate SOA product, the iteration yielded two converged values of $\omega_i(T)$, namely $\omega_i(T^{*})^{\mathrm{chamber}}$ and $\omega_i(T^{*})^{\mathrm{fitted}}$: the agreement was within a few percent in every case. Even though binary mixtures of different compounds will not in general reflect exact ideality, the $N\bullet 2\mathrm{p}$ assumption of $\zeta_i = 1$ was maintained throughout the iteration (see Eq.(3.7)). However, because a ζ_i prediction method such as CP-Wilson.1 will not in general yield $\zeta_i = 1$ in any OPM mixture, after the fitting, results obtained for one parent HC using the $(N\bullet 2\mathrm{p})^{\zeta,\overline{\mathrm{MW}},\theta}$ approach will not collapse at RH = 0% to the corresponding 2p results if that parent HC is considered to lead to two products.

The final assumed structures for the surrogate SOA products are given in Fig.3.1; corresponding inferred molecular parameters are given in Table 3.1. While there is some arbitrariness in the selection of each final $\nu_{k,i}$ set and the corresponding structure, this is not considered problematic given the considerable approximations that are already built into the 2p model: simply finding a structure that matches the value of $\omega_i(T)$ derived using Eq.(3.4) provides meaningful insight regarding aggregate compound polarity that can be used to predict ζ_i effects in OPM systems.

3.2.2. Partitioning POA Compounds

15 POA surrogate compounds (P1-P15) were selected to cover a broad range of source types; all 15 compounds were considered subject to G/P partitioning (Fig. 3.1). Structures for P1-P8 were obtained from Griffin et al. (2003) for mobile (P1-4, P7), mobile/natural (P5), and general cooking (P6) sources. P9, P10, and P15 were selected based on Nolte et al. (1999) as being relevant for meat cooking sources. Levoglucosan (P11) was selected as relevant for biomass burning (Simoneit et al., 2000; Fraser et al. 2002; Zhao et al., 2007). P8, P12, and P13 were selected as representatives of unresolved complex mixture (UCM) materials found in primary mobile emissions. P8 was considered by Griffin et al. (2003). P12 and P13 were included here to expand the volatility range of UCM related materials considered.

3.2.3. Chang-Pankow-Wilson (CP-Wilson) Activity Coefficient Method

Equations. The approach developed here to calculate ζ_i values is based on the equation of Wilson (1964), with modifications introduced for use in a group-contribution manner and for consideration of T effects by application of a $1/T$ factor as suggested by the Scatchard-Hildebrand equation (Flory, 1953). For each neutral compound i in a mixture of other such compounds, each group is therefore assumed here to contribute additively to ζ_i according to

$$\ln \zeta_i = \frac{\sum_k (-n_{k,i} \ln \Gamma_k) - C_i}{T/300} \tag{3.11}$$

where: $n_{k,i}$ is the number of groups of type k in i; Γ_k is the activity coefficient of group k; and C_i is a compound specific constant that functions as a reference-state correction term. While k is again used as the group index for the summation, the set of groups used for the CP-Wilson method with coefficients $n_{k,i}$ is not synonymous with the set used by Asher and Pankow (2007) with coefficients $\nu_{k,i}$.

The equation for Γ_k is assumed here to take the same form as that originally proposed by Wilson (1964) so that

$$\ln \Gamma_k = -\ln(\sum_j x_j \Lambda_{kj}) + 1 - \sum_l \frac{x_l \Lambda_{lk}}{\sum_j x_j \Lambda_{lj}} \tag{3.12}$$

The summations occur over all groups in the mixture wherein: j and l providing indexing through the groups; x_j is the group mole fraction; and Λ_{kj} is the interaction parameter between groups k and j. For each compound i, the constant C_i is evaluated according to

$$C_i = \sum_k n_{k,i} \ln \Gamma_k^{(i)} \tag{3.13}$$

where $\Gamma_k^{(i)}$ is the activity coefficient of group k in pure i and is evaluated using Eq (3.12). Eqs.(3.11-3.13) compose the CP-Wilson method. Values of C_i for the compound structures considered here are given Table 3.1.

In its original form, the Wilson equation is less general than the CP-Wilson method because it is not a group-contribution method. Rather, it handles each compound in the mixture as a full chemical entity, and so its implementation requires specific chemical property information for all the compounds in the mixture. This poses an obvious problem for atmospheric applications: even if the composition of a given atmospheric OPM sample could be accurately characterized, the property information needed for use with the Wilson equation would not be available, not even for some appropriate list of lumped/surrogate compounds. The group contribution approach utilized in the CP-Wilson method overcomes this problem: this method only requires parameter information for the constituent groups, and not property data for all compounds of interest. In general, then, the CP-Wilson method will be significantly more computationally economical than UNIFAC because it requires fewer logarithm and double summation operations, and because the empirical treatment for the T dependence in Eq.(3.11) allows the C_i to be computed once, and thereafter acquired from a look-up table.

Parameter Fitting for CP-Wilson.1. The parameter values needed for a group contribution method are generally obtained by a fitting that minimizes some measure of the difference, for the parameter of interest, between: a) the group-contribution predicted values; vs. b) corresponding experimental values. The particular fitting parameters obtained here combined with the governing equations compose version CP-Wilson.1. Ideally, the fit carried out here would utilize experimental ζ_i values obtained for mixtures involving compounds similar to those of interest. Since such experimental data are not currently available, UNIFAC-generated values (i.e., ζ_i^{U} values) were used as the best, readily available substitute. The ζ_i^{U} values were obtained for mixtures involving compounds with the mix of functionalities and structures of interest, plus water. For SOA compounds, the preliminary structures given in the Supplementary Materials were used; for the POA compounds, the structures in Fig. 3.1 were used. While the nitrate (ONO_2) group is an SOA functionality of interest here, it is not currently a UNIFAC group, and needed experimental thermodynamic data do not exist. The UNIFAC group $CHNO_2$ was therefore substituted for nitrate during the fitting. Some degree of caution should therefore be exercised with considering predictions made using CP-Wilson.1 for nitrate-containing compounds. Overall, fitting to ζ_i^{U} values was considered adequate given the high general merits of the UNIFAC method, and because use of the 2p model and the assumed structures for the SOA compounds (Fig. 3.1) already represents a significant degree of approximation. At some future point, the CP-Wilson method could be re-fit using the extensive experimental ζ_i data set used by Fredenslund et al. (1975) to fit the UNIFAC method, and using new data for organic nitrate compounds (see above), the result perhaps designated as version CP-Wilson.2.

A total of 13,338 ζ_i^{U} values were generated for various binary mixtures of the 41 compounds (40 organic compounds and water) over the mole fraction range 0.2 to 0.8 within the temperature range −10 to 50 °C. Although some of these mixtures are not stable (i.e., would separate into two phases), that did not affect the inherent utility of the associated ζ_i^{U} values. Parameter optimization was performed on the total of 441 Λ_{kj} parameters describing interactions among the 21 constituent groups. The fitting (optimization) occurred by use of the Levenberg-Marquardt algorithm (Levenberg, 1944) to minimize the function $\chi^2 = \sum_1^n \left(1 - \zeta_i^{\mathrm{CPW.1}} / \zeta_i^{\mathrm{U}}\right)^2$ wherein $n = 13{,}338$.

The optimization was performed in three stages. In the first stage, a subset containing 4,446 ζ_i^{U} values for mixtures at 20 °C was extracted from the entire pool to perform a preliminary optimization. Seven different sets of initial values for the Λ_k were involved in the fitting: all $\Lambda_{kj} = 250$, all $\Lambda_{kj} = 500$; all $\Lambda_{kj} = 1000$; all $\Lambda_{kj} = 3000$; all $\Lambda_{kj} = 5000$; all $\Lambda_{kj} = 7000$; and all $\Lambda_{kj} = 10{,}000$. During the fitting runs, the Λ_{kj} were restricted within $0 < \Lambda_{kj} < 10{,}000$. (Due to the presence of the natural logarithm term in Eq.(3.12), it is required that each $\Lambda_{kj} > 0$.) The mean and standard deviation of the seven χ^2 were 228 and 205. The best fit yielded $\chi^2 = 24$ and $0 < \Lambda_{kj} < 6{,}000$. The set of Λ_{kj} yielding $\chi^2 = 24$ was further refined by performing 10 additional optimizations in which the initial Λ_{kj} were varied randomly within ±30%, but still so that $0 < \Lambda_{kj} < 6{,}000$. The resulting best fit yielded $\chi^2 = 22.8$. Consideration of other initial Λ_{kj} sets outside the ±30% range did not improve χ^2. In the second fitting stage, an optimization involving the entire set of 13,338 ζ_i^{U} values was performed five times using the best preliminary Λ_{kj} fit, but randomly varying the values within ±30% (but still so that $0 < \Lambda_{kj} < 6{,}000$). The resulting χ^2 range was 124 to 127. The Λ_{kj} set giving $\chi^2 = 124$ was then used as input for a final optimization during which the step size was reduced three times. The resulting Λ_{kj} set gave $\chi^2 = 120$; further optimization did not reduce χ^2.

3.2.4. $(N{\bullet}2\mathrm{p})^{\zeta,\overline{\mathrm{MW}},\theta}$ *Approach Implementation*

Phase separation considerations. Some of the surrogate compounds considered possess substantial polarity (e.g., the SOA products of isoprene with OH radical), and some are completely non-polar (e.g., the POA compound *n*-nonacosane). A liquid PM mixture containing significant proportions of both types of compounds will be unstable relative to phase separation (Erdakos and Pankow, 2004). At constant P and T in a one-phase liquid system, phase separation will tend to occur when the liquid can find a lower Gibbs free energy by separating into two phases. Similarly, in a gas+liquid system (also at constant P and T) that is initially at equilibrium between the gas and a single-phase liquid, phase separation in the liquid will tend to occur when the overall system can find a lower Gibbs free energy by transformation into a three-phase system (a gas phase and two liquid phases); the transformation is likely to be accompanied by some net exchange with the gas phase of the partitioning compounds. Following Erdakos and Pankow (2004), when two liquid phases exist, then $\theta = \alpha$ and β (see above). $K_{\mathrm{p},i}^{\theta}$ values were calculated by means of Eq.(3.2) using $K^{*}_{\mathrm{p},i}$ values. For most of the SOA surrogate compounds, actual chamber-derived $K^{*}_{\mathrm{p},i}$ and α_i values were used. For three SOA surrogate compounds (S23, S24, and S25), because the experimental data were not available, the Caltech Atmospheric Chemistry Mechanism (CACM) (Griffin et al., 2002) and the Model to Predict the Multi-phase Partitioning of Organics (MPMPO) (Griffin et al., 2003) were used to predict a yield versus organic PM mass concentration (M_{o}) curve so that $K^{*}_{\mathrm{p},i}$ and α_i values could be generated for each compound. For the POA surrogate compounds, chamber-derived $K^{*}_{\mathrm{p},i}$ do not exist, so $K^{*}_{\mathrm{p},i}$ values were calculated directly by means of Eq (3.1) assuming ζ_i =1 and $\overline{\mathrm{MW}} = \mathrm{MW}_i$ and using the SIMPOL.1 method of Pankow and Asher (2007) to estimate $p^{\mathrm{o}}_{\mathrm{L},i}(T^{*} = 293\ \mathrm{K})$ based on structure.

*PM mass calculations***.** All 40 lumped surrogate compounds and water were assumed subject to G/P partitioning. $\mathcal{F}_i$ (μg m^{-3}) represents the PM-associated level of *i*. (The related parameter F_i (ng m^{-3}) has been used in prior work from this group.) If two PM phases are
present, then

$$\mathcal{F}_i \ = \ \mathcal{F}_i^{\alpha} + \mathcal{F}_i^{\beta} \tag{3.14}$$

$\mathcal{T}_i$ (=$\mathcal{A}_i$ + $\mathcal{F}_i$) is the sum of the G- and total P-phase concentrations. At equilibrium the G-phase concentration $\mathcal{A}_i$ (μg m^{-3}) can be calculated based on the value of $K_{\mathrm{p},i}$ and $\mathcal{F}_i$. In the case of phase separation,

$$\mathcal{T}_i \ = \ \frac{\mathcal{F}_i^{\theta}}{M^{\theta}_{\mathrm{TPM}}\ K^{\theta}_{\mathrm{p},i}} + \mathcal{F}_i \tag{3.15}$$

wherein the first term on the RHS represents $\mathcal{A}_i$, as based on equilibrium with either liquid phase (θ = α or β), whichever is more convenient. $M^{\theta}_{\mathrm{TPM}}$ (μg m^{-3}) represents the total mass concentration of the θ phase. In this work, a constant RH was assumed in each case considered. At equilibrium, the statement of equality of water activity between the gas and particle phases is

$$\mathrm{RH}/100 = \zeta^{\theta}_{\mathrm{w}} x^{\theta}_{\mathrm{w}} \tag{3.16}$$

which is thermodynamically equivalent to Eq.(3.1). As with Eq.(3.15), θ = α or β, and in the absence of phase separation, the θ is dropped.

Iterational solutions of the overall G/P distribution problem represented by Eqs.(3.14-3.16) were obtained by applying a liquid-liquid-equilibrium (LLE) flash calculation in each iteration as described by Chang and Pankow (2006). Using the index θ as needed, relationships used in consideration of the results are:

$$M_{\mathrm{o}}^{\theta} = \sum_{\mathrm{organic}\, i} \mathcal{F}_i^{\theta} \tag{3.17}$$

$$M_{\mathrm{o}} = M_{\mathrm{o}}^{\alpha} + M_{\mathrm{o}}^{\beta} \tag{3.18}$$

$$M_{\mathrm{w}} = M_{\mathrm{w}}^{\alpha} + M_{\mathrm{w}}^{\beta} \tag{3.19}$$

$$M_{\mathrm{TPM}} = M_{\mathrm{o}} + M_{\mathrm{w}} = M_{\mathrm{TPM}}^{\alpha} + M_{\mathrm{TPM}}^{\beta} \tag{3.20}$$

where: M_{o}^{θ} (μg m^{-3}) is total organic mass concentration associated with phase θ; M_{o} (μg m^{-3}) is the total organic mass concentration over all PM phases; M_{w}^{α} and M_{w}^{β} (μg m^{-3}) are the water mass concentrations associated with the α and β phases; M_{w} (μg m^{-3}) is the total water mass concentration over all PM phases; and M_{TPM} (μg m^{-3}) is the total PM mass concentration. As noted in Eq.(3.20), for the systems considered here, M_{TPM} (μg m^{-3}) is considered to be comprised of organic compounds and water (and no salt), and a maximum of two phases.

3.2.5. Cases

Computational Efficiency (CE) Test Case (Liquid Phase Only). For a given group-contribution ζ_i prediction method, the PM property that affects the computation time is the number of constituent groups and the number of compounds. Thus, a one-phase liquid mixture at T = 300 K was invoked containing water and 40 organic compounds (the 25 preliminary surrogate SOA compounds in the Supplementary Materials) and the 15 surrogate POA compounds in Fig. 3.1), all at $x_i = 1/41$. The fact that such a system would not remain a single phase at equilibrium at 300 K was not a problem because the only issue was the speed of the ζ_i calculations. The speed of the calculations was compared for CP-Wilson.1 vs. five existing ζ_i estimation methods, namely UNIFAC, NRTL (Renon and Prausnitz, 1968), TK-Wilson (Tsuboka and Katayama, 1975), UNIQUAC (Abram and Prausnitz, 1975), and the unmodified Wilson equation. For each method, the CPU time required to compute the ζ_i values for 41 components in the mixture was obtained 100,000 different times, the large number allowing an averaging of the fluctuations in the CPU operation due to temporal variations in the system resource availability.

Performance Evaluation (PE) Case for ζ_i Prediction. A performance evaluation (PE) aerosol case at T = 298 K for consideration of CP-Wilson.1 and UNIFAC in PM calculations with the $(N\bullet2\text{p})^{\zeta,\overline{\text{MW}},\theta}$ approach was selected to involve all 40 final surrogate compounds in Table 3.1 (and Fig. 3.1) each at $\mathcal{T}_i = 0.3\ \mu\text{g m}^{-3}$, plus water at RH = 50%.

Chamber Based (CB) Cases with RH = 41 to 58%, ΔHC = 386 to 986 μg m^{-3}). Cases CB.1 to CB.3 involve α-pinene/O_3 at RH values in the range 41 to 58% (Table 3.2), and were studied experimentally in the chamber study of Cocker et al. (2001). With α-pinene as the only parent HC, only two surrogate product compounds from Table 3.1 (and Fig.3.1) were considered, namely S3 and S4. The goal here was to allow a comparison of observed chamber PM levels with predictions based on: a) the $(N\bullet2\text{p})^{\zeta,\overline{\text{MW}},\theta}$ approach using the structures in Fig. 3.1 with CP-Wilson.1 for the ζ_i calculations; and b) the conventional $N\bullet2\text{p}$ approach.

Hypothetical Varying Humidity Cases. To investigate RH effects at a lower ΔHC than in the CB cases, an α-pinene/O_3 series was considered assuming ΔHC = 30 μg m^{-3} with RH = 20 to 80% at T = 301 K. Also, a hypothetical mixed SOA+POA series was developed with T = 301 K and two values of RH (5 and 80%); all compounds were considered subject to G/P partitioning. The individual $\mathcal{T}_i$ values for the SOA+POA series are given in Table 3.3 with $\sum_{\text{SOA}} \mathcal{T}_i = 10\ \mu\text{g m}^{-3}$ and $\sum_{\text{POA}} \mathcal{T}_i = 10\ \mu\text{g m}^{-3}$.

3.3 Results

3.3.1. Fit Quality for CP-Wilson.1 Relative to UNIFAC

Table 3.4 gives the best-fit values for the 441 Λ_{kj} parameters for CP-Wilson.1. The averaged unsigned percentage error for ζ_i relative to UNIFAC was calculated based on the 13,338 pairs of predicted $\zeta_i^{\text{CP-W.1}}$ and ζ_i^{U} values according to:

$$\sigma_{\text{FIT}}\,(\%) \quad = \quad \frac{\sum^{13{,}338} \left| \dfrac{\zeta_i^{\text{CP-W.1}} - \zeta_i^{\text{U}}}{\zeta_i^{\text{U}}} \right| \times 100\%}{13{,}338} \qquad (3.21)$$

The overall fit quality was very good ($\sigma_{\text{FIT}} = 6$ %). Fig. 3.2 provides a plot of the 13,338 points for $\zeta_i^{\text{CPW.1}}$ vs. ζ_i^{U}. When $\zeta_i^{\text{U}} < 1000$, where >99% of the points are located, the values are in good agreement. (The good quality of the fit is masked to a considerable extent by the fact that many of the 13,338 points are near the 1:1 line, and plot essentially on top of one another.) For $\zeta_i^{\text{U}} > 1000$, the agreement is still within a factor of ~2. Moreover, contributions to prediction errors for the mass totals given by Eqs.(3.17-3.20) are not likely to be caused simply by incorrectly estimating a large ζ_i value. Indeed, when there is one liquid phase, such an error can only be significant if the corresponding x_i is also of a significant magnitude. However, in that case, the phase would very likely be unstable relative to phase separation, in which case the *i*-related prediction error for the mass total would become small because most of the *i* would retreat into the new, second phase in which ζ_i would be relatively close to 1 and thus reliably estimated.

3.3.2. CP-Wilson.1 vs. Other Methods for the Computational Efficiency (CE) Case

Table 3.5 compares the CPU requirements of CP-Wilson.1 with five other ζ_i methods for the CE case. CP-Wilson.1 gave the best result. The economy of this method is achieved by the combination of its group contribution nature (21 groups for the CE case instead of 41 compounds), and its relatively small need for logarithm and double summation operations. While not implemented here, the computational efficiency of a

CP-Wilson.1 code can be assisted by utilizing a lookup table to evaluate the logarithm term in Eq.(3.12).

3.3.3. CP-Wilson.1 vs. UNIFAC for Performance Evaluation (PE) Case

When CP-Wilson.1 is used in the $(N\bullet 2\mathrm{p})^{\zeta,\overline{\mathrm{MW}},\theta}$ approach to predict ζ_i in the liquid PM formed in the PE case (all $\mathcal{T}_i$ = 0.3 μg m^{-3} for the organic components, and RH = 50%), two phases are revealed as being present in the PM at equilibrium; use of UNIFAC leads to the same result. For each phase θ, relative to UNIFAC, the unsigned prediction difference (%) for x_i^{θ} is defined

$$\delta_{x,i}^{\theta} = \frac{\left| x_i^{\theta,\mathrm{CP\text{-}W.1}} - x_i^{\theta,\mathrm{U}} \right|}{x_i^{\theta,\mathrm{U}}} \times 100\% \qquad (3.22)$$

where the superscripts on x_i denote the phase and ζ_i method. For the α phase, a plot of $\delta_{x,i}^{\alpha}$ vs. $\log_{10} x_i^{\alpha,\mathrm{U}}$ is given in Fig. 3.3.a for the 40 compounds and water. A corresponding plot for the β phase is given in Fig. 3.3.b. Consistent with the results in Fig. 3.2, $\delta_{x,i}^{\alpha}$ is small when $x_i^{\alpha,\mathrm{U}} > 0.01$, and the corresponding $\delta_{x,i}^{\beta}$ are small when $x_i^{\beta,\mathrm{U}} > 0.01$.

Table 3.6 provides observed and predicted results for M_{o}, M_{w}, and M_{TPM} for the PE case. While UNIFAC does not provide perfect estimates of ζ_i, the similarity of the predicted results as obtained using CP-Wilson.1 vs. UNIFAC supports the view discussed above that errors associated with large ζ_i^{θ} are not likely to have significant effects on the quality of predictions for gross parameters such as M_{o}, M_{w}, and M_{TPM} (= M_{o} and M_{w}).

The extent to which an error in a given x_i^{θ} value translates into an error in M_{TPM} depends on the magnitude of x_i^{θ} and on the size of the θ phase. For UNIFAC-based predictions, the fraction (%) of the total PM phase identified with *i* in the θ-phase equals $\mathcal{F}_i^{\theta,\mathrm{U}} \times 100\% / M_{\mathrm{TPM}}^{\mathrm{U}}$. While UNIFAC is certainly also subject to increasing prediction error as any given ζ_i increases, it is again perhaps the best available benchmark for evaluating the results obtained using CP-Wilson.1. Thus, as an means to evaluate the implications of incorrectly predicting $\mathcal{F}_i^{\theta}$ we define

$$\varepsilon_i^{\theta} = \left| \frac{(\mathcal{F}_i^{\theta,\text{CP-W.1}} - \mathcal{F}_i^{\theta,\text{U}}) \times 100\%}{(M_{\text{TPM}})^{\text{U}}} \right| \tag{3.23}$$

If ε_i^{θ} is small, either $\mathcal{F}_i^{\theta,\text{CP-W.1}} \approx \mathcal{F}_i^{\theta,\text{U}}$, or both are small relative to M_{TPM}. Figs. 3.4.a and 3.4.b provide plots of ε_i^{θ} vs. $\log_{10} x_i^{\theta,\text{U}}$ for the PE case. For both $\theta = \alpha$, and $\theta = \beta$, ε_i^{θ} becomes small as $\log_{10} x_i^{\theta,\text{U}}$ increases. This is a consequence of the fact that when phase separation occurs, if ζ_i^{α} is large (and thus subject to some error regardless of the prediction method used), then ζ_i^{β} is relatively close to 1 (and vice versa), the overall result being a thermodynamically driven minimization of the mass amount of *i* in the less-hospitable phase where ζ_i is more difficult to predict (see discussion above). This type of hyperbolic behavior in $\log_{10}\zeta_i^{\alpha}$ vs. $\log_{10}\zeta_i^{\beta}$ is clearly evident in Fig. 3.5. For compounds that fall in the middle of the hydrophobicity↔hydrophilicity scale, both ζ_i^{α} and ζ_i^{β} are neither near 1 nor very large. E.g., for P6, both ζ_i^{α} and ζ_i^{β} are of order 10 because P6 is not particularly "comfortable" in either phase.

3.3.4. Predictions for Chamber Based (CB) and Hypothetical Cases

CB Cases for α-Pinene/O$_3$ with RH = 41 to 58%. Table 3.2 provides M_{TPM} values measured by Cocker et al. (2001) along with the predicted values of M_{o}, M_{w}, and M_{TPM} using the $(N{\bullet}2\text{p})^{\zeta,\overline{\text{MW}},\theta}$ approach with CP-Wilson.1 and the assumed structures for products S3 and S4. For all three CB cases, use of CP-Wilson.1 indicates a single PM phase. (In this and all other respects for these cases, UNIFAC gives similar results.) At these moderate RH values, water uptake is low and ζ_{S3} and ζ_{S4} values are ~1.3, i.e., relatively close to unity. The prediction errors for M_{TPM} as compared to the chamber experiments ranged from −17 to 3% for the three cases. Table 3.2 also provides M_{o} as predicted using the $N{\bullet}2\text{p}$ approach for which, as has been noted, all $\zeta_i \equiv 1$, $M_{\text{o}} \equiv M_{\text{TPM}}$, and $\overline{\text{MW}} \equiv$ constant. The prediction errors for the $N{\bullet}2\text{p}$ approach ranged from −22 to −5 %. The two approaches give nearly the same results because the assumed structures for S3 and S4 have similar polarities and MW$_i$ values, and the water uptake is low.

Hypothetical α*-pinene/O₃ Series*. Results based on the $N\bullet 2\text{p}$ and $(N\bullet 2\text{p})^{\zeta,\overline{\text{MW}},\theta}$ approaches for the α-pinene/O₃ series are given in Fig. 3. 6. As with the CB cases, use of CP-Wilson.1 in the $(N\bullet 2\text{p})^{\zeta,\overline{\text{MW}},\theta}$ approach indicates a single PM phase for the entire RH range (20 to 80%). However, the difference in the M_o predictions obtained using the $N\bullet 2\text{p}$ approach with no water uptake and $(N\bullet 2\text{p})^{\zeta,\overline{\text{MW}},\theta}$ with water uptake is much greater in the Fig. 3.6 series than in the CB cases: M_o by the $(N\bullet 2\text{p})^{\zeta,\overline{\text{MW}},\theta}$ approach in Fig. 3.6 increases by more than 3× as RH increases from 20 to 80%. The increase in M_o by the $(N\bullet 2\text{p})^{\zeta,\overline{\text{MW}},\theta}$ approach is driven mostly by the decreasing $\overline{\text{MW}}$ brought about by water absorption ($\overline{\text{MW}}$ = 151 g mol^{-1} at RH = 20%, and 64 g mol^{-1} at RH = 80%), but is also compounded somewhat by the behavior of ζ_{S3}, which changes from 1.6 at RH = 20%, to 1.1 at RH = 80% (ζ_{S4} remains essentially unchanged at 1.3).

For mono-phasic PM, based on Liang and Pankow (1996), the fraction of i in the particle phase is given by

$$f_{\text{p},i} = \frac{K_{\text{p},i}M_{\text{TPM}}}{1 + K_{\text{p},i}M_{\text{TPM}}} \tag{3.24}$$

(Donahue et al. (2006) denote $f_{\text{p},i}$ as ξ_i .) When $K_{\text{p},i}M_{\text{TPM}}$ is large relative to 1, $f_{\text{p},i} \approx 1$, and the contribution that i makes to M_{TPM} is relatively insensitive to changes in $K_{\text{p},i}$ that may be caused by changes in RH, T, and other factors. However, as $f_{\text{p},i}$ decreases away from 1, that sensitivity increases. Thus, as compared to the CB cases and as compared to the monoterpene cases considered by Seinfeld et al. (2001), M_{TPM} in the series in Fig. 3.6 is much lower, and M_o is thus much more sensitive to RH. Pankow and Chang (2008) provide additional perspective on why the sensitivity of M_o and M_{TPM} predictions will tend to increase as the levels of condensable compounds decrease.

SOA+POA System. Table 3.7 provides predicted results assuming the Table 3.3 levels of SOA+POA compounds at T = 301 K for RH = 5% and 80%. In each of these two cases, the $(N\bullet 2\text{p})^{\zeta,\overline{\text{MW}},\theta}$ approach using CP-Wilson.1 predicts two liquid phases in the PM, with the α phase containing mostly SOA compounds and water, and the β phase containing mostly POA compounds and little water. At RH = 5%, for the major components in each PM phase, $\zeta_i^\theta \approx 1$. Because of the considerable mutual exclusion of the SOA and POA compounds, the effective size of the PM compartment at RH = 5% is significantly lower than is predicted using the N•2p approach: M_w and M_o based on the $(N\bullet 2\mathrm{p})^{\zeta,\overline{\mathrm{MW}},\theta}$ approach are 0.001 and 6.5 μg m^{-3}. By the N•2p approach, the corresponding values are 0 and 9.2 μg m^{-3}. For the RH = 80% case, significant mutual exclusion of the SOA and POA compounds still operates. However, significant water uptake into the α phase is now predicted. This tends to increase the $f_{\mathrm{p},i}$ values of the more polar compounds because M_TPM^α is relatively larger and $\overline{\mathrm{MW}}^\alpha$ relatively smaller than at RH = 5%. Moreover, because of the resulting increased M_w^α value, several of the rather polar compounds take on significantly reduced ζ_i^α values (for S8, 10, 12, 14, 20 and P11, the range for ζ_i^α is 0.2 to 0.6). The overall result is that at RH = 80%, M_w and M_o based on the $(N\bullet 2\mathrm{p})^{\zeta,\overline{\mathrm{MW}},\theta}$ approach are 1.3 and 10.0 μg m^{-3} vs. 0 and 9.2 μg m^{-3} by the N•2p approach.

3.4 Conclusions

The approximations for the particulate matter (PM) phase incorporated in the multiple lumped "two-product" N•2p approach for SOA PM (*i.e.*, all $\zeta_i = 1$, $\overline{\mathrm{MW}}$ is constant, and no water uptake occurs at ambient RH levels) will become increasingly problematic as M_o levels decrease. Also, the approximation of a single-absorbing phase as utilized in the N•2p approach can become invalid when RH levels are high, and/or when significant levels of both SOA and POA compounds are present. The structures proposed here for partitioning SOA and POA compounds will allow first stage usage of the $(N\bullet 2\mathrm{p})^{\zeta,\overline{\mathrm{MW}},\theta}$ approach for ambient PM modeling; the CP-Wilson.1 ζ_i–prediction method developed here allows consideration of computationally intensive space-time domains.

3.5 References

Abram, D.S., Prausnitz, J.M., 1975. Statistical thermodynamics of liquid mixtures: a new expression for the excess Gibbs energy of partly or completely miscible systems. AIChE Journal 21, 116-128.

Barsanti, K.C., Pankow, J.F., 2004. Thermodynamics of the formation of atmospheric organic particulate matter by accretion reactions, Part 1: aldehydes and ketones Atmospheric Environment 38, 4371-4382.

Barsanti, K.C., Pankow, J.F., 2005.Thermodynamics of the formation of atmospheric organic particulate matter by accretion reactions-2. Dialdehydes, methylglyoxal, and diketones. Atmospheric environment 39, 6597-6607.

Barsanti, K.C., Pankow, J.F., 2006. Thermodynamics of the formation of atmospheric organic particulate matter by accretion reactions-Part 3: Carboxylic and dicarboxylic acids. Atmospheric environment 40, 6676-6686.

Bates, T. S., Anderson, T. L., Baynard, T., Bond, T., Boucher, O., Carmichael, G., Clarke, A., Erlick, C., Guo, H., Horowitz, L., Howell, S., Kulkarni, S., Maring, H., McComiskey, A., Middlebrook, A., Noone, K., O'Dowd, C. D., Ogren, J., Penner, J., Quinn, P. K., Ravishankara, A. R., Savoie, D. L., Schwartz, S. E., Shinozuka, Y., Tang, Y., Weber, R. J., Wu, Y., 2006. Aerosol direct radiative effects over the northwest Atlantic, northwest Pacific, and North Indian Oceans: estimates based on in-situ chemical and optical measurements and chemical transport modeling. Atmospheric Chemistry and Physics 6, 1657-1732.

Bowman, F. M., Karamalegos, A. M., 2002. Estimated effects of composition on secondary organic aerosol mass concentrations. Environmental Science & Technology 36, 2701-2707.

Bowman, F.M., Melton, J.A., 2004. Effect of activity coefficient models on predictions of secondary organic aerosol partitioning. Journal of aerosol science 35, 1415-1438.

Chang, E.I., Pankow, J.F., 2006. Prediction of activity coefficients in liquid aerosol particles containing organic compounds, dissolved inorganic salts, and water-Part 2: Consideration of phase separation effects by an X-UNFIAC model. Atmospheric Environment 40, 6422-6436.

Cocker III, D.R., Cleggb, S. L., Flagana, R. C., Seinfelda, J. H., 2001.The effect of water on gas–particle partitioning of secondaryorganic aerosol. Part I: α-pinene/ozone system Atmospheric Environment 35, 6049–6072.

Donahue, N.M., Robinson, A.L., Stanier, C.O., Pandis, S.N. (2006) Coupled partitioning, dilution, and chemical aging of semivolatile organics. Environmental Science and Technology 40, 2635-2643.

Erdakos, G.B., Pankow, J.F., 2004. Gas/particle partitioning of neutral and ionizing compounds to single- and multi-phase aerosol particles. 2. Phase separation in liquid particulate matter containing both polar and low-polarity organic compounds. Atmospheric environment 38, 1005-1013.

Flory, P. J., 1953. Principles of Polymer Chemistry, Cornell University Press, Ithaca, New York.

Fraser, M.P., Yue, Z.W., Tropp, R.J., Kohl, S.D., Chow, J.C., 2002. Molecular composition of organic fine particulate matter in Houston, TX. Atmospheric Environment 36, 5751-5758.

Fredenslund, A., Jones, R.L., Prausnitz, J.M., 1975.Group-contribution estimation of activity coefficients in nonideal mixtures. AIChE Journal 21, 1086-1099.

Griffin, R. J., Cocker III, D.R., Flagan, R. C., Seinfeld, J. H., 1999. Organic aerosol formation from the oxidation of biogenic hydrocarbons, Journal of Geophysical Research 104, 3555–3568.

Griffin, R. J., Dabdub, D., Kleeman, M. J., Fraser, M. P., Cass, G.R., Seinfeld, J. H., 2002a. Secondary organic aerosol. 3. Urban/regional scale model of size- and composition-resolved aerosols. Journal of geophysical research 107, AAC5.1-AAC5.14.

Griffin, R. J., Dabdub, D., Seinfeld, J. H.,2002b. Secondary organic aerosol. 1. Atmospheric chemical mechanism for production of molecular constituents. Journal of geophysical research 107, AAC3.1-AAC3.26.

Griffin, R.J., Nguyen, K., Dabdub, D., Seinfeld, J.H., 2003. A coupled hydrophobic-hydrophilic model for predicting secondary organic aerosol formation. Journal of Atmospheric Chemistry 44, 171-190.

Griffin, R.J. (2007) personal communication.

Henze, D.K., Seinfeld, J.H., 2007. Global secondary organic aerosol from isoprene oxidation. Geophysical Research Letters 33, L09812, doi:10.1029/2006GL025976.

Hoffman, T., Odum, J. R., Bowman, F., Collins, D., Klockow, D., Flagan, R. C., Seinfeld, J. H., 1997. Formation of organic aerosols from the oxidation of biogenic hydrocarbons, J. Atmospheric Chemistry 26, 189–222.

Kalberer, M., Paulsen, D., Sax, M., Dommen, J., Prevot, A.S.H., Fisseha, R., Weingartner, E., Frankevich, V., Zenobi, R., Baltensperger, U., 2004. Identification of polymers as major components of atmospheric organic aerosols. Science 303, 1659-1662.

Kanakidou, M., Tsigaridis, K., Dentener, F. J., and Crutzen, P. J., 2000. Human-activity-enhanced formation of organic aerosols by biogenic hydrocarbon oxidation. Journal of Geophysiccal Research 105, 9243–9254.

Liang, C., Pankow, J.F. 1996. Gas/particle partitioning of organic compounds to environmental tobacco smoke: partition coefficient measurements by desorption and comparison to urban particulate material. Environmental Science and Technology 30, 2800-2805.

Levenberg, K., 1944. A method for the solution of certain problems in least Squares. Quarterly of Applied Mathematics 2, 164-168.

Mazurek, M., Masonjones, M. C., Masonjones, H. D., Salmon, L. G., Cass, G. R., Hallock, K. A., Leach, M., 1997. Visibility-reducing organic aerosols in the vicinity of Grand Canyon National Park: Properties observed by high resolution gas chromatography. Journal of Geophysical Research 102, 3779–3794.

Nolte, C.G., Schauer, J.J., Cass, G.R., Simoneit, B.R.T., 1999. Highly polar organic compounds present in meat smoke. Environmental Science and Technology 33, 3313-3316.

Odum, J.R., Hoffmann, T., Bowman, F., Collins, D., Flagan, R.C., and Seinfeld, J. H., 1996. Gas/particle partitioning and secondary organic aerosol yields. Environmental Science &. Technology 30, 2580 -2585.

Odum, J.R., Jungkamp, T.P.W., Griffin, R.J., Forstner, H.J.L., Flagan, R. C., Seinfeld, J. H., 1997. Aromatics, reformulated gasoline, and atmospheric organic aerosol formation. Environmental Science &. Technology 31, 1890 -1897.

Pankow, J.F., 1994a.An absorption model of gas/particle partitioning of organic compounds in the atmosphere. Atmospheric Environment 28, 185-188.

Pankow, J.F., 1994b.An absorption model of the gas/aerosol partitioning involved in the formation of secondary organic aerosol. Atmospheric Environment 28, 189-193.

Pankow, J.F., Asher, W.E., 2007. SIMPOL.1: A simple group contribution method for predicting vapor pressures and enthalpies of vaporization of multifunctional organic compounds. Atmospheric Chemistry and Physics Discussion 7, 11839-11894.

Pankow, J.F. and Barsanti, K.C. 2008. Framework for managing the complexity of the compounds involved in organic particulate matter formation in the atmosphere: the carbon number-polarity grid (in preparation).

Pope, C. A., 2000. Epidemiology of fine particulate air pollution and human health: biologic mechanisms and who's at risk. Environ Health Perspect 108, 713–723.

Pun, B. K., Zhang, Y., Vijayaraghavan, K., Wu, S., Seigneur, C., Seinfeld, J. H., 2001. Development and initial application of the model for aerosol dynamics, reaction, ionization, and dissolution (MADRID). Regional Haze and Global Radiation Balance: Aerosol Measurements and Models--Closure, Reconciliation and Evaluation, Proceedings of a Specialty Conference, Bend, OR, United States, Oct. 2-5, 2001, 104-113.

Pun,B.K., Wu, S. Y., Seigneur, C., Seinfeld, J. H., Griffin, R. J., Pandis S. N., 2003. Uncertainties in modeling secondary organic aerosols: three-dimensional modeling studies in Nashville/western Tennessee. Environmental Science and Technology 37, 3647-3661.

Renon, H., Prausnitz, J.M., 1968. Local compositions in thermodynamic excess functions for liquid mixtures. AIChE Journal 14, 135-144.

Seinfeld, J. H., Erdakos,G.B., Asher, W.E., Pankow, J. F., 2001. Modeling the formation of secondary organic aerosol (SOA). 2. The predicted effects of relative humidity on aerosol formation in the α-pinene-, β-pinene-, sabinene-, Δ3-carene-, and cyclohexene-ozone systems. Environmental Science & Technology 35, 1806 - 1817.

Simoneit, B.R.T., Rogge, W.F., Lang, Q., Jaffe, R., 2000. Molecular characterization of smoke from campfire burning of pine wood (Pinus elliottii). Chemosphere: Global Change Science 2, 107-122.

Surratt, J. D., Murphy, S. M., Kroll, J. H., Ng, N. L., Hildebrandt, L., Sorooshian, A., Szmigielski, R., Vermeylen, R., Maenhaut, W., Claeys, M., Flagan, R. C., Seinfeld, J. H., 2006. Chemical composition of secondary organic aerosol formed from the photooxidation of isoprene . Journal of Physical Chemistry A 110, 9665 -9690.

Tsigaridis, K., Kanakidou, M., 2003. Global modeling of secondary organic aerosol in the troposphere: a sensitivity analysis. Atmospheric Chemistry and Physics 3, 1849–1869.

Tsuboka, T., Katayama, T., 1975. Modified Wilson equation for vapor-liquid and liquid-liquid equilibria. Journal of Chemical Engineering of Japan 8, 181-187.

Wilson, G. M., 1964. Vapor-Liquid Equilibrium. XI. A new expression for the excess free energy of mixing. Journal of American Chemical Society 86,127-130.

Zhao, Y., Hu, M., Slanina, S., Zhang, Y., 2007. Chemical compositions of fine particle organic matter emitted from Chinese cooling. Environmental Science and Technology 41, 99-105.

Table 3.1. Assumed properties of 25 SOA and 15 POA surrogate compounds, and water.

SOA Compounds				chamber-derived parameters				other parameters				
compound	reaction	parent HC	oxidant	T^* (K)	$K^*_{\mathrm{p},i}(T^*)$	α_i	ref.	$\overline{\mathrm{MW}}^{*\,a}$ (g mol^{-1})	MW_i ^{b} (g mol^{-1})	CP-Wilson parameter C_i ^{c}	ΔH_{vap} (303) ^{d} (kJ mol^{-1})	$p^{\mathrm{o}}_{\mathrm{L}}(T^*)$ ^{d} (atm)
S1	1	α - pinene	OH	310	0.171	0.038	A	189	188	70.90	99.1	7.38 E-10
S2					0.004	0.326		189	190	59.07	85.7	3.82 E-08
S3	2	α - pinene	O_3	310	0.088	0.125	A	194	214	41.76	74.3	1.34 E-09
S4					0.0788	0.102		194	174	69.75	89.7	1.52 E-09
S5	3	β - pinene	OH	310	0.044	0.13	A	194	186	56.44	100.6	3.63 E-09
S6					0.0049	0.041		194	172	52.63	78.6	2.75 E-08
S7	4	β - pinene	O_3	310	0.195	0.026	A	188	202	56.92	103.9	7.32 E-10
S8					0.003	0.485		188	174	64.41	77.1	4.18 E-08
S9	5	β - pinene	NO_3	310	0.0163	1.000	A	245	245	69.29	80.3	7.61 E-09
S10	6	isoprene	OH	295	0.0086	0.232	B	177	136	52.68	90.3	1.36 E-08
S11					1.62	0.029		177	218	76.27	87.5	8.68 E-11
S12	7	limonene	OH	310	0.055	0.239	A	195	188	51.90	79.8	2.33 E-09
S13					0.0053	0.363		195	202	43.32	90.0	2.57 E-08
S14	8	ocimene	OH	310	0.174	0.045	A	152	146	32.46	105.5	1.06 E-09
S15					0.0041	0.149		152	158	37.15	90.2	3.36 E-08
S16	9	terpinene	OH	310	0.081	0.091	A	174	202	62.45	111.3	1.46 E-09
S17					0.0046	0.367		174	146	24.88	79.7	3.52 E-08
S18	10	toluene	OH	310	0.053	0.071	C,D	173	148	38.63	95.6	2.54 E-09
S19					0.0019	0.138		173	197	48.12	81.4	8.21 E-08
S20	11	xylene	OH	310	0.042	0.038	C,D	187	176	31.03	87.5	2.64 E-09
S21					0.0014	0.167		187	197	48.12	81.4	8.21 E-08
S22	12	humulene	OH	310	0.0501	1.000	A	270	270	72.94	73.9	1.80 E-09
S23	13	2-ring PAH	OH	298	0.015	0.156	E	175	186	68.19	94.5	8.14 E-09

S24					0.002	0.777		175	164	47.75	81.5	7.05 E-08
S25	14	C_{16} *n*-alkane	OH	298	0.0229	1.173	E	301	301	94.58	100.9	3.28 E-09

POA Compounds

Compound		T^* (K)	$K^*_{\mathrm{p},i}(293)$	MW_i (g mol^{-1})	CP-Wilson parameter C_i [c]	ΔH_{vap} (303) [d] (kJ mol^{-1})	$p^{\mathrm{o}}_{\mathrm{L}}(293)$ [d]
P1	2,6-naphthalene diacid		101.68	216	69.62	118.9	1.09 E-12
P2	benzo[ghi]perylene		43.83	276	119.40	112.7	1.99 E-12
P3	butanedioic acid		0.0025	118	26.59	84.0	8.31 E-08
P4	17(α)H-21(β)H-hopane		72.83	412	172.24	123.1	8.01 E-13
P5	*n*-nonacosane		33.62	409	166.96	149.2	1.75 E-12
P6	Octadecanoic acid		1.14	284	107.03	123.4	7.41 E-11
P7	phthalic acid		0.48	166	47.60	101.4	3.01 E-10
P8	UCM2 (unresolved complex mixture 2)		10.45	390	162.46	132.4	5.90 E-12
P9	monoglyceride		433.96	330	123.00	138.8	1.68 E-13
P10	triglyceride		1.72E+17	860	299.04	280.0	1.63 E-28
P11	levoglucosan		0.167	162	57.14	94.4	8.88 E-10
P12	UCM1 (unresolved complex mixture 1)		1.42E-05	210	87.12	79.2	8.07 E-06
P13	UCM3 (unresolved complex mixture 3)		16381.2	487	202.35	158.2	3.01 E-15
P14	hexadecanoic acid		0.14	256	95.49	114.3	6.58 E-10
P15	glycerol		0.0005	92	39.10	78.0	5.02 E-07
c. Water	H_2O			18	7.15		

Footnotes:

a. Calculated as the mean of the inferred MW_i values
b. Inferred based on chamber data using iterative process outlined in Eqs.(3.5-3.10).
c. Calculated based on Eq.(3.13).
d. Calculated based on parameters given in Pankow and Asher (2007).

References:

A. Griffin et al. (1999); B. Henze and Seinfeld (2006); C. Odum et al. (1997b); D. Pun et al. (2003); E. Estimated by CACM and MPMPO (Griffin 2007).

Table 3.2. Results for chamber-based (CB) cases with α-pinene/O_3 as measured by Cocker et al. (2001) and as predicted using the $N{\bullet}2\mathrm{p}$ approach and using the $(N{\bullet}2\mathrm{p})^{\zeta,\overline{\mathrm{MW}},\theta}$ approach with the CP-W.1 method for prediction of ζ_i values.

				Measured	$N{\bullet}2\mathrm{p}$ Predictions				$(N{\bullet}2\mathrm{p})^{\zeta,\overline{\mathrm{MW}},\theta}$ Predictions			
case	*T* (K)	ΔHC (μg m^{-3})	RH (%)	M_{TPM} (μg m^{-3})	M_{o} (μg m^{-3})	M_{w} (μg m^{-3})	M_{TPM} (μg m^{-3})	error[a] in M_{TPM}	M_{o} (μg m^{-3})	M_{w} (μg m^{-3})	M_{TPM} (μg m^{-3})	error[a] in M_{TPM}
CB.1	301.8	386.3	41.0	86	82	0[b]	82	-5%	83	6	89	+3%
CB.2	301.8	675.0	57.7	177	148	0[b]	148	-16%	150	18	168	-5%
CB.3	302.7	986.5	37.3	281	218	0[b]	218	-22%	219	13	232	-17%

[a] error based on measured value of Cocker et al. (2001).

[b] by definition

Table 3.3. Total mass concentration $\mathcal{T}_i$ values for the hypothetical SOA + POA cases.

SOA Compounds				
Rxn.	Parent	Oxidant	Compound	$\mathcal{T}_i$ (μg m^{-3})
1	α - pinene	OH	S1	0.104
			S2	0.896
2	α - pinene	O_3	S3	0.551
			S4	0.449
3	β - pinene	OH	S5	0.380
			S6	0.120
4	β - pinene	O_3	S7	0.025
			S8	0.475
5	β - pinene	NO_3	S9	0.500
6	isoprene	OH	S10	0.111
			S11	0.014
7	limonene	OH	S12	0.397
			S13	0.603
8	ocimene	OH	S14	0.029
			S15	0.096
9	terpinene	OH	S16	0.025
			S17	0.100
10	toluene	OH	S18	0.849
			S19	1.651
11	xylene	OH	S20	0.324
			S21	1.426
12	humulene	OH	S22	0.125
13	2-ring PAH	OH	S23	0.125
			S24	0.125
14	C_{16} *n*-alkane	OH	S25	0.500
POA Compounds				
	2,6-naphthalene diacid		P1	0.083
	benzo-ghi-perylene		P2	0.083
	butanedioic acid		P3	0.083
	17(α)H-21(β)H-hopane		P4	0.083
	n-nonacosane		P5	0.083
	Octadecanoic acid		P6	0.083
	phthalic acid		P7	0.083
	UCM2		P8	3.000
	monoglyceride		P9	0.083
	triglyceride		P10	0.083
	levoglucosan		P11	0.083
	UCM1		P12	3.000
	UCM3		P13	3.000
	hexadecanoic acid		P14	0.083
	glycerol		P15	0.083

Table 3.4. Fitted interaction parameters (Λ_{ki}) for 21 groups.

	CH_3	CH_2	CH	C	CH=CH	(Aromatic C)-H	Aromatic C	(Aromatic C)-CH_3	(Aromatic C)-CH_2	OH
CH_3	3.88E+02	3.75E+01	9.26E+01	1.96E+01	6.73E+02	1.31E+02	1.75E+01	5.44E+02	1.21E+02	2.34E+03
CH_2	8.74E+02	3.19E+02	3.85E+02	3.40E+02	3.94E+01	6.59E+01	1.56E+02	5.48E+02	3.66E+02	1.89E+03
CH	6.39E+02	2.42E+02	3.02E+02	2.71E-02	3.33E-07	2.15E+01	1.50E+02	5.05E+02	4.22E+02	1.52E+03
C	9.70E+02	2.05E+02	3.65E+02	1.20E-02	6.33E+02	4.89E+02	3.92E+02	4.95E+02	5.19E+02	8.80E+02
CH=CH	3.52E+00	1.23E+02	9.92E+01	3.37E+01	6.52E-03	2.01E+02	1.37E+01	6.78E-05	2.95E-02	7.22E+02
(Aromatic C)-H	5.44E+02	4.49E+02	4.27E+02	7.76E-02	4.83E+01	2.55E+02	4.10E+02	3.59E+02	3.06E+02	7.54E+02
Aromatic C	7.70E+02	4.95E+02	4.06E+02	6.70E-05	3.19E+02	2.33E+01	2.98E+02	3.97E+02	3.28E+02	1.72E+03
(Aromatic C)-CH_3	3.27E+01	3.12E+01	2.57E+01	1.98E+01	2.04E+00	8.87E+00	6.52E+01	1.63E+02	1.23E+02	5.67E+02
(Aromatic C)-CH_2	8.08E+01	7.63E+01	1.70E+01	4.39E+01	2.83E-01	2.06E+01	7.85E+01	1.42E-01	1.70E+02	8.87E+02
OH	9.39E+01	7.06E+01	5.13E+01	1.79E+02	4.30E+02	1.92E+02	2.15E-04	2.90E-03	2.22E-02	8.20E+02
H_2O	5.88E+01	7.68E+01	4.15E+01	1.19E+02	1.02E-01	2.49E-01	1.38E+02	5.90E-03	3.62E+02	2.31E+02
(Aromatic C)-OH	8.85E+01	3.89E+01	1.34E-02	1.77E-05	4.47E+03	1.32E+02	2.33E+02	8.82E-04	3.22E-02	6.12E+02
CH_3CO	6.08E+01	7.34E+01	4.81E+02	4.40E+02	7.32E+02	1.82E+02	2.17E+01	9.17E+02	1.36E-12	8.79E+02
CH_2CO	1.75E+00	3.94E+01	7.04E+01	6.78E-02	1.94E+02	5.62E+01	9.94E-04	1.36E+00	1.17E-12	3.53E+02
CHO	9.86E+02	3.67E+02	1.53E-02	2.13E+02	5.00E-02	3.57E+02	1.08E-01	2.97E-12	3.24E-12	9.65E+02
CH2COO	8.59E+02	3.81E+02	1.53E+00	5.27E-07	4.40E-01	7.33E+02	4.83E-01	4.46E+02	2.64E-02	7.65E+02
CH_2O	4.55E+00	1.43E+02	1.24E+00	8.39E+01	5.47E+02	8.17E+01	1.01E-12	5.64E+02	1.22E-12	6.98E+02
CH-O	1.95E+03	9.69E+02	1.54E+02	1.00E+00	1.50E+03	4.01E+02	6.40E+01	7.16E+02	9.19E+02	2.23E+02
COOH	4.30E+02	1.23E+02	4.79E-05	6.64E+02	1.60E+03	3.78E+02	1.38E-05	5.49E-01	2.80E-03	1.14E+03
NO_3	3.44E+00	8.56E+01	1.47E+02	9.11E-02	1.02E-12	5.41E-04	8.61E+01	2.08E+02	6.45E+02	4.26E+02
(Aromatic C)-NO_2	4.18E+02	2.63E+02	1.46E+02	2.45E-01	1.96E-03	2.33E+02	7.32E-02	1.79E-02	4.76E+02	1.19E+03

	H_2O	Aromatic OH	CH_3CO	CH_2CO	CHO	CH_2COO	CH_2O	CH-O	COOH	NO_3	(Aromatic C)- NO_2
CH_3	2.71E+03	3.50E+03	1.94E+03	1.94E+03	1.25E+03	7.66E+02	6.04E+02	1.23E+03	1.69E+03	2.08E+03	4.51E+02
CH_2	1.94E+03	2.47E+03	1.79E+03	1.18E+03	1.03E+03	9.28E+02	5.16E+02	4.19E+02	1.63E+03	1.12E+03	3.23E+02
CH	1.50E+03	2.03E+03	5.53E+02	4.96E+02	9.81E+02	1.24E+03	4.19E+02	3.01E+02	1.25E+03	4.09E+02	7.65E-08
C	1.25E+03	1.34E+03	7.47E+02	7.64E+02	4.86E+02	2.51E+02	1.69E-02	1.19E+03	3.48E+02	7.63E+02	6.05E+02
CH=CH	1.11E+03	2.77E-01	7.88E-04	2.29E-01	4.32E+02	7.14E+02	8.36E-02	3.09E-12	2.66E+02	4.90E+02	5.08E+02
(Aromatic C)-H	1.12E+03	1.01E+03	7.18E+02	6.13E+02	3.54E+02	2.13E+02	4.15E+02	5.35E+02	3.84E+02	3.65E+02	2.44E-01
Aromatic C	2.15E+03	1.69E+03	1.26E+03	9.01E+02	1.04E+03	4.19E+02	4.18E+02	1.09E+03	1.42E+03	1.24E+03	5.70E+02
(Aromatic C)-CH_3	7.21E+02	9.31E+02	1.01E+02	4.45E+02	3.71E+02	1.73E+02	1.59E-12	1.27E-12	4.75E+02	2.12E+02	1.07E-01
(Aromatic C)-CH_2	1.13E+03	2.04E+03	4.25E+02	2.96E+02	3.83E+02	3.76E-12	3.67E+02	1.10E-02	1.07E+03	2.87E+02	4.02E-03
OH	1.52E+03	1.45E-12	2.00E+03	1.21E+03	6.16E+02	1.35E+03	1.04E+03	9.18E+02	7.23E+02	2.41E+03	4.19E+01
H_2O	1.28E+03	1.09E-12	3.58E+02	2.62E+02	1.68E+02	6.76E+01	1.07E-12	1.10E-12	2.39E+02	1.45E+03	8.47E-02
(Aromatic C)-OH	4.98E+02	3.96E+03	1.00E+03	2.01E-04	1.36E-02	4.14E-01	3.96E+02	4.78E+02	1.52E+03	2.00E-12	4.27E-04
CH_3CO	2.25E+03	1.55E+03	1.42E+03	5.74E+02	1.40E+03	1.37E+03	9.32E+02	8.14E+02	1.03E+03	1.40E+02	5.79E-02
CH_2CO	6.15E+02	5.82E+02	6.60E+02	2.98E+02	3.14E+02	3.23E+02	6.32E+02	4.43E+02	3.44E+02	8.54E-02	4.30E-03
CHO	2.27E+03	1.82E+03	9.71E+02	4.01E+02	7.51E+02	5.14E+02	7.41E+02	9.91E+02	5.55E+02	5.31E+03	2.79E+03
CH2COO	2.18E+03	9.61E-12	2.49E-01	3.71E+02	9.29E+02	1.13E+03	3.94E+00	1.05E-11	2.42E-03	1.10E-12	2.15E+00
CH_2O	3.08E+02	1.03E-12	1.94E+03	4.98E-02	8.19E+02	9.52E-12	4.40E+02	4.40E+02	8.98E+02	1.22E+03	8.06E-07
CH-O	5.01E+02	2.00E-04	4.58E+02	5.88E+02	1.47E+00	4.10E+03	1.78E+03	1.78E+03	3.46E+02	3.03E+03	3.39E+03
COOH	1.98E+03	3.44E+03	7.47E+02	1.19E+02	1.15E+03	7.10E+02	1.03E-02	1.01E-12	1.09E+03	3.67E+03	2.98E+03
NO_3	1.29E+03	1.32E+03	1.13E+03	8.20E+02	2.21E+02	3.86E-04	1.22E+00	1.25E+00	1.34E+03	4.59E+02	2.11E-01
(Aromatic C)-NO_2	2.39E+03	1.05E+03	3.51E+02	1.08E-12	2.62E-12	6.03E+02	3.60E+02	4.78E+02	8.69E+02	1.51E+03	3.43E-02

Table 3.5. Comparison of relative computer processing time required for six ζ_i prediction methods.

ζ_i Method	Method type	Number of groups or compounds	Relative computer processing time
CP-Wilson.1	group	21	0.1
Wilson	compound	41	0.6
UNIQUAC	compound	41	0.6
TK-Wilson	compound	41	0.7
NRTL	compound	41	0.8
UNIFAC	compound	21	1.0

Table 3.6. Comparison of predictions for the performance evaluation (PE) case by the $(N\bullet 2\mathrm{p})^{\zeta,\overline{\mathrm{MW}},\theta}$ approach using the CP-Wilson.1 method and the UNIFAC method (*T* = 298K, RH = 50%).

	ζ_i Method	
Result	CP-Wilson.1	UNIFAC
Number of PM phases	2	2
M_{o}^{α}, M_{o}^{β} (µg/m^3)	3.63, 1.79	3.62, 1.79
$M_{\mathrm{o}} = M_{\mathrm{o}}^{\alpha} + M_{\mathrm{o}}^{\beta}$ (µg/m^3)	5.42	5.41
M_{w}^{α}, M_{w}^{β} (µg/m^3)	0.29, 0.001	0.29, 0.0005
$M_{\mathrm{w}} = M_{\mathrm{w}}^{\alpha} + M_{\mathrm{w}}^{\beta}$ (µg/m^3)	0.29	0.29
$M_{\mathrm{TPM}}^{\alpha}$ (µg/m^3)	3.92	3.92
M_{TPM}^{β} (µg/m^3)	1.79	1.79
M_{TPM} (µg/m^3)	5.71	5.71

Table 3.7. Results for the hypothetical SOA + POA cases at 300 K as predicted using the $N\bullet 2\mathrm{p}$ approach and using the $(N\bullet 2\mathrm{p})^{\zeta,\overline{\mathrm{MW}},\theta}$ approach with the CP-Wilson.1 method for prediction of ζ_i values. (See Table 3.3 for all $\mathcal{T}_i$ values.)

	$N\bullet 2\mathrm{p}$ Prediction				$(N\bullet 2\mathrm{p})^{\zeta,\overline{\mathrm{MW}},\theta}$ Prediction				
RH (%)	M_o (μg m^{-3})	M_w (μg m^{-3})	M_TPM (μg m^{-3})	PM phases	M_o (μg m^{-3})	M_w (μg m^{-3})	M_TPM (μg m^{-3})	PM phases	phase mass distribution $M^{\alpha}_{\mathrm{TPM}}/M^{\beta}_{\mathrm{TPM}}$
5	9.23	0 [a]	9.23	1 [a]	6.48	0.001	6.48	2	0.19/6.29
80	9.23	0 [a]	9.23	1 [a]	10.00	1.28	11.28	2	5.02/6.26

[a] by definition

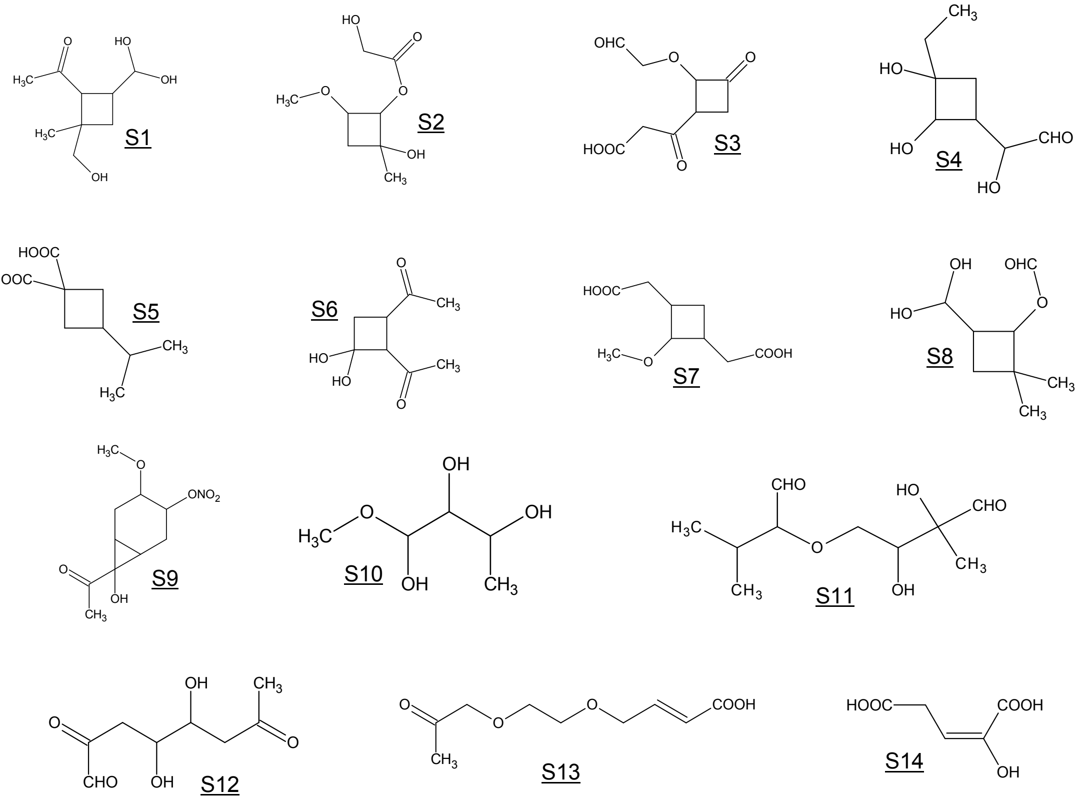

Figure 3.1. Molecular structures of lumped SOA products and surrogate POA compounds.‡R_1 = C_{16} alkyl chain; R_2 = C_{18} alkyl chain; R_3 = C_{18} alkyl chain with one double bond.

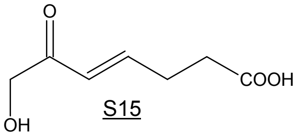

S15

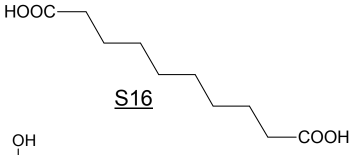

S16

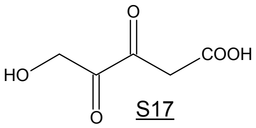

S17

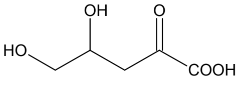

S18

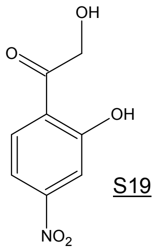

S19

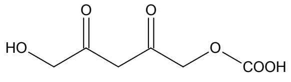

S20

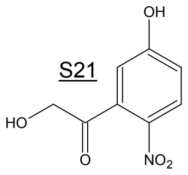

S21

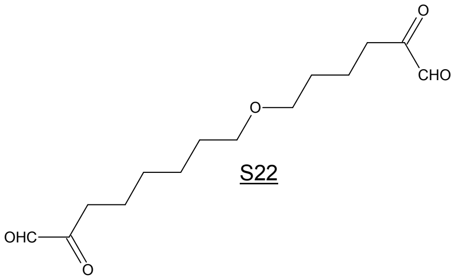

S22

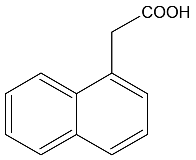

S23

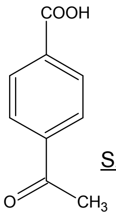

S24

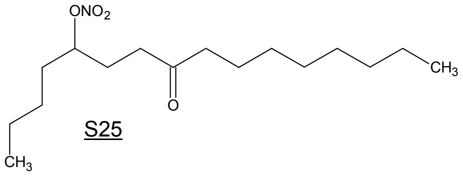

S25

Figure 3.1. (continued)

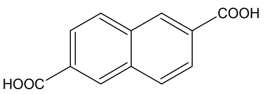

P1

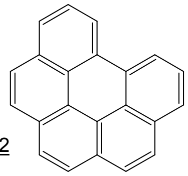

P2

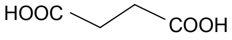

P3

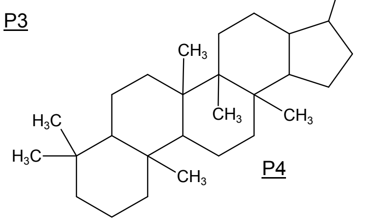

P4

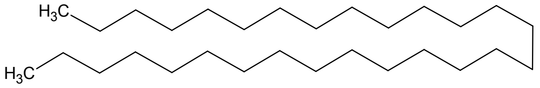

P5

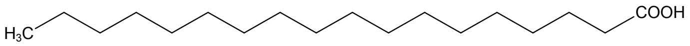

P6

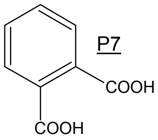

P7

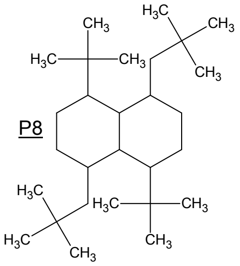

P8

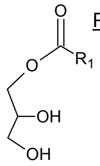

P9‡

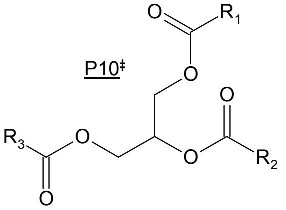

P10‡

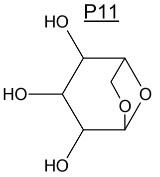

P11

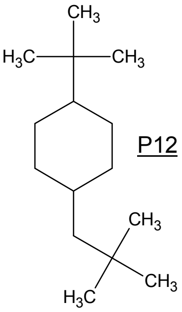

P12

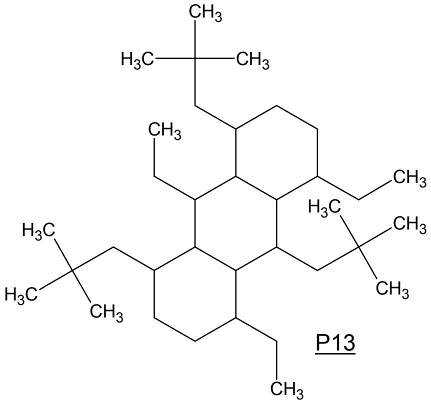

P13

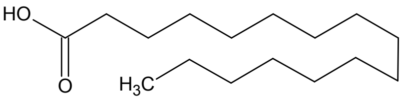

P14

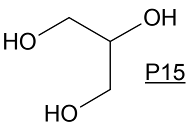

P15

Figure 3.1 (continued).

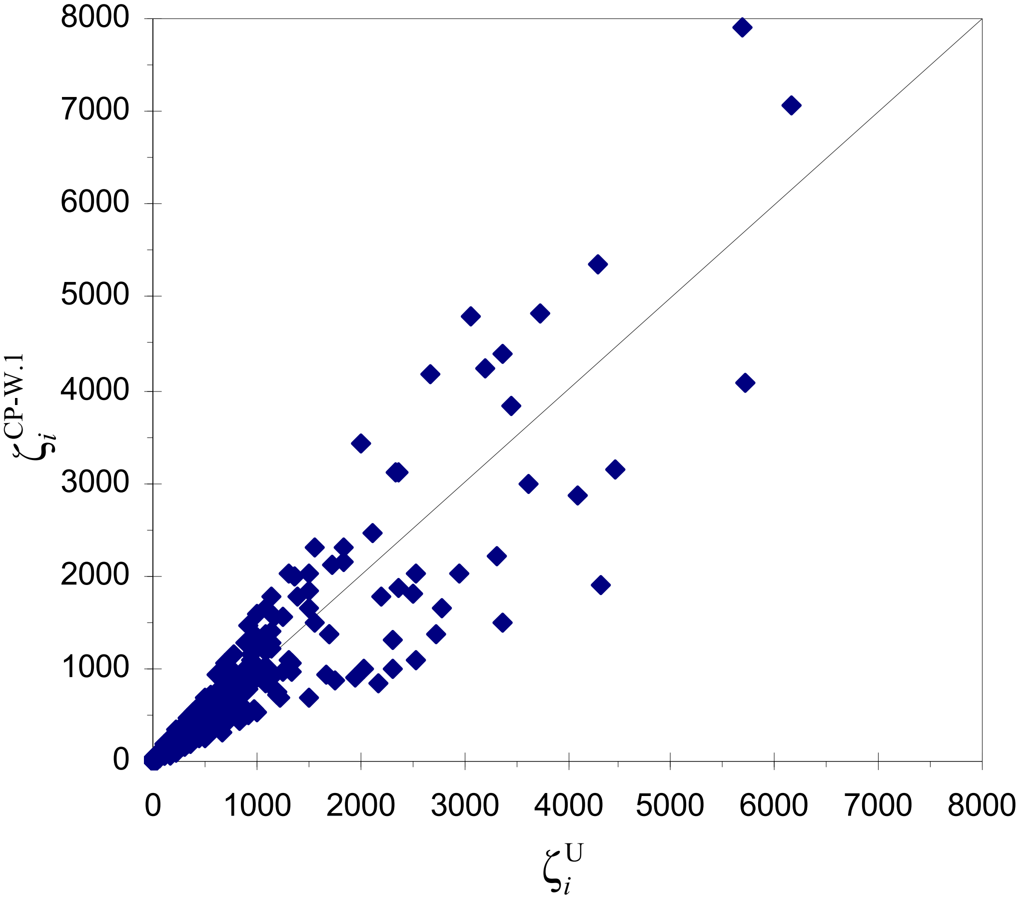

Figure 3.2. ζ_i calculated by CP-W.1 vs. ζ_{i} calculated by UNIFAC for 13,338 points used in the fitting of CP-W.1 to UNIFAC.

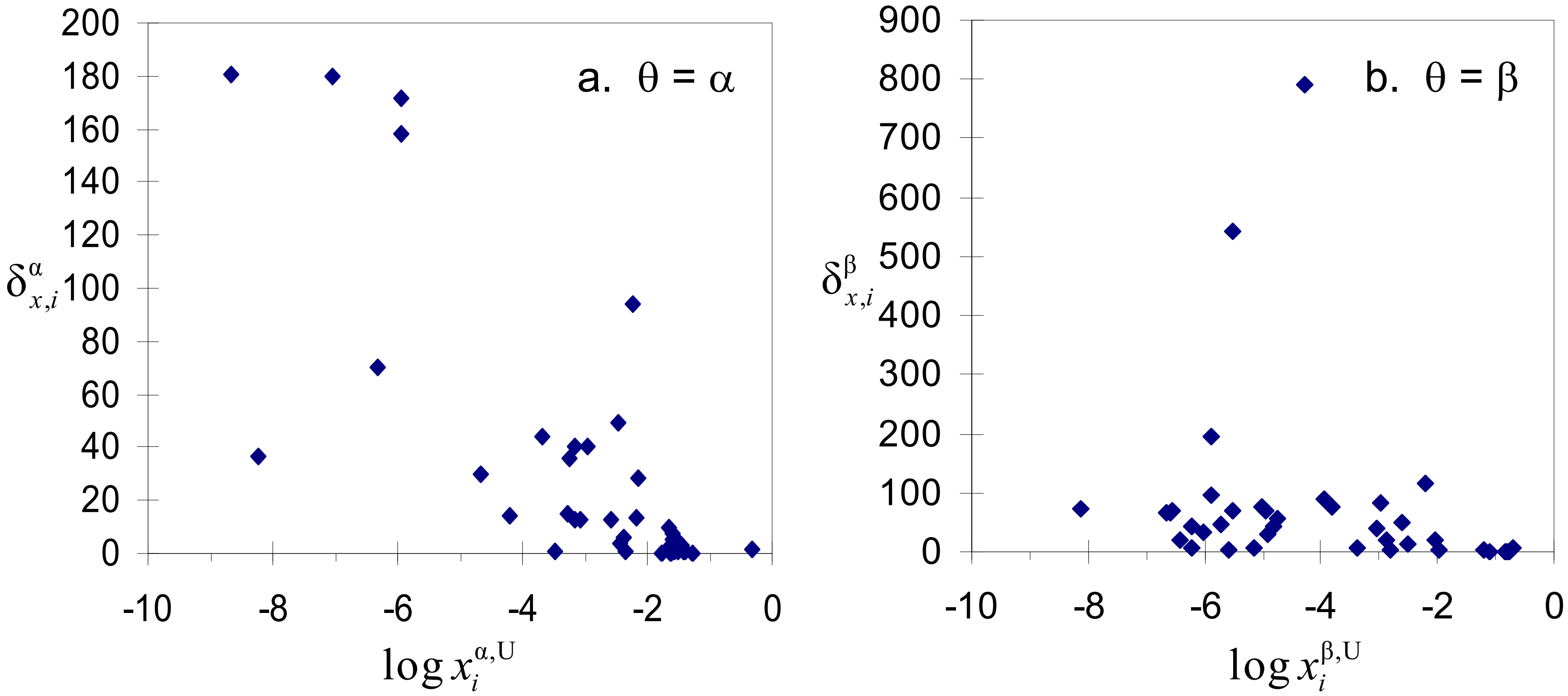

Figure 3.3. Unsigned percentage difference between the values of x_i^{θ} as predicted using CP-W.1 and UNIFAC plotted vs. log $x_i^{\theta,\mathrm{U}}$ (U = UNIFAC) for $\theta = \alpha$ and for $\theta = \beta$ in the performance evaluation (PE) case.

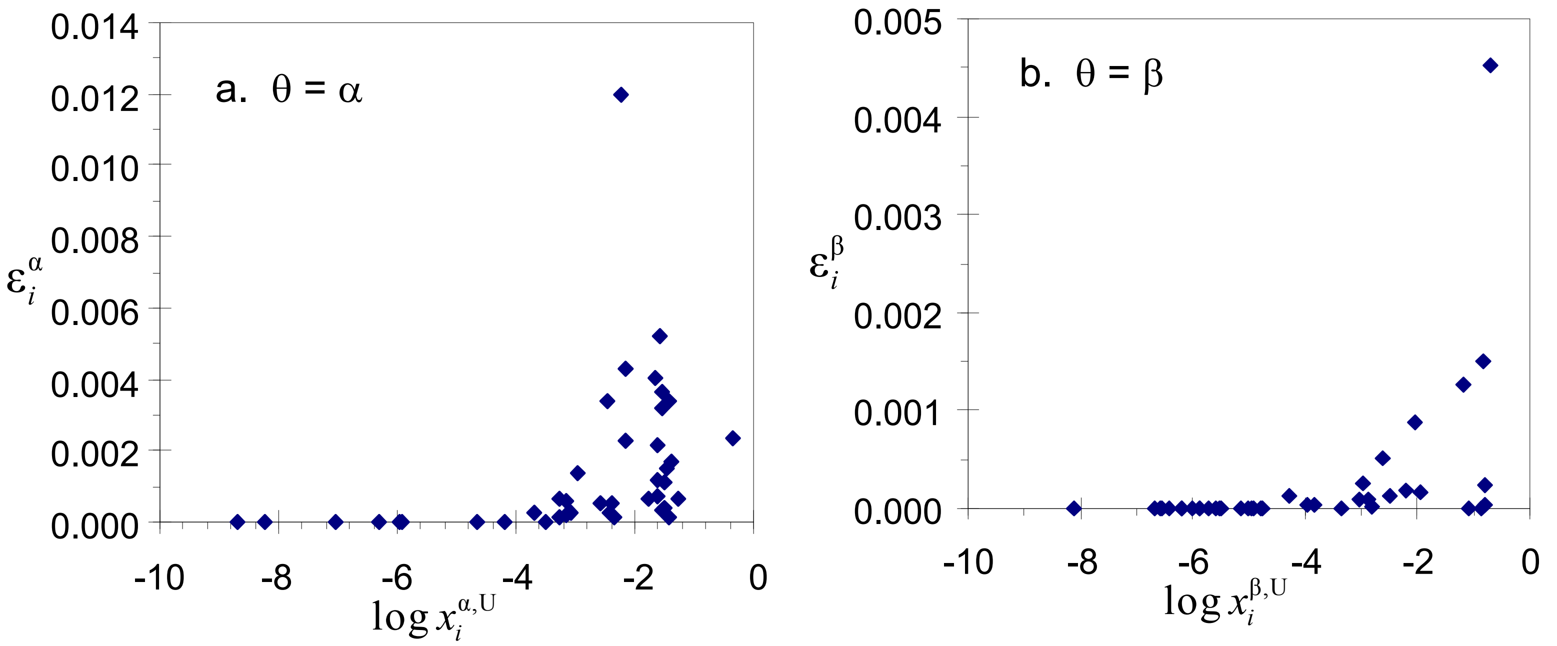

Figure 3.4. Unsigned difference between the values of $\mathcal{F}_i^{\theta}$ as predicted using CP-W.1 and UNIFAC expressed as a percentage of $(M_{\text{TPM}})^{\text{U}}$ vs. $\log x_i^{\theta,\text{U}}$ (U = UNIFAC) for θ = α and for θ = β in the performance evaluation (PE) case.

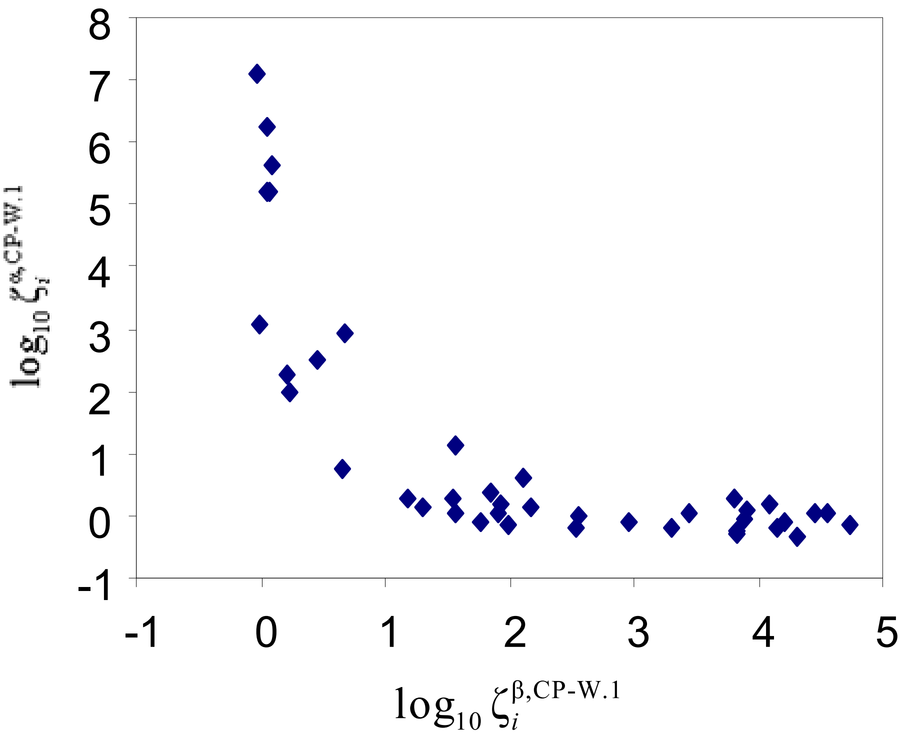

Figure 3.5. Hyperbolic relationship between $\log_{10} \zeta_i^{\alpha}$ vs. $\log_{10} \zeta_i^{\beta}$ as calculated in the performance evaluation (PE) case by the CP-W.1 method

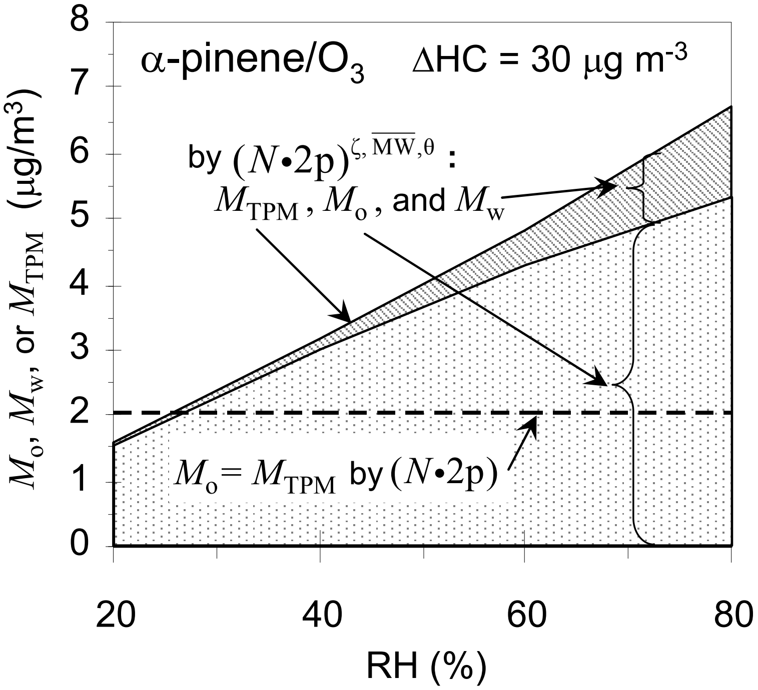

Fig. 3.6. M_o , M_w , and M_{TPM} by the $(N\bullet 2p)^{\zeta,\overline{MW},\theta}$ approach using the CP-Wilson.1 method for the activity coefficients for α-pinene/O$_3$ with ΔHC = 30 μg m^{-3}; for comparison, M_o = M_{TPM} by the $N\bullet 2p$ approach is also given.

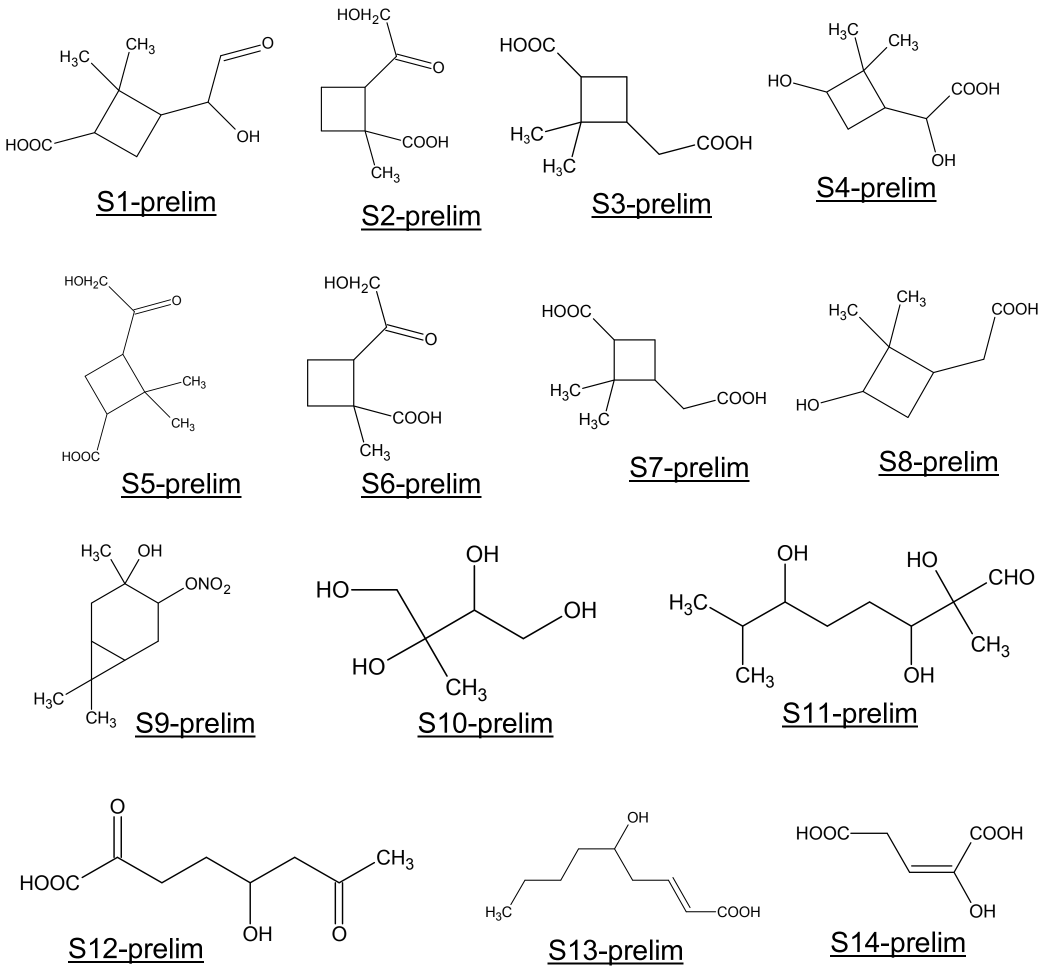
S1-prelim S2-prelim S3-prelim S4-prelim

S5-prelim S6-prelim S7-prelim S8-prelim

S9-prelim S10-prelim S11-prelim

S12-prelim S13-prelim S14-prelim

Figure S3.1. Preliminary fitted surrogate structures.

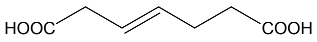

S15-prelim

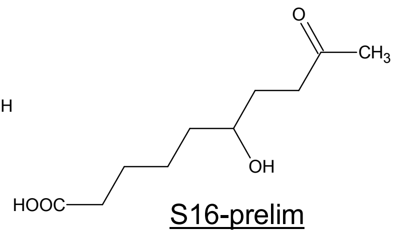

S16-prelim

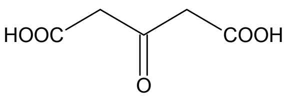

S17-prelim

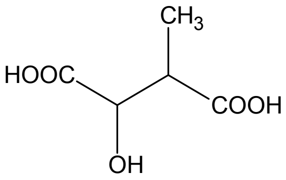

S18-prelim

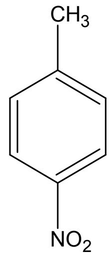

S19-prelim

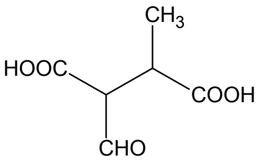

S20-prelim

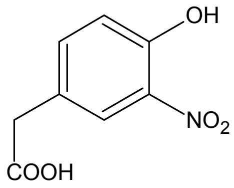

S21-prelim

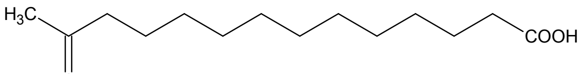

S22-prelim

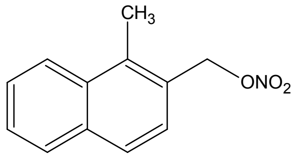

S23-prelim

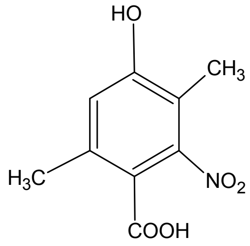

S24-prelim

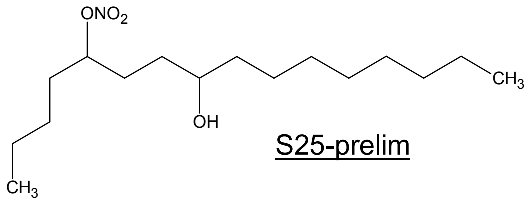

S25-prelim

Figure S3.1 (continued).

CHAPTER 4

Using Two Simple Pure Compound Properties to Model Complex Gas/Particle Partitioning for Non-aqueous Particulate Matter

4.1 Introduction

Chemical composition of atmospheric particulate matter (PM) is extremely complex and only a small fraction of organic compounds in PM has been identified (typically less than 10% by weight) (Rogge et al., 1993). Under such circumstance, a model of partitioning based on individual compounds is not possible and treatments based on lumped PM properties are often used. For examples, secondary organic aerosol (SOA) compounds are often modeled using model of Odum et al. (1996). For each photo-oxidation reaction of a parent hydrocarbon compound, Odum et al. (1996) lumped produced oxidation products into one or two products and the partitioning coefficients for the products were fitted using chamber experimental data. At present, primary organic aerosol (POA) are assumed to remain entirely in the particle (i.e., non-volatile) in most of the models.

The model of Odum et al. (1996) is attractive to large scale, three-dimensional (3-D) atmospheric modeling since it can be translated to simple computer algorithms for more economical computation. However, the model assumes a fixed gas/particle (G/P) partitioning coefficient ($K_{\mathrm{p},i}$) value for each compound even when relative humidity and aerosol composition can vary significantly in atmosphere. Based on the absorption model of Pankow (1994), besides vapor pressure ($p^{\circ}_{\mathrm{L},i}$), $K_{\mathrm{p},i}$ is a function of mean molecular weight ($\overline{\text{MW}}$) and activity coefficient (ζ_i). As $\overline{\text{MW}}$ and ζ_i depend on in-situ PM composition, $K_{\text{p},i}$ should be updated dynamically according to the temporal and special conditions. Neglecting PM composition dependence of $K_{\text{p},i}$ can result in large errors in predicted PM mass concentrations (Bowman et al., 2004). Pankow and Chang (2008) have estimated that the error in organic mass predictions can be as large as a factor of 1000 when total particulate matter (TPM) level is low. Chang and Pankow (2008) have advanced the model of Odum et al. (1996) by incorporating the dynamic $\overline{\text{MW}}$ and ζ_i so that the composition dependence of $K_{\text{p},i}$ is captured. A surrogate molecular structure for each lumped SOA product was extracted from the reported experimental $K_{\text{p},i}$ values based on the $p^{\text{o}}_{\text{L},i}$ - functional groups relationship (Pankow and Asher, 2007). These individual molecular structures allow the estimation of dynamic $\overline{\text{MW}}$ and ζ_i.

Donahue et al. (2006) have proposed a simple basis set of lumped partitioning coefficients (determined mainly by variation of $p^{\text{o}}_{\text{L},i}$) in one dimension to model organic particulate matter (OPM) levels in the atmosphere. The basis set treats both POA and SOA as semi-volatile compounds and thus allows gas/particle (G/P) partition. Like the Odum et al. (1996) model, while the simple view provides computational advantage to the application to large scale air quality modeling, it carries the disadvantage of not allowing the effects of variations in ζ_i and $\overline{\text{MW}}$ values. In recognition of the complicating effects of compound ζ_i, Donahue et al. (2006) do suggest that a suitable two-dimensional (2-D) characterization of the partitioning compounds might be obtained by supplementing p^{o}_{L} with carbon oxidation state. Carbon oxidation state, however, is an imperfect characteristic for the problem at hand as explained by Pankow and Barsanti (2008), because of the inflexible electron assignment rules (and thus potentially misleading).

Suitable parameters for 2-D characterization of the partitioning compounds may be related to the fundamental driving forces of ζ_i levels. Factors that determine the activity coefficient for a compound in a mixture include molecular size, polarity, and intermolecular forces (dispersion forces, polar forces, and hydrogen-bonding). Some pure compound properties that are associated with these factors have been used in ζ_i

models by Hildebrand et al. (1970) and Mermehrabi et al. (2006). Model of Hildebrand et al. (1970) used molar volumes and Hildebrand solubility parameters (indicating the solvency behavior of a specific solvent) to predict ζ_i for binary mixtures:

$$\ln\zeta_2 = \frac{\upsilon_2\varphi_1^2(\delta_1-\delta_2)^2}{\mathrm{R}T} \tag{4.1}$$

where subscripts 1 and 2 refer to the solvent and solute, respectively. δ is the Hildebrand solubility parameter $(\mathrm{J/cm^3})^{0.5}$, ζ_2 is the activity coefficient of the solute, υ is the specific volume ($\mathrm{cm^3/mol}$), T is temperature (K), and ϕ is the volume fraction. This model applies well on mixtures with similar compounds, but it failed to predict mixtures that contain dissimilar molecules or have interactions between different compounds. This limitation may be due to the lack of the consideration of compound polarity and polarizability in the model (Mermehrabi et al., 2006). Mermehrabi et al. (2006) have proposed an improved model that incorporates dielectric constant into the ζ_i expression in order to account for degrees of compound polarities and dipole-dipole interactions:

$$\ln\zeta_i = \frac{cA^a}{\mathrm{R}T}(x_1^b \ldots x_m^b)_{j\neq i}\left[bx_i^{(b-1)} + (1-mb)x_i^b\right] \tag{4.2}$$

$$A = \left|(\delta_{\mathrm{solute}}-\bar{\delta})^2 \times (\upsilon_{\mathrm{solute}}-\bar{\upsilon}) \times (\varepsilon_{\mathrm{solute}}-\bar{\varepsilon})^d\right| \tag{4.3}$$

where m is the number of compounds in the mixture; a, b, c, and d are constants; x_i is the mole fraction, δ_{solute} and $\bar{\delta}$ are solute and average Hildebrand solubility parameters; $\upsilon_{\mathrm{solute}}$ and $\bar{\upsilon}$ are the solute and average molar volumes; $\varepsilon_{\mathrm{solute}}$ and $\bar{\varepsilon}$ are the solute and average dielectric constants.

4.2 Method

4.2.1. Simple Activity Coefficient (SimAct.1) Estimation Method for Organic Mixtures

Equations. Like the models of Hildebrand et al. (1970) and Mermehrabi et al. (2006) (see Eqs 4.1 and 4.2), the expression of ζ_i in SimAct.1 also follows the "like dissolves like" principle. SimAct.1 accounts for degrees of the differences between the pure properties of organic compound *i* and the averaged bulk properties of the whole mixture. Vapor pressure ($p^{\mathrm{o}}_{\mathrm{L},i}$) and octanol-water partitioning coefficient ($K_{\mathrm{ow},i}$) are used to characterize organic compounds. $p^{\mathrm{o}}_{\mathrm{L},i}$ is directly related to heat of vaporization and thus can reflect the sum of intermolecular attractions that act to hold the pure liquid molecules of i together. $K_{\mathrm{ow},i}$ reflects the hydrophilic/hydrophobic tendency of a compound and thus is a good indication of the ratio (polar forces + hydrogen bond)/(dispersion forces) of the compound. Compounds will be miscible in each other not only if their total intermolecular forces are similar, but also if their composite forces are made up in the same way. In SimAct.1, the total intermolecular attraction and its composite are captured by $p^{\mathrm{o}}_{\mathrm{L},i}$ and $K_{\mathrm{ow},i}$ respectively and, thus, one can expect that compounds with similar $p^{\mathrm{o}}_{\mathrm{L},i}$ and similar $K_{\mathrm{ow},i}$ values would be miscible. Based on this rational, the SimACt.1 ζ_i is expressed as:

$$\ln\zeta_i = \frac{\mathrm{Co2}\bullet\left(\left|\log_{10} p^{\mathrm{o}}_{\mathrm{L},i} - \overline{\log_{10} p^{\mathrm{o}}_{\mathrm{L},i}}\right|^{\mathrm{Co3}} + \left|\log_{10} K_{\mathrm{ow},i} - \overline{\log_{10} K_{\mathrm{ow},i}}\right|^{\mathrm{Co4}}\right)^{\mathrm{Co1}}}{\mathrm{R}T} \tag{4.4}$$

with $$\overline{\log_{10} p^{\mathrm{o}}_{\mathrm{L},i}} = \sum_i x_i \log_{10} p^{\mathrm{o}}_{\mathrm{L},i} \quad \text{and} \quad \overline{\log_{10} K_{\mathrm{ow},i}} = \sum_i x_i \log_{10} K_{\mathrm{ow},i} \tag{4.5}$$

where i is the organic compound in the non-aqueous mixture, Co1-4 are fitting constants (universal for all organic compounds), $K_{\mathrm{ow},i}$ is octanol-water partitioning coefficient at 298K (mole fraction/mole fraction), $p^{\mathrm{o}}_{\mathrm{L},i}$ is liquid vapor pressure(sub-cooled if necessary) at 298 K (atm), R is the ideal gas constant (8.31 m^3 Pa K^{-1} mol^{-1}), T is temperature (K), x_i is the mole fraction.

As $p^{\mathrm{o}}_{\mathrm{L},i}$ and $K_{\mathrm{ow},i}$ of compound i deviate from that of the surrounding compounds, i becomes less miscible in the mixture and ζ_i increases. As the properties of i and the surrounding become identical, $\left|\log_{10} p^{\mathrm{o}}_{i,\mathrm{L}} - \overline{\log_{10} p^{\mathrm{o}}_{\mathrm{L}}}\right|$ and $\left|\log_{10} K_{\mathrm{ow},i} - \overline{\log_{10} K_{\mathrm{ow},i}}\right|$ both approach zero and ζ_i becomes unity. Like Eqs 4.1 and 4.2, the temperature dependence is in the reciprocal form in the SimAct.1 ζ_i expression.

Parameter Fitting. The parameter values needed for an activity coefficient estimation method are generally obtained by a fitting that minimizes some measure of the difference, for the parameter of interest, between: a) the predicted values; vs. b) corresponding experimental values. The particular fitting parameters obtained here combined with the governing equations compose version SimAct.1. Ideally, the fit carried out here would utilize experimental ζ_i values obtained for mixtures involving compounds similar to those of interest. Since such experimental data are not currently available, UNIFAC-generated values (i.e., ζ_i^{U} values) were used as the best, readily available substitute. The ζ_i^{U} values were obtained for mixtures involving 14 organic surrogate compounds taken directly from Chang and Pankow (2008) (see Fig. S3.1). These organic compounds were selected to cover a wide range of compound types (including multiple functional, di-acid, long-chain, mono-aromatic, poly-aromatic, mono-cyclic, poly-cyclic, and nitrated compounds) that are relevant to atmospheric partitioning species. Overall, fitting to ζ_i^{U} values was considered adequate given the high general merits of the UNIFAC method, and because use of the basis set model already represents a significant degree of approximation. At some future point, the SimAct.1 method could be re-fit using the extensive experimental ζ_i data set used by Fredenslund et al. (1975) to fit the UNIFAC method.

A total of 1694 ζ_i^{U} values were generated for total 823 mixtures (819 binary, 4 fourteen-compound mixtures) over mole fraction range 0.1 to 0.9 at 298 K. These mixtures were extracted from various combinations out of 14 compounds. Although some of these mixtures are not stable (i.e., would separate into two phases), that did not affect the inherent utility of the associated ζ_i^{U} values. Parameter optimization was performed on the total of four parameters (Co1-4). The fitting (optimization) occurred by use of the Differential Evolution algorithm (Storn et al, 1996) to minimize the function $\chi^2 = \sum_{1}^{1694}\left(\ln\zeta_i^{\mathrm{SimAct.1}}\text{-}\ln\zeta_i^{\mathrm{U}}\right)^2$. Differential Evolution algorithm (DE) is a population based, stochastic function minimizer, which applies genetic scheme for generating trial parameter vectors. In a population of potential solutions within an n-dimensional search space (in this case, $n = 4$), a fixed number of vectors are randomly initialized, then evolved over time to explore the search space and to locate the minima of the objective function. At each iteration, new vectors are generated by the combination of vectors randomly chosen from the current population (mutation). The resulting vectors are then combined with a predetermined target vector to produce the trial vector. Finally, the trial vector is accepted for the next generation if and only if it yields a reduction in the value of the objective function.

4.2.2. Molecular Weight as a Function of $p^{\mathrm{o}}_{\mathrm{L},i}$ *and* $K_{ow,i}$

To estimate $\overline{\mathrm{MW}}$ of OPM, it requires information about molecular weights (MW_i) of individual partitioning compounds. MW_i of i is assumed to be approximately proportional to its molecular size. For compounds of the same class such as n-alkane as an example, larger molecules such as n-hexadecane show lower $p^{\mathrm{o}}_{\mathrm{L},i}$ than their corresponding smaller homologues (e.g., n-hexane). This is because that those larger molecules have more contact area for each molecule and thus have a greater tendency to maximize the dispersion attractions. However the dispersion force is not the sole factor that drives the $p^{\mathrm{o}}_{\mathrm{L},i}$ level, polar force and hydrogen bonding force also play roles in determining $p^{\mathrm{o}}_{\mathrm{L},i}$. As the result, the described relationship between molecular sizes and $p^{\mathrm{o}}_{\mathrm{L},i}$ levels may not hold for compounds across a wide range of polarities. In this study, $K_{\mathrm{ow},i}$ is used to correct $p^{\mathrm{o}}_{\mathrm{L},i}$ in order to factor out the polarity contribution (polar and hydrogen bonding forces). The schematic in the following illustrates the assumed theory:

(a) $p^{\mathrm{o}}_{\mathrm{L},i}$: represents dispersion forces + polar forces + hydrogen bonding forces.

(b) $K_{\mathrm{ow},i}$: indicates the portion of polar forces + hydrogen bonding forces.

(a) – (b) : reflects dispersive forces, which is directly related to molecular size and, thus, to $\mathrm{MW}_{i.}$

Based on this assumption, MW_i can be expressed as a function of $p^{\mathrm{o}}_{\mathrm{L},i}$ and $K_{\mathrm{ow},i}$:

$$\mathrm{MW}_i = a\,\mathrm{Log}_{10}(p^{\mathrm{o}}_{\mathrm{L},i}) + b\,\mathrm{Log}_{10}(K_{\mathrm{ow},i}) + c \tag{4.6}$$

where constant coefficients a, b, c were fitted using values of MW_i, $p^{\mathrm{o}}_{\mathrm{L},i}$, and $K_{\mathrm{ow},i}$ for 14 organic compounds (see Table 4.1).

4.2.3. $\log_{10} p^{\mathrm{o}}_{\mathrm{L},i}$ vs. $\log_{10} K_{ow,i}$ Basis Set Approach Implementation

Partitioning is assumed to occur to a liquid or liquid-like phase and the partitioning coefficient for compound *i* is calculated according to (Pankow, 1994)

$$K_{\mathrm{p},i}\ (\mathrm{m}^3\ \mu g) = \frac{c_{\mathrm{g},i}}{c_{\mathrm{p},i}\ M_{\mathrm{TPM}}} = \frac{RTf}{10^6\,\overline{\mathrm{MW}}\,p^{\mathrm{o}}_{\mathrm{L},i}\,\zeta_i} \tag{4.7}$$

where $c_{\mathrm{g},i}$ (ng m^{-3}) and $c_{\mathrm{p},i}$ (ng μg^{-1}) are the gas- and particle-phase concentrations of *i*, *R* (m^3 atm mol^{-1} K^{-1}) is the gas constant, *T* (K) is temperature, *f* is the absorptive mass fraction of the PM and is assumed unity in this study, $\overline{\mathrm{MW}}$ (g mol^{-1}) is the mean molecular weight of the absorbing phase, $p^{\mathrm{o}}_{\mathrm{L},i}$ (Pa) is the pure compound vapor pressure of *i*, and ζ_i is the mole-fraction scale activity coefficient of *i* in the absorbing phase.

In conjunction with the SimAct.1 method and the proposed MW_i expression (see Eqs 4.4 - 4.7), $K_{\mathrm{p},i}$ can be treated as a function of only two independent variables, $p^{\mathrm{o}}_{\mathrm{L},i}$ and $K_{\mathrm{ow},i}$ at a given temperature. A 2-D basis set was created by assigning $\log_{10} p^{\mathrm{o}}_{\mathrm{L},i}$ (-15 to -5) and $\log_{10} K_{\mathrm{ow},i}$ (-4 to 19) to x and y axis respectively. The intervals for $\log_{10} p^{\mathrm{o}}_{\mathrm{L},i}$ and $\log_{10} K_{\mathrm{ow},i}$ are 1 and 2 respectively. A point on this $\log_{10} p^{\mathrm{o}}_{\mathrm{L},i}$ vs. $\log_{10} K_{\mathrm{ow},i}$ surface represents a partitioning compound with specific values of volatility, polarity, MW_i and $K_{\mathrm{p},i}(p^{\mathrm{o}}_{\mathrm{L},i}, K_{\mathrm{ow},i})$ value. All compounds characterized by the 2D basis set were assumed subject to G/P partitioning and each was assigned with a sum of the G- and total P-phase concentrations $\mathcal{T}_i$ $(=\mathcal{A}_i + \mathcal{F}_i)$. $\mathcal{F}_i$ (μg m^{-3}) and $\mathcal{A}_i$ (μg m^{-3}) represent the PM-associated and the G-phase associated concentrations of *i* respectively. (The related parameter $\mathcal{F}_i$ (ng m^{-3}) has been used in prior work from this group.) At equilibrium $\mathcal{A}_i$ can be expressed based on the value of $K_{\mathrm{p},i}$ and $\mathcal{F}_i$:

$$\mathcal{T}_i = \frac{\mathcal{F}_i}{M_{\mathrm{TPM}}\, K_{\mathrm{p},i}} + \mathcal{F}_i \tag{4.8}$$

wherein the first term on the RHS represents $\mathcal{A}_i$, as based on equilibrium with the liquid phase. M_{TPM} (μg m^{-3}) represents the total particulate matter mass concentration ($M_{\mathrm{TPM}}=\sum\mathcal{F}_i$). Eq (4.8) must be solved iteratively for M_{TPM} and at each iteration $K_{\mathrm{p},i}$ is updated based on the PM composition using the 2-D basis set (i.e., utilizing Eqs. (4.4) - (4.7)).

4.2.4. Cases

Performance Evaluation (PE) Cases for ζ_i *Prediction.* Three performance evaluation (PE) aerosol cases at T = 298 K for consideration of SimAct.1 and UNIFAC in PM calculations were selected to involve 14 compounds in Table 4.1 (also see Fig. S3.1). Among the 14 compounds (c1-c14), c1-c7 have relatively lower $p^{\mathrm{o}}_{\mathrm{L},i}$ values (the l-pol group) as compared with c8-c14 (the h-pol group). The settings of the three performance evaluation cases (PE1-3) are based on the relative mass proportions of the h-pol and the l-pol groups. PE1 represents the case in that total mass of each group is evenly distributed (each compound at $\mathcal{T}_i$ = 0.05 μg m^{-3}). PE2 represents the case in that the h-pol group dominates (c1-c7: each at $\mathcal{T}_i$ =0.05 μg m^{-3}, c8-c14: each at $\mathcal{T}_i$ = 0.1 μg m^{-3}). PE3 represents the case in that the l-pol group dominates (c1-c7: each at $\mathcal{T}_i$ =0.1 μg m^{-3}, c8-c14: each at $\mathcal{T}_i$ = 0.05 μg m^{-3}).

The 2-D Basis Set Case for Modeling G/P Partitioning. The hypothetical aerosol case involves multiple compounds characterized by a 2-D basis set with $\log_{10} p^{\mathrm{o}}_{\mathrm{L},i}$ (-15 to -5, separated by 1) and $\log_{10} K_{\mathrm{ow},i}$ (-4 to 19, separated by 2) on the two axis. There are total 143 grid points representing 143 partitioning compounds in the system. $\mathcal{T}_i$ values for individual compounds are provided in Table 4.2 and Fig. 4. 6A. System T is 300 K.

4.3 Result

4.3.1. Fit Quality for SimAct.1 Relative to UNIFAC

Table 4.3 gives the best-fit values for parameters Co1-Co4 for SimAct.1. The averaged unsigned percentage error for ζ_i relative to UNIFAC was calculated based on the 1694 pairs of predicted $\zeta_i^{\mathrm{SimAct.1}}$ and ζ_i^{U} values according to:

$$\sigma_{\mathrm{FIT}}\,(\%) \quad = \quad \frac{\displaystyle\sum_{i=1}^{1694}\left|\frac{\zeta_i^{\mathrm{SimAct.1}}-\zeta_i^{\mathrm{U}}}{\zeta_i^{\mathrm{U}}}\right|\times 100\%}{1694} \tag{4.9}$$

The overall fit quality is satisfying (σ_{FIT} = 50 %) given that the expression for $\zeta_i^{\mathrm{SimAct.1}}$ is simpler than the UNIFAC by a significant degree and, moreover, only four parameters (universal to all compounds) are allowed to flow in the fitting process (very limited freedom). Fig. 4.1 provides the plot of the 1694 points for $\ln\zeta_i^{\mathrm{SimAct.1}}$ vs. $\ln\zeta_i^{\mathrm{U}}$ and it shows that the overall trend of the model predictions is correct. For $0 < \ln\zeta_i^{\mathrm{U}} < 4$, there are some over- and under-prediction scatters. These scattered points generally involve mixtures containing hexadecanoic acid, a free fatty acid possessing both polar and non-polar properties. The carboxylic acid end of the fatty acid is very hydrophilic and thus dissolves readily in polar compounds; the long carbon chain end is very hydrophobic and thus dissolves in non-polar compounds. The fatty acids will naturally align themselves such that the hydrophobic long carbon ends will point upwards into the non-polar layer and the hydrophilic carboxylic acid ends will point downwards into the polar layer. The extremely simplified SimAct.1 model might not be able to model this type of compound as the unique properties of a 16 carbon fatty acid may not be reflected well purely by $K_{\mathrm{ow},i}$ and $p_{\mathrm{L},i}^{\mathrm{o}}$. Most of the existing activity coefficient models, including UNIFAC, generally cannot model this type of mixture structure well. Therefore, the scattering points should be well expected. Extra caution should be paid when applying the model to systems dominated with long chain fatty acids.

Errors in $\zeta_i^{\mathrm{SimAct.1}}$ tend to increase with increasing ζ_i^{U}. The contributions to prediction errors for the mass totals are not likely to be caused simply by incorrectly estimating a large ζ_i value. Indeed, when there is one liquid phase, such an error can only be significant if the corresponding x_i is also of a significant magnitude. However, in that case, the phase would very likely be unstable relative to phase separation, in which case the i-related prediction error for the mass total would become small because most of the i would retreat into the new, second phase in which ζ_i would be relatively close to 1 and thus reliably estimated.

The model cannot predict ζ_i less than unity. $\zeta_i<1$ corresponds to compounds with very strong attractions to each other (even stronger than the pure solution) and usually are mixtures of extremely polar compounds. In atmosphere, compounds constitute PM are very diverse in terms of polarity. Therefore, the case with $\zeta_i<1$ should be very rare.

4.3.2. Molecular Weight as a Function of $p^{\mathrm{o}}_{\mathrm{L},i}$ and $K_{ow,i}$

Table 4.4 provides the best fit values for coefficients *a*, *b*, *c* of Eq. (4.6). Fig. 4.2 provides a plot of the 14 points for $\mathrm{MW}_i^{\mathrm{cal}}$ vs. $\mathrm{MW}_i^{\mathrm{obs}}$ (predicted vs. observed values). The averaged unsigned percentage error for $\mathrm{MW}_i^{\mathrm{cal}}$ was calculated according to $\sigma_{\mathrm{FIT}}\ (\%) = 100\% \times \sum_{i=1}^{14} \left|(\mathrm{MW}_i^{\mathrm{cal}} - \mathrm{MW}_i^{\mathrm{obs}}) / \mathrm{MW}_i^{\mathrm{obs}}\right| / 14$. The resulting σ_{FIT} is 9 % indicating the very good fit quality. This result also supports the assumption that the dispersive force can be singled out from the total attraction interaction by using the function of $p^{\mathrm{o}}_{\mathrm{L},i}$ (represents dispersive forces + polar forces + hydrogen bonding forces) and $K_{\mathrm{ow},i}$ (indicates the portion of polar forces + hydrogen bonding forces).

4.3.3. SimAct.1 vs. UNIFAC for Performance Evaluation (PE) Cases

Relative to UNIFAC, the unsigned prediction difference (%) for $\mathcal{F}_i$ is defined

$$\delta^{\theta}_{\mathcal{F},i} = \frac{\left|\mathcal{F}_i^{\mathrm{SimAct.1}} - \mathcal{F}_i^{\mathrm{U}}\right|}{\mathcal{F}_i^{\mathrm{U}}} \times 100\% \tag{4.10}$$

where the superscripts on $\mathcal{F}_i$ denote the ζ_i method. The plots of $\delta_{\mathcal{F},i}$ vs. x_i^{U} for Cases PE1-3 are given in Figs. 4.3.A, 4.4.A, and 4.5.A for the 14 compounds. Plots of $\mathcal{F}_i^{\mathrm{SimAct.1}}$ vs. $\mathcal{F}_i^{\mathrm{U}}$ for all 14 compounds in Cases PE1-3 are also provided (Figs 4.3.B, 4.4.B, and 4.5.B). For all PE cases, $\delta_{\mathcal{F},i}$ is small when $x_i^{\alpha,\mathrm{U}} > 0.06$. This indicates that the prediction deviations do not affect much on major compounds in PM and thus are not likely have significant effects on the quality of predictions for total PM concentrations (M_{TPM}). Table 4.5 provides observed and predicted results for M_{TPM} for the PE case. The low percentage errors in M_{TPM} support the view discussed above.

4.3.4. Predictions for $\log_{10} p^{\mathrm{o}}_{\mathrm{L},i}$ vs. $\log_{10} K_{ow,i}$ Basis Set Case

Table 4.2 provide assigned $\mathcal{T}_i$ values for compounds characterized by the $\log_{10} p^{\mathrm{o}}_{\mathrm{L},i}$ vs. $\log_{10} K_{\mathrm{ow},i}$ grid. Predicted $\mathcal{F}_i$ and $\mathcal{A}_i$ values are provided in Table 4.6. Plots of $\log_{10} p^{\mathrm{o}}_{\mathrm{L},i}$ vs. $\log_{10} K_{\mathrm{ow},i}$ vs. $\mathcal{T}_i$, $\log_{10} p^{\mathrm{o}}_{\mathrm{L},i}$ vs. $\log_{10} K_{\mathrm{ow},i}$ vs. $\mathcal{A}_i$, and $\log_{10} p^{\mathrm{o}}_{\mathrm{L},i}$ vs. $\log_{10} K_{\mathrm{ow},i}$ vs. $\mathcal{F}_i$ are also provided (Figs 4.6.A-C). The result shows that for compounds of extremely high or low volatility, the G/P partitions are mainly controlled by the $p^{\mathrm{o}}_{\mathrm{L},i}$ (for example, for compounds with $\log_{10} p^{\mathrm{o}}_{\mathrm{L},i} = 6$, the $\mathcal{F}_i$ values stay almost constant regardless the variation in $\log_{10} K_{\mathrm{ow},i}$). In contrast, for compounds with medium volatilities, the polarity effects (reflected by $\log_{10} K_{\mathrm{ow},i}$) become significant on the G/P partitioning (for example, for compounds with $\log_{10} p^{\mathrm{o}}_{\mathrm{L},i} = -10$, $\mathcal{F}_i$ decreases by 60% as $\log_{10} K_{\mathrm{ow},i}$ decreases from 16 to 8). These results indicate that 2-D (volatility vs. polarity) basis set provides a much better resolution in both compound characterization and G/P partition prediction than the1-D (volatility) basis set approach. This 2-D method should especially improve the predictions for SOA compounds as they typically possess medium volatilities (semi-volatile) and the partitions can be very sensitive to the polarity effects.

4.4 Conclusions

When dealing modeling, one of the toughest problems is the dilemma of choosing between the economic computation and sophisticated equations based on sound theories. The $\log_{10} p^{\mathrm{o}}_{\mathrm{L},i}$ vs. $\log_{10} K_{\mathrm{ow},i}$ basis set approach developed here is the balance between the two objectives above. The method is extremely simple and computationally economic. At the same time, it advanced the commonly used models that utilize fixed $K_{\mathrm{p},i}$ by considering both compound volatility and polarity and thus can better estimate dynamic $K_{\mathrm{p},i}$. The success in developing the new activity coefficient model, SimAct.1, and the expression of MW_i ($p^{\mathrm{o}}_{\mathrm{L},i}$, $K_{\mathrm{ow},i}$) is especially crucial to this advance in modeling of G/P partitioning.

4.5 References

Bowman, F. M., Karamalegos, A. M., 2002. Estimated effects of composition on secondary organic aerosol mass concentrations. Environmental Science & Technology 36, 2701-2707.

Chang, E.I., Pankow, P.F., 2007. Organic particulate matter at varying relative humidity using surrogate primary and secondary organic compounds with a method based on the Wilson Equation for activity corrections in the condensed phase. Atmospheric Chemistry and Physics Discussion 8, 1–45.

Donahue, N.M., Robinson, A.L., Stanier, C.O., Pandis, S.N., 2006. Coupled partitioning, dilution, and chemical aging of semivolatile organics. Environmental Science and Technology 40, 2635-2643.

Fredenslund, A., Jones, R.L., Prausnitz, J.M., 1975.Group-contribution estimation of activity coefficients in nonideal mixtures. AIChE Journal 21, 1086-1099.

Hildebrand, J.H., Prausnitz, J.M., Scott, R.L., 1970. Regular and related solutions. New York: Van Nostrand Reinhold. 22p.

Mermehrabi, M., Rohani, S., Perry, L., 2006. Thermodynamic modeling of avtivity coefficient and prediction of solubility: Part 1. Predictive models. Journal of Pharmaceutical Sciences 95, 790-797.

Odum, J.R., Hoffmann, T., Bowman, F., Collins, D., Flagan, R.C., and Seinfeld, J. H., 1996. Gas/particle partitioning and secondary organic aerosol yields. Environmental Science &. Technology 30, 2580 -2585.

Pankow, J.F., 1994.An absorption model of gas/particle partitioning of organic compounds in the atmosphere. Atmospheric Environment 28, 185-188.

Pankow, J.F., Asher, W.E., 2007. SIMPOL.1: A simple group contribution method for predicting vapor pressures and enthalpies of vaporization of multifunctional organic compounds. Atmospheric Chemistry and Physics Discussion 7, 11839-11894.

Pankow, J.F., Barsanti, K.C., 2008. Framework for considering the complexity of the compounds present in organic particulate matter in the atmosphere (in preparation).

Pankow, J.F., Chang, E.I., 2008. Variation in the Sensitivity of Predicted Levels of Atmospheric Organic Particulate Matter (OPM). Atmospheric Chemistry and Physics Discussion (in press).

Politzer, P., Murray, J. S., 1994. Theoretical and Computational Chemistry, Quantitative Treatment of Solute/Solvent Interactions, Elsevier Publishers.

Rogge, W.F., Mazurek, M.A., Hildemann, L.M., Cass, G.R., Simoneit, B.R.T., 1993. Quantification of urban organic aerosols at a molecular-level-identification, abundance and seasonal-variation. Atmospheric Environment 27A, 1309-1330.

Storn, R., and Price, K.V., 1996. Minimizing the real function of the ICEC'96 contest by differential evolution. IEEE Conference on Evolutionary Computation, 842-844.

Table 4.1. Compounds taken from Chang and Pankow (2008) for SimAct.1 parameter fitting.

	Volatility Group [a]	Number [b]	Product Name	log $p^{o}_{L,i}$ [c] (log atm)	log $K_{ow,i}$ [c] (log $x_{o,i}/x_{w,i}$)	MW$_i$ (g/mol)
1	l-pol	P13-Prelim	unresolved complex mixture	-13.38	18.51	487
2	l-pol	P10-Prelim	monoglyceride	-13.22	5.61	330
3	l-pol	P1-Prelim	2,6-naphthlene diacid	-13.09	2.78	216
4	l-pol	S17-Prelim	hopane	-12.56	-2.38	146
5	l-pol	P4-Prelim	nonacosane	-11.7	15.18	412
6	l-pol	P5-Prelim	isoprene/OH product	-10.37	17.71	409
7	l-pol	P1-Prelim	α-pinene/O_3 product	-10.32	-0.67	186
8	h-pol	P11-Prelim	toluene/OH product	-9.98	-3.45	162
9	h-pol	S4-Prelim	α-pinene/OH product	-9.74	0.21	174
10	h-pol	S21-Prelim	hexadecanoic acid	-9.68	1.93	197
11	h-pol	P14-Prelim	levoglucosan	-9.12	6.65	256
12	h-pol	S18-Prelim	terpene/OH product	-8.69	-0.87	148
13	h-pol	S11-Prelim	xylene/OH product	-8.1	-0.12	170
14	h-pol	P15-Prelim	glycerol	-6.22	-2.52	92

Footnotes:

a. l-pol and h-pol groups indicate relatively lower and higher $p^{o}_{L,i}$ values respectively.

b. Reference numbers to Fig. S3.1.

c. Estimated using SPARC (Politzer and Murray, 1994) at 298 K.

Table 4.2. Assigned total mass concentration for each compound, $\mathcal{T}_i$ (μg m^{-3}), used in the $\log_{10} p^{o}_{L,i}$ vs. $\log_{10} K_{ow,i}$ basis set case.

		Log$_{10}$ $p^{o}_{L,i}$ (log$_{10}$ atm)										
		-15	-14	-13	-12	-11	-10	-9	-8	-7	-6	-5
Log$_{10}$ $K_{ow,i}$ (log$_{10}$$x_{o,i}/x_{w,i}$)	20	0.1	0.1	0.1	0	0	0	0	0	0	0	0
	18	0	0.1	0.1	0.1	0	0	0	0	0	0	0
	16	0	0	0.1	0.1	0.1	0.1	0.1	0	0	0	0
	14	0	0	0	0.1	0.1	0.1	0.1	0.1	0.1	0.1	0
	12	0	0	0	0.1	0.1	0.1	0.1	0.1	0.1	0.1	0.1
	10	0	0	0	0	0.1	0.1	0.1	0.1	0.1	0.1	0.1
	8	0	0	0	0	0.1	0.1	0.1	0.1	0.1	0.1	0.1
	6	0	0	0	0	0	0.1	0.1	0.1	0.1	0.1	0.1
	4	0	0	0	0	0	0	0.1	0.1	0.1	0.1	0.1
	2	0	0	0	0	0	0	0	0.1	0.1	0.1	0.1
	0	0	0	0	0	0	0	0	0.1	0.1	0.1	0.1
	-2	0	0	0	0	0	0	0	0	0.1	0.1	0.2
	-4	0	0	0	0	0	0	0	0	0	0.1	0.2

Table 4.3. Fitted parameters for SimAct.1 equation.

$$\ln \zeta_i = \frac{\mathrm{Co2}\bullet\left(\left|\log_{10} p^{\mathrm{o}}_{\mathrm{L},i} - \overline{\log_{10} p^{\mathrm{o}}_{\mathrm{L},i}}\right|^{\mathrm{Co3}} + \left|\log_{10} K_{\mathrm{ow},i} - \overline{\log_{10} K_{\mathrm{ow},i}}\right|^{\mathrm{Co4}}\right)^{\mathrm{Co1}}}{\mathrm{R}T}$$

Co1	Co2	Co3	Co4
4.2449	14.9493	0.0459	0.5163

Table 4.4. Fitted parameters for $\mathrm{MW}_i = a\ \mathrm{Log}_{10}(\ p^{\mathrm{o}}_{\mathrm{L},i}\ ) + b\ \mathrm{Log}_{10}(K_{\mathrm{ow},i}) + c$

a	*b*	*c*
-1.90E+01	1.14E+01	1.67E+00

Table 4.5. Comparison of predictions for the performance evaluation (PE) cases using the UNIFAC method and the SimAct.1 method (T = 298K, RH = 50%).

Case	$\mathcal{T}_i$ (µg m^{-3}) [§]		M_{TPM} (µg m^{-3})		Error in M_{TPM} [‡]
	l-pol group	h-pol group	UNIFAC prediction	SimAct.1 prediction	%
PE1	0.05	0.05	0.18	0.19	5.6
PE2	0.05	0.1	0.215	0.209	-2.8
PE3	0.1	0.05	0.42	0.44	4.8

Footnotes:

[§] for each compound in the specified group.

[‡] error based on UNIFAC predictions as observed values.

Table 4.6. Predicted gas ($\mathcal{A}_i$) and liquid ($\mathcal{F}_i$) mass concentrations for the log$_{10}$ $p^{o}_{L,i}$ vs. log$_{10}$ $K_{ow,i}$ basis set case (T = 300K). Predicted M_{TPM}=1.64 μg m^{-3}.

a. $\mathcal{A}_i$ (μg/m^3)		Log$_{10}$ $p^{o}_{L,i}$ (log$_{10}$ atm)										
		-15	-14	-13	-12	-11	-10	-9	-8	-7	-6	-5
	20	2.93E-06	2.86E-05	2.75E-04	0	0	0	0	0	0	0	0
	18	0	1.67E-05	1.63E-04	1.51E-03	0	0	0	0	0	0	0
	16	0	0	1.14E-04	1.10E-03	1.02E-02	5.34E-02	9.20E-02	0	0	0	0
	14	0	0	0	1.04E-03	9.62E-03	5.17E-02	9.15E-02	9.91E-02	9.99E-02	1.00E-01	0
	12	0	0	0	1.37E-03	1.27E-02	5.97E-02	9.38E-02	9.93E-02	9.99E-02	1.00E-01	1.00E-01
Log$_{10}$ $K_{ow,i}$	10	0	0	0	0	1.89E-02	7.08E-02	9.61E-02	9.96E-02	1.00E-01	1.00E-01	1.00E-01
(log$_{10}$$x_{o,i}$/$x_{w,i}$)	8	0	0	0	0	3.05E-02	8.24E-02	9.80E-02	9.98E-02	1.00E-01	1.00E-01	1.00E-01
	6	0	0	0	0	0	9.13E-02	9.91E-02	9.99E-02	1.00E-01	1.00E-01	1.00E-01
	4	0	0	0	0	0	0	9.97E-02	1.00E-01	1.00E-01	1.00E-01	1.00E-01
	2	0	0	0	0	0	0	0	1.00E-01	1.00E-01	1.00E-01	1.00E-01
	0	0	0	0	0	0	0	0	1.00E-01	1.00E-01	1.00E-01	1.00E-01
	-2	0	0	0	0	0	0	0	0	1.00E-01	1.00E-01	2.00E-01
	-4	0	0	0	0	0	0	0	0	0	1.00E-01	2.00E-01

b. $\mathcal{F}_i$(μg/m^3)		Log$_{10}$ $p^{o}_{L,i}$ (log$_{10}$ atm)										
		-15	-14	-13	-12	-11	-10	-9	-8	-7	-6	-5
	20	1.00E-01	1.00E-01	9.97E-02	0	0	0	0	0	0	0	0
	18	0	1.00E-01	9.98E-02	9.85E-02	0	0	0	0	0	0	0
	16	0	0	9.99E-02	9.89E-02	8.98E-02	4.66E-02	7.97E-03	0	0	0	0
	14	0	0	0	9.90E-02	9.04E-02	4.83E-02	8.50E-03	9.18E-04	9.23E-05	9.22E-06	0
	12	0	0	0	9.86E-02	8.73E-02	4.03E-02	6.24E-03	6.54E-04	6.53E-05	6.49E-06	6.46E-07
Log$_{10}$ $K_{ow,i}$	10	0	0	0	0	8.11E-02	2.92E-02	3.86E-03	3.93E-04	3.89E-05	3.85E-06	3.81E-07
(log$_{10}$$x_{o,i}$/$x_{w,i}$)	8	0	0	0	0	6.95E-02	1.76E-02	2.02E-03	2.01E-04	1.97E-05	1.94E-06	1.91E-07
	6	0	0	0	0	0	8.69E-03	8.97E-04	8.72E-05	8.48E-06	8.28E-07	8.11E-08
	4	0	0	0	0	0	0	3.37E-04	3.23E-05	3.11E-06	3.01E-07	2.94E-08
	2	0	0	0	0	0	0	0	1.02E-05	9.72E-07	9.36E-08	9.06E-09
	0	0	0	0	0	0	0	0	2.74E-06	2.59E-07	2.48E-08	2.38E-09
	-2	0	0	0	0	0	0	0	0	5.90E-08	5.59E-09	1.07E-09
	-4	0	0	0	0	0	0	0	0	0	1.07E-09	2.03E-10

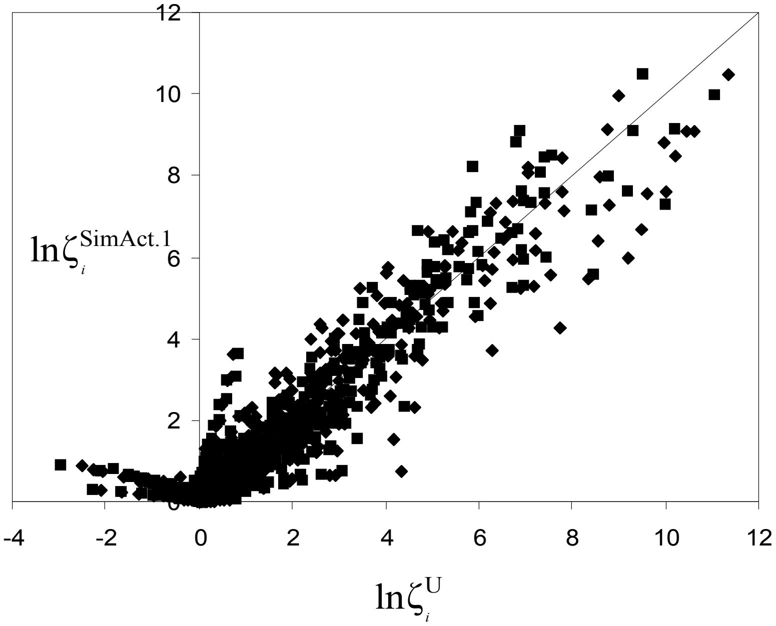

Figure 4.1. ζ_i calculated by SimAct.1 vs. ζ_{i} calculated by UNIFAC for 1,694 points used in the fitting of SimAct.1 to UNIFAC.

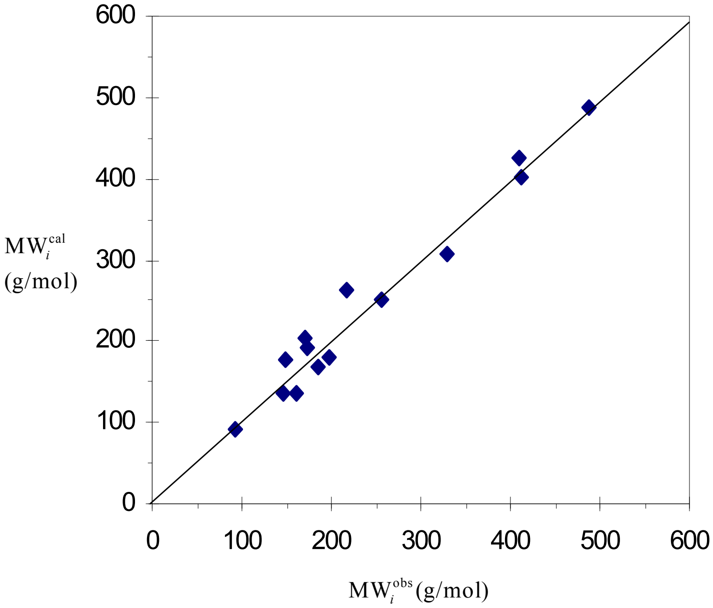

Figure 4.2. Calculated molecular weights ($\mathrm{MW}_i^{\mathrm{cal}} = a\ \mathrm{Log}_{10}\, p^{\mathrm{o}}_{\mathrm{L},i} + b\ \mathrm{Log}_{10}\, K_{\mathrm{ow},i} + c$) vs. observed values ($\mathrm{MW}_i^{\mathrm{obs}}$) for 14 compounds used in the fitting of SimAct.1 to UNIFAC.

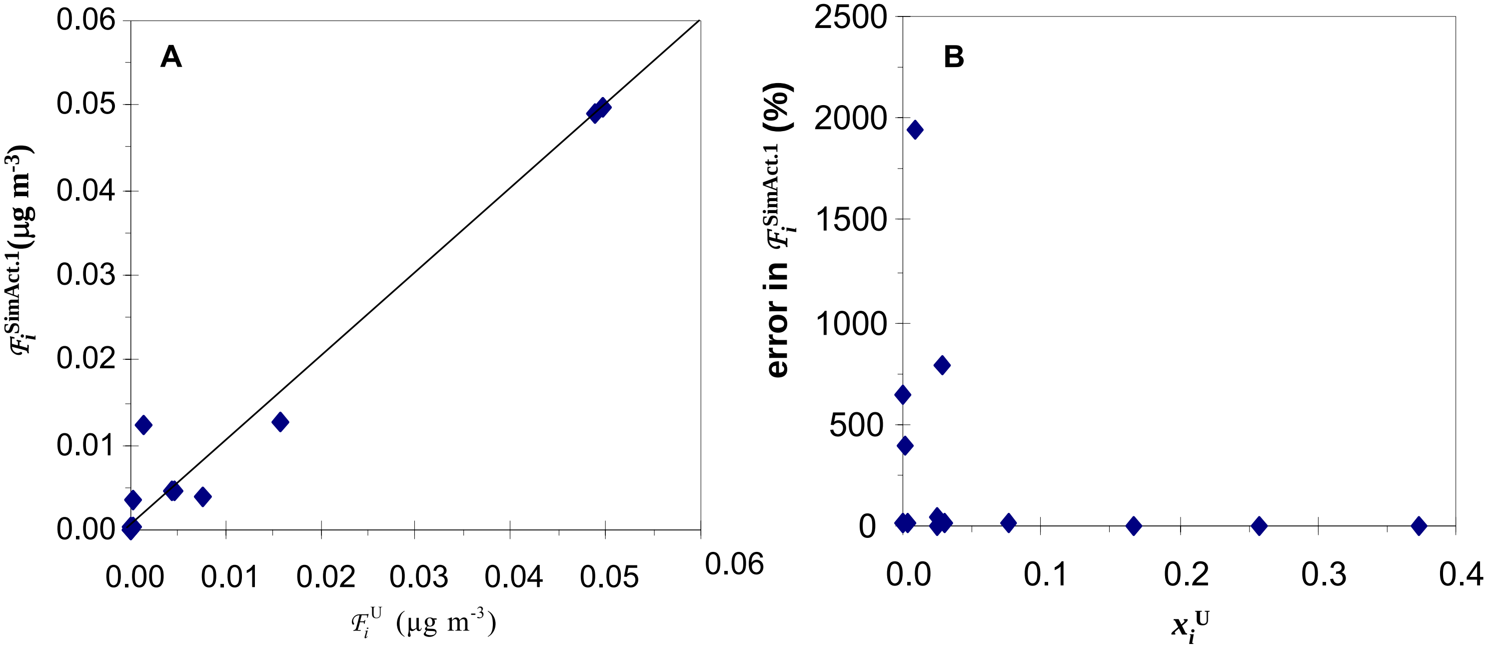

Figure 4.3. Results for Case PE1: A. total mass concentrations predicted by SimAct.1 vs. UNIFAC; B. unsigned percentage difference between the values of $\mathcal{F}_i^{\text{SimAct.1}}$ as predicted using SimAct.1 and UNIFAC plotted vs. x_i^{U}.

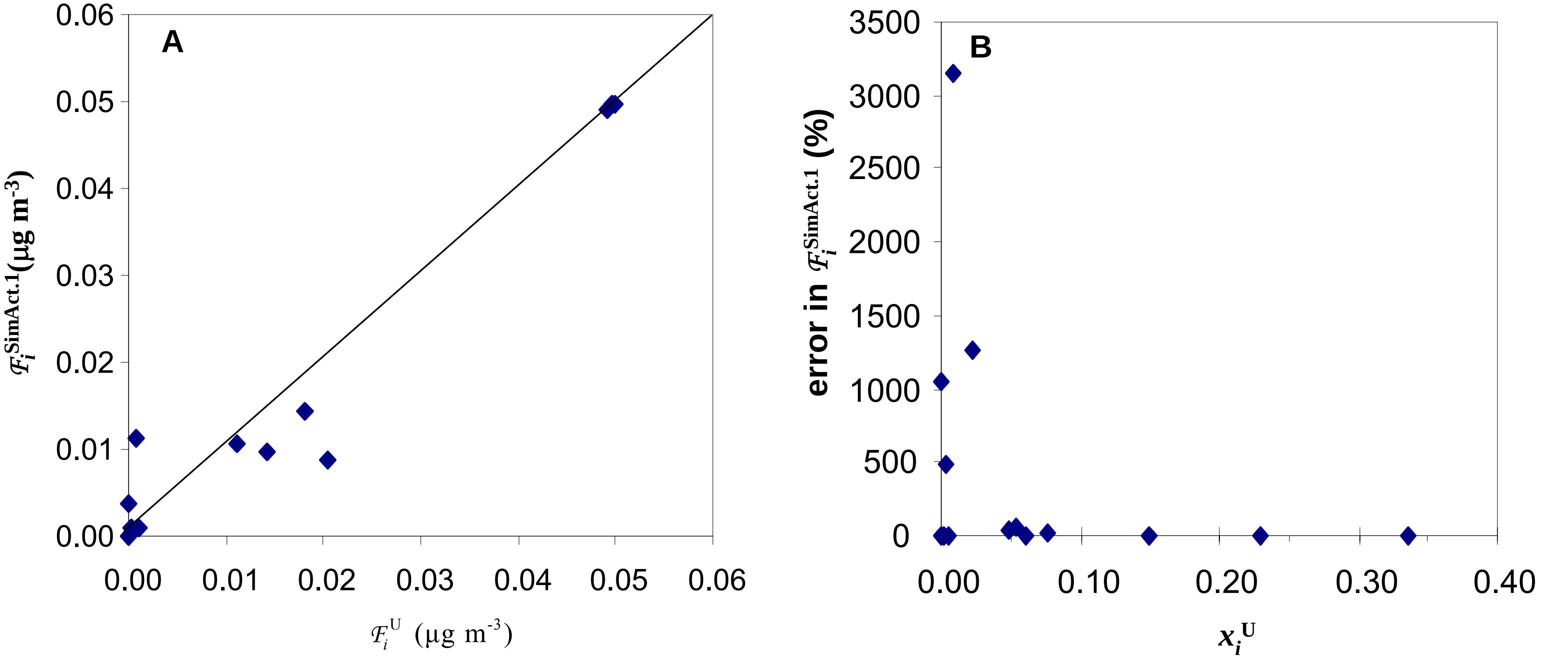

Figure 4.4. Results for Case PE2: A. total mass concentrations predicted by SimAct.1 vs. UNIFAC; B. unsigned percentage difference between the values of $\mathcal{F}_i^{\mathrm{SimAct.1}}$ as predicted using SimAct.1 and UNIFAC plotted vs. x_i^{U}.

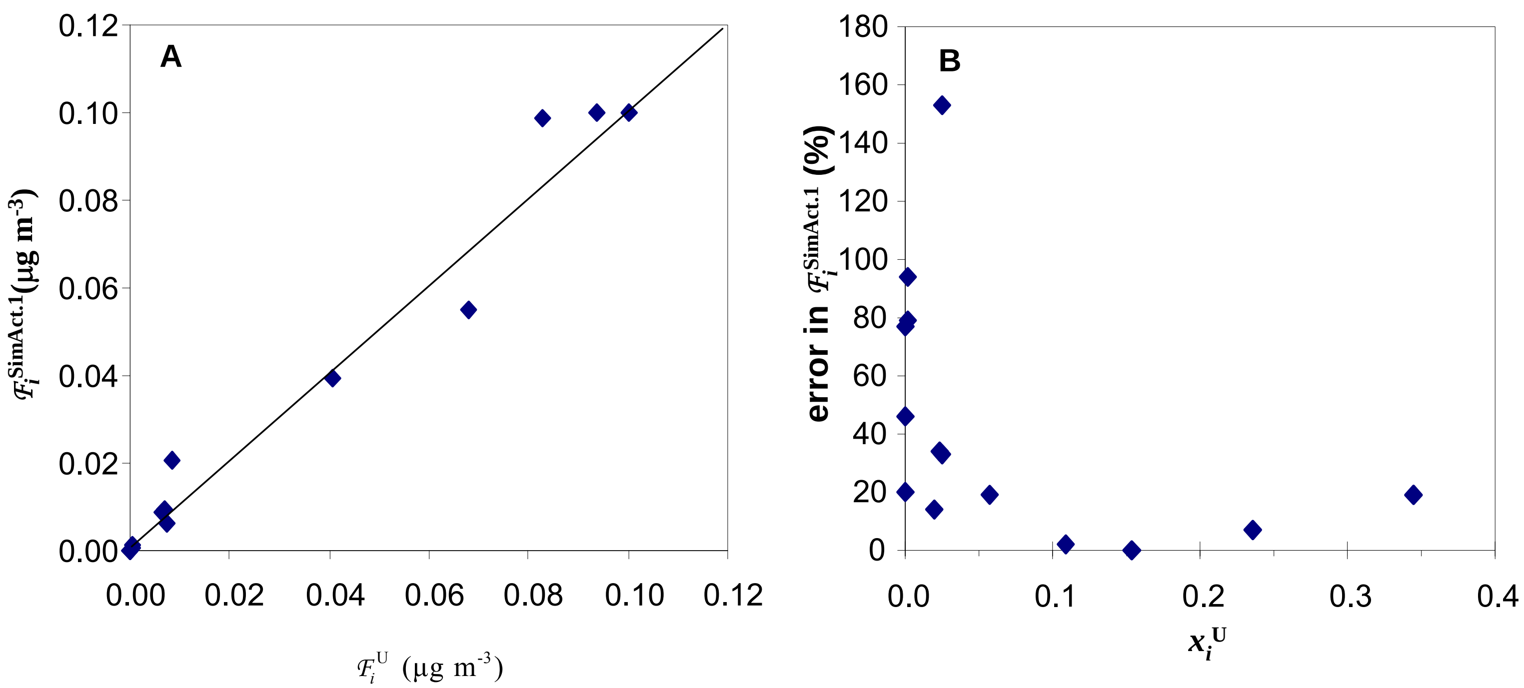

Figure 4.5. Results for Case PE3: A. total mass concentrations predicted by SimAct.1 vs. UNIFAC; B. unsigned percentage difference between the values of $\mathcal{F}_i^{\text{SimAct.1}}$ as predicted using SimAct.1 and UNIFAC plotted vs. x_i^{U}.

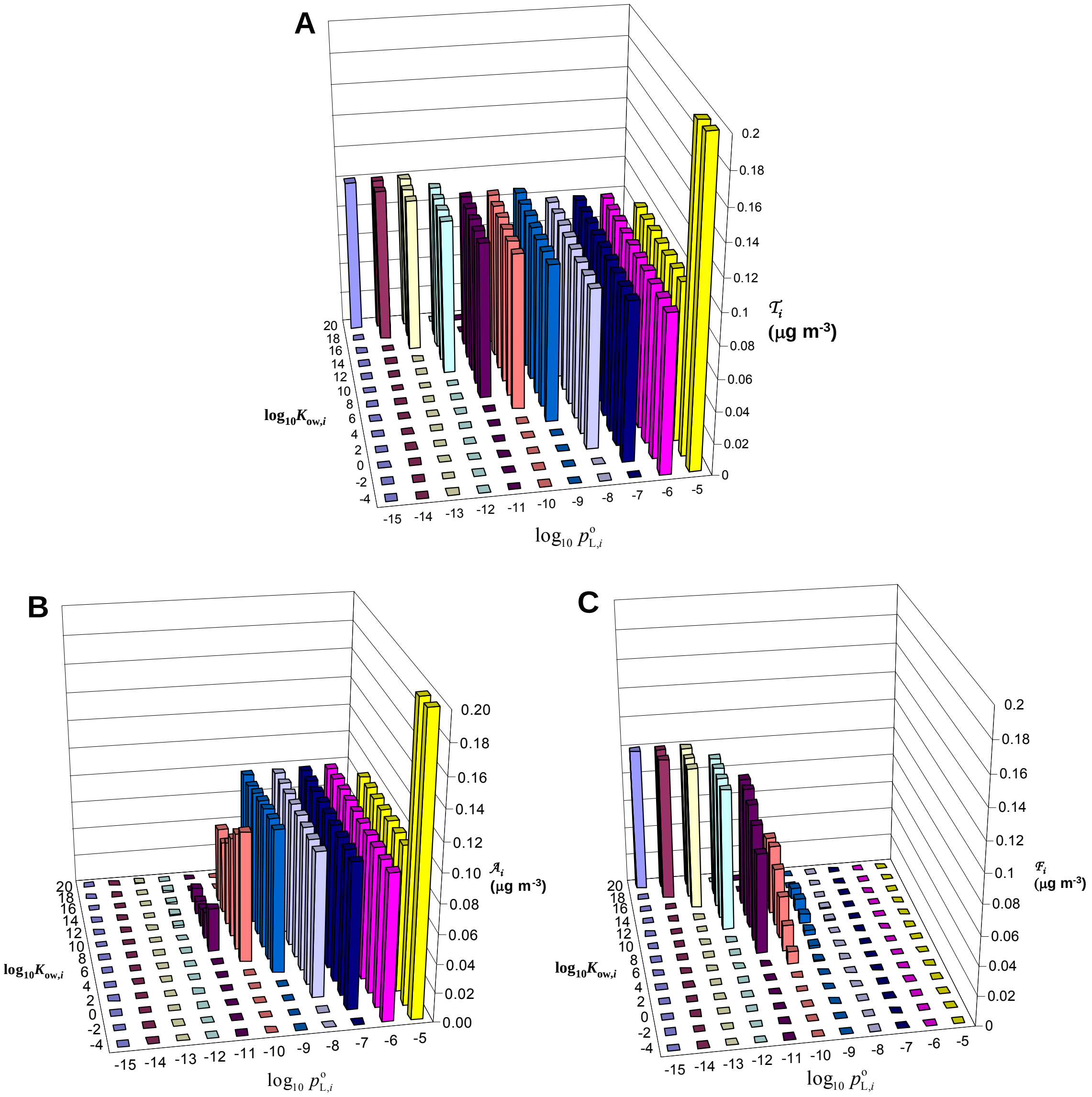

Figure 4.6. Results for predictions using the log$_{10}$ $p^{\text{o}}_{\text{L},i}$ vs. log$_{10}$ $K_{\text{ow},i}$ basis set: A. assumed total mass concentration for each compound ($\mathcal{T}_i$), B. predicted gas mass concentration ($\mathcal{A}_i$), C. predicted liquid mass concentrations ($\mathcal{F}_i$).

BIOGRAPHICAL SKETCH

Elsa was born in Norman, Oklahoma in January of 1977. She grew up in Taipei, Taiwan and received her Bachelor of Science degree in Environmental Engineering from National Chung-Hsing University. To pursuit higher education, Elsa joined Cornell University in 1999 and researched the development of a sensing process to detect pollutants in drinking water. This work led to a breakthrough patent (US patent: 10/650,042). These efforts also led to the receipt of the Nanobiotechnology Center (NBTC) Fellowship from the National Science Foundation (NSF). Elsa received the Master of Science degree in Biological and Environmental Engineering from Cornell University in 2001. In 2002, Elsa joined OGI and started to research the development of chemical models to predict atmospheric particulate matter levels and properties. She has been an active member of the American Aerosol Association of Research (AAAR) and the American Chemical Society (ACS) speaking at several national and international conferences and publishing a number of scientific articles in peer-reviewed journals. Elsa is currently working at Bonneville Power Administration as a Physical Scientist in Portland, Oregon.

Publications

Celebucki, C.C., Ferris Wayne, G., Connolly, G.N., Pankow, J.F., Chang, E.I., 2005. When “light” means more: characterization of measured menthol in 48 U.S. cigarette sub-brands. Nicotine & Tobacco Research 7, 523–531.

Chang, E.I., Pankow, J.F., 2006. Prediction of activity coefficients in liquid aerosol particles containing organic compounds, dissolved inorganic salts, and water-Part 2: Consideration of phase separation effects by an X-UNFIAC model. Atmospheric Environment 40, 6422-6436.

Chang, E.I., Pankow, J. F., 2008. Organic particulate matter formation at varying relative humidity using surrogate secondary and primary organic compounds with activity corrections in the condensed phase obtained using a method based on the Wilson equation. Atmospheric Chemistry and Physics Discussion 8, 995-1039.

Chang, E.I., Pankow, J. F., 2008. Using two simple pure compound properties to model complex gas/particle partitioning for atmospheric organic particulate matter (OPM) (in preparation).

Erdakos, G.B., Chang, E.I., Pankow, J.F., Seinfeld, J.H., 2006. Prediction of activity coefficients in liquid aerosol particles containing organic compounds, dissolved inorganic salts, and water—Part 3: Organic compounds, water, and ionic constituents by consideration of short-, mid-, and long-range effects using X-UNIFAC. Atmospheric Environment 40, 6437-6452.

Pankow, J.F., Chang, E.I., 2008. Variation in the sensitivity of predicted levels of atmospheric organic particulate matter (OPM). Environmental Science & Technology (in press).